

REPORT NO. AER 1263

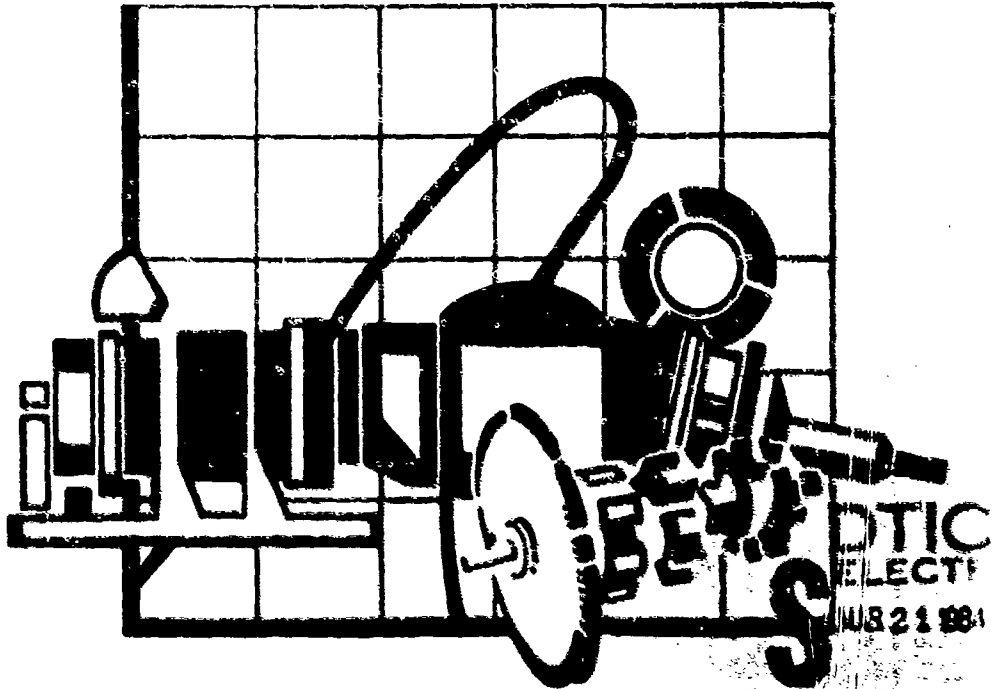
AD

ORGANIC RANKINE CYCLE SILENT POWER PLANT, 1.5 KW, 28 VDC

FOR
U. S. ARMY MOBILITY R & D CENTER
FORT BELVOIR, VIRGINIA

AD A 139160

DTS FILE COPY



Sundstrand Energy Systems

DISTRIBUTION STATEMENT A

Approved for public release
Distribution Unlimited

DC 14-897

NOTICES
DISTRIBUTION STATEMENT

THIS DOCUMENT HAS BEEN APPROVED FOR PUBLIC RELEASE AND SALE.
ITS DISTRIBUTION IS UNLIMITED.

DISCLAIMERS
THE FINDINGS IN THIS REPORT ARE NOT TO BE CONSTRUED AS AN
OFFICIAL DEPARTMENT OF THE ARMY POSITION, UNLESS SO DESIGNATED
BY OTHER AUTHORIZED DOCUMENTS.
THE CITATION OF TRADE NAMES AND NAMES OF MANUFACTURERS IN
THIS REPORT IS NOT TO BE CONSTRUED AS OFFICIAL GOVERNMENT
ENDORSEMENT OR APPROVAL OF COMMERCIAL PRODUCTS OR SERVICES
REFERENCED HEREIN

DISPOSITION
DESTROY THIS REPORT WHEN IT IS NO LONGER NEEDED.
DO NOT RETURN IT TO THE ORIGINATOR.

Accession Per	
NTIS GRAFI	<input checked="" type="checkbox"/>
DTIC TAB	<input type="checkbox"/>
Unannounced	<input type="checkbox"/>
Justification	
By Per DTIC Form 10	
Distribution/on file	
Availability Codes	
Avail and/or Dist	Special
R/I	

REPORT NO. AER 1263
 DATE 9/22/75
 REVISION _____ DATE _____

SUNDSTRAND AVIATION
 DIVISION OF SUNDSTRAND CORPORATION
 ROCKFORD, ILLINOIS

DAAK02-72-C-0472

ENGINEERING REPORT

ORGANIC RANKINE CYCLE
 SILENT POWER PLANT, 1.5 KWe, 28v DC
 FOR
 ELECTROTECHNOLOGY DEPARTMENT
 ELECTROMECHANICAL DIVISION
 U. S. ARMY MOBILITY R & D CENTER
 FORT BELVOIR, VIRGINIA 22060

DISTRIBUTION STATEMENT A
 Approved for public release
 Distribution Unlimited

DTIC
 ELECTE
 MAR 21 1984
 S D

APPROVAL AND CLASSIFICATION		
INITIALS	DATE	INITIALS
BUDGETOR ONLY	DIRECTOR OF ENGINEERING	DATE
EQUIPMENT	S. S. Bush	11-18-75
BUDGETOR	DIRECTOR OF ENGINEERING	DATE
15M EN 10 891		
BUDGETOR	DIRECTOR OF ENGINEERING	DATE
FINANCIAL		
MILITARY EQUIPMENT	DIRECTOR OF ENGINEERING	DATE
INSTRUMENTS OR EQUIPMENT		
DATA RELATED TO THIS ORIGIN	SAM HOGAN, MUSC PGSB	DATE
DATA RELATED TO THIS SUBMISSION		
MERIT/QUALITY ASSURANCE		
DRAFTED BY: [Signature]		
REVIEWED BY: [Signature]		
APPROVED BY: [Signature]		
DATE: 11-18-75		
FORM 5160.7		

SECTION I
ACKNOWLEDGEMENT

I. ACKNOWLEDGEMENT

Many individuals and groups have worked enthusiastically toward developing this Organic Rankine Cycle Silent Power Plant. While all individuals cannot be identified, following is a list of those who formed a nucleus on this extension program. Louis Suit, Roland Christen, Gary Peach, Timothy Bland, William Smith, and many other support individuals and groups.

SECTION II
TABLE OF CONTENTS

TABLE OF CONTENTS

<u>Section</u>	<u>Page No</u>
I ACKNOWLEDGEMENT	1
II TABLE OF CONTENTS	2
III INTRODUCTION	3
Set 1 Development Summary and Conclusions	4
Set 2 Improvement Plan	6
IV SUMMARY	10
V DESCRIPTION	15
VI COMPONENT DEVELOPMENT	24
Constant Frequency Motor	24
Noise	24
Gearbox Noise	24
Noise Frequencies Identification from Test Data	28
Improvements in Gear Noise Reduction	29
CRU Noise	34
Offset Gearbox	35
CRU (Combined Rotating Unit)	44
Valves	56
Pitot Pump	56
Boost Pump	56
Start Approach	60
VII SYSTEM DEVELOPMENT	69
Steady State Operation	69
VIII IMPROVEMENTS	98
Startup	98
Output Power and Efficiency	98
Repackaging Concept	108
IX CALIBRATION REQUIREMENTS SUMMARY	110

SECTION III

INTRODUCTION

III. INTRODUCTION

Under USAMERDC Contract DAAK02-72-C-0472, Sundstrand has been developing an organic Rankine cycle, 1.5 KWe, 28 VDC, portable silent power plant. A summary of the specification requirements is presented in Table III-A. To date, two (2) development sets have been delivered to USAMERDC, Ft. Belvoir, Va. The development of Set 1 is described in Sundstrand Report ATR 1182, 6-24-74; the following report describes the development of Set 2. The following introductory paragraphs summarize the results of Set 1 development and the basis for improvements planned for Set 2.

Table III-A Specification Requirements

- 1.5 KW, 28 VDC, Closed Rankine Cycle
- Portable, skid mounted
- Silent at 100 meters
- Capable of withstanding extremely hard usage encountered in military field application simulated by free fall flat and end drop (18 and 12 inches respectively), vibration, railroad impact at 10 mph and in transit road test
- Locally or remote station startup within 10 minutes by an integral stored energy source and a manual or external energy source
- 65°F to +125°F ambient temperature, any humidity
- Minimum 3000 hours operating life
- Minimum 7.5% Set efficiency at 1.5 KW output
- Maximum 150 lb. dry weight
- Maximum 8 cubic foot volume
- Multi fuel operation
- Inclined operation, 31° from horizontal
- Minimum 95% Set reliability
- Start and operate at 1.5 KW in rain and wind (12 in/hr and 40 mph respectively)
- 4% voltage regulation, 2 seconds recovery time, 2% voltage stability, 26-34 volts adjustment, 3% voltage ripple, adjustable current limit, 30% voltage dip and rise, overload of 110% and overspeed of 125%
- Design for human performance and engineering
- Major component characteristics
 - Boiler-Burner: Heatup to operating temperature and pressure in three minutes, equipped with automatic controls, electrical power supplied from alternators
 - Working Fluid Circulating System: Includes condenser, preheater if required, feed pump. No significant working fluid loss for two years or 10,000 hours of operation
 - Throttle Valve: Used to control vapor flow
 - Governor: Required to sense and control engine speed to essentially a constant level
 - Condenser: Must be compact, light weight, vapor to air using blower(s).
 - Regenerator: Utilize if overall cycle efficiency can be improved
 - Lubrication System: Must be suitable for moving parts and hermetically sealed for engine
 - Alternator: To be brushless and have a static excitation system
 - Fuel System: Includes ignition source, integral fuel pump capable of pumping through a 25 foot line with a six foot static suction head, lines, filter and positive shutoff
 - Battery and Charger
 - Controls for pressure, speed, temperature and power conditioning

SET 1 DEVELOPMENT SUMMARY AND CONCLUSIONS

The program consisted of:

- Packaged development Set and breadboard controls
- Limited component and subsystem testing
- No breadboard system testing

In terms of development effort, some of the critical subsystems of Set No. 1 resulted in:

- Air/Fuel System developed - more than 100 hours of operation
- Turbine development - 2900 hours of bearing testing
- Breadboard control system demonstrated/operational

A significant amount of set testing resulted in:

- 69 hot tests
- 15 hours of hot testing on the turboalternator, regenerator and condenser
- 20 hours of hot testing on the heater and burner
- 75 hours of operation on all accessories

There were several nuisance types of problems encountered throughout the Set 1 development period, some of these were resolved. There were major problems which were identified, including potential solutions. These prevented complete self-contained operation and full power output from being demonstrated and are listed below.

- Low turbine performance
- Apparent low turbine exhaust temperature
- Structural flexibility of the turbine balanced assembly and hotwell
- Pitot pump performance

It was demonstrated that low turbine performance was primarily due to too large spacing of the turbine nozzles and correcting this would enable at least 84% of predicted turbine power to be achieved. Figure III-1 shows the data for the Set No. 1 nozzle plate and a test nozzle plate with close-spaced (touching edge-to-edge) nozzles (Figure III-2). With the exception of the one point taken from set data, all data are for tests conducted on a test rig using high pressure nitrogen to drive the turbine. It can be seen that the original nozzle plate produced 88% of the predicted turbine efficiency. By reducing the nozzle spacing, the turbine views a continuous rather than intermittent driving gas stream as the wheel rotates past each nozzle. The result is a substantial increase in turbine efficiency.

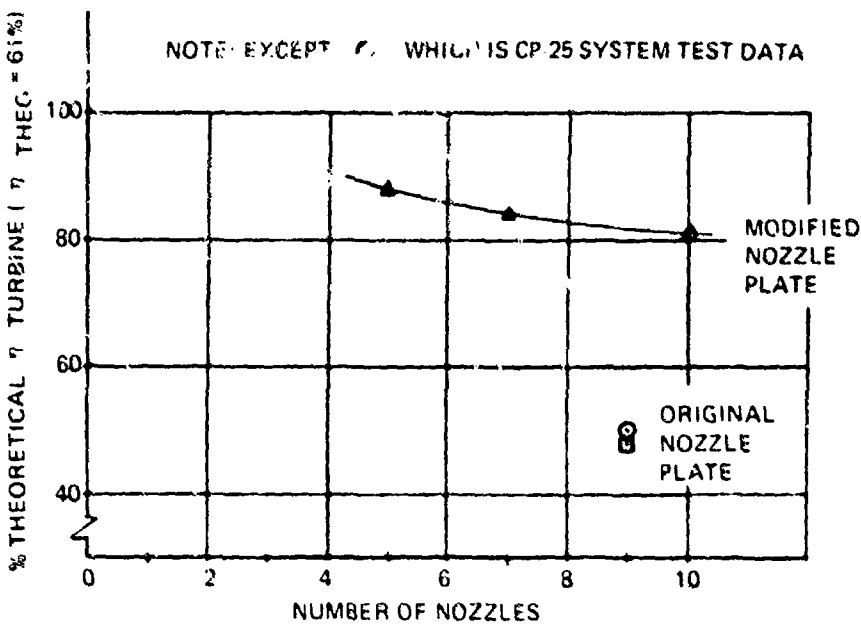


Figure III-1 N₂ Test Results

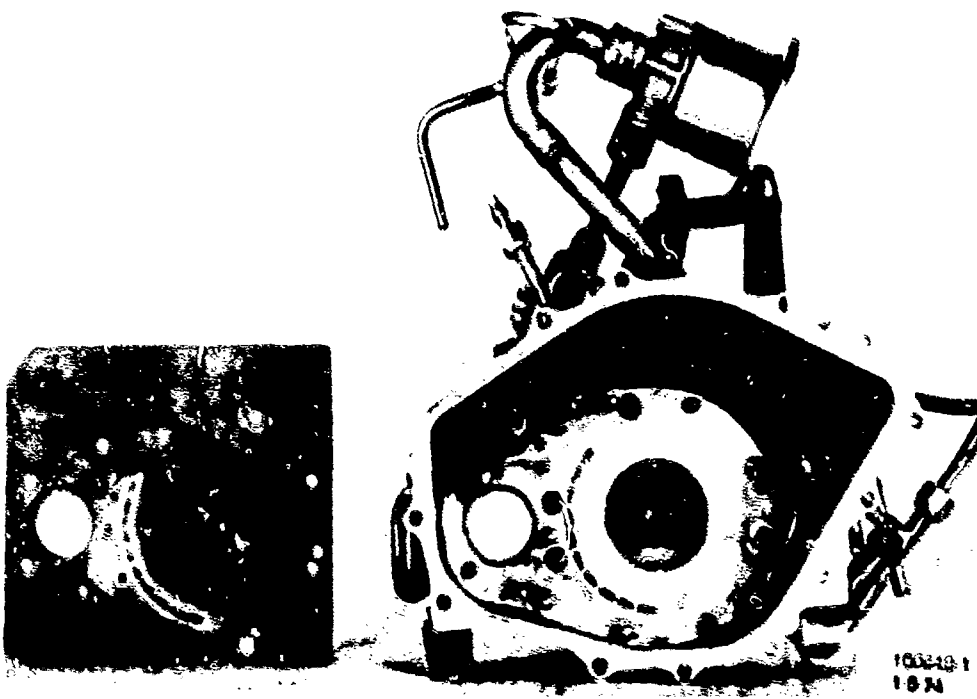


Figure III-2 Test and End 1 Nozzle Plates

The resultant projected system performance with the modified nozzle plate is shown in Figure III 3 to be 1.1 KW net output at an average 8 1/2 active nozzles which corresponds to the maximum flow that the system can support. The burner has overfire capability but of unknown extent. However, at 10 active nozzles (the limit of the present design), 1.47 KW net output power can be produced. Whether this can be achieved is dependent upon the extent of the overfire capability, the heat exchangers, the achievable reduction in parasitic power and the turbine/pump characteristics.

Another problem was low turbine exhaust temperature. It was hypothesized that quenching of the turbine exhaust was occurring due to fluid migrating from the pitot pump area. Shifting the pitot pump from the turbine wheel end of the assembly would permit any leakage to fall to the hotwell. The Set No. 1 and revised configurations are shown in Figure III 4.

Also, the flexibility of the turbine balance assembly and hotwell, or the CRU (combined rotating unit), has resulted in rubbing at the turbine wheel hub and pitot pump housing regions. These have all been light and non-damaging in nature but nonetheless result in undesirable noise, vibration and power consumption. Improved balancing, an increase in the shaft diameter and noncantilevered mounting of the turbine balance assembly in the hotwell have shown by test to be an improvement.

SET 2 IMPROVEMENT PLAN

The following improvements were considered advantageous to incorporate into Set No. 2 which comprises the basis of this report.

CRU redesign	Includes a new, close spaced nozzle plate, stiffening of the forward and aft hotwell housings, larger diameter shaft, shifting the pitot pump aft and moving the bending critical speeds above the 55,000 rpm operating speed.
Boost pump	Improving the capability of the boost pump to operate with a boiling fluid will improve operation margin.
Noise reduction	Several sources of emitted noise include the CRU (housing resonance) and accessories such as condenser fan and gearbox, should be identified and reduced to acceptable level.
Control valves	Sticking of the control valves appears to be related to clearances, contamination and coil size, reliability of operation should be improved through correction.
Packaged controller	The present (Set No. 1) breadboard controller should be packaged into a configuration consistent with mounting in the wave.

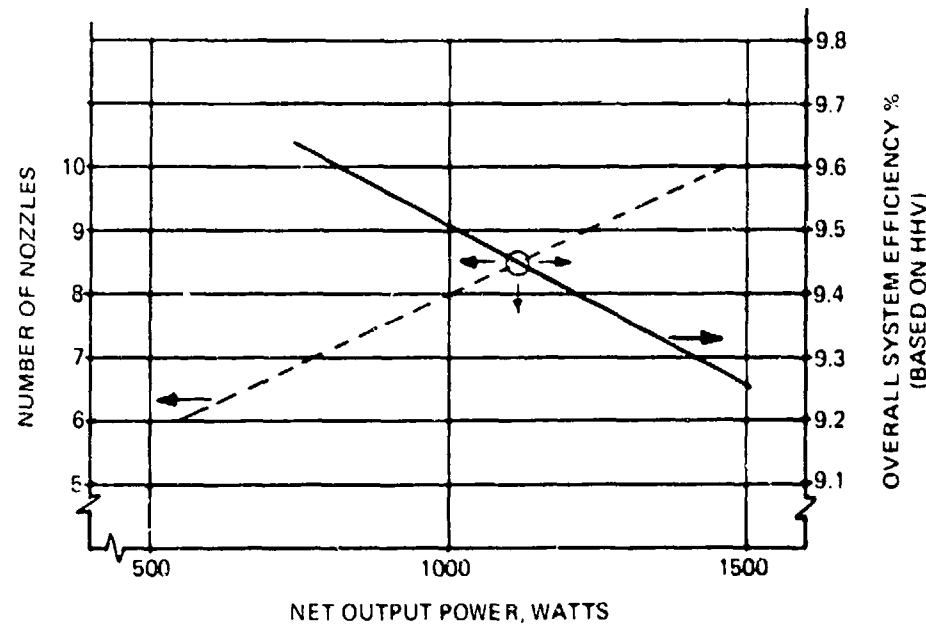
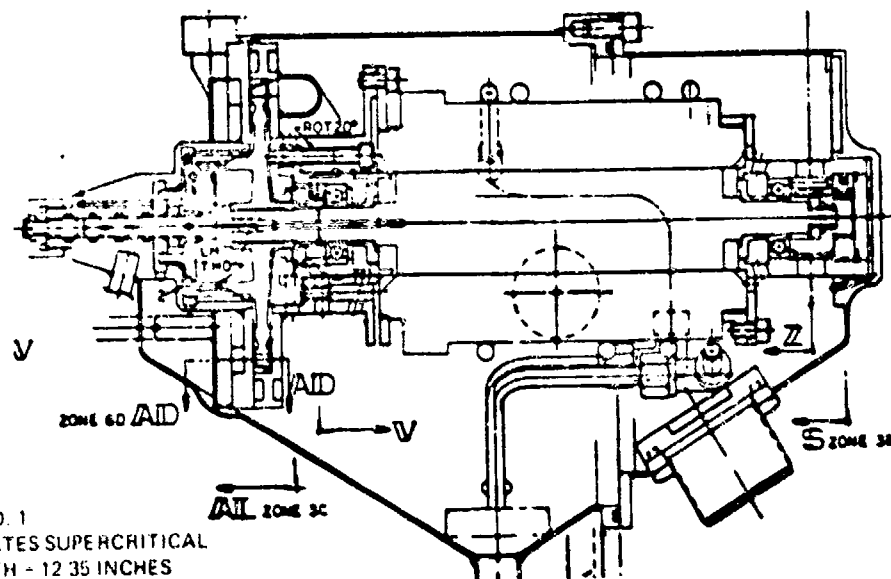
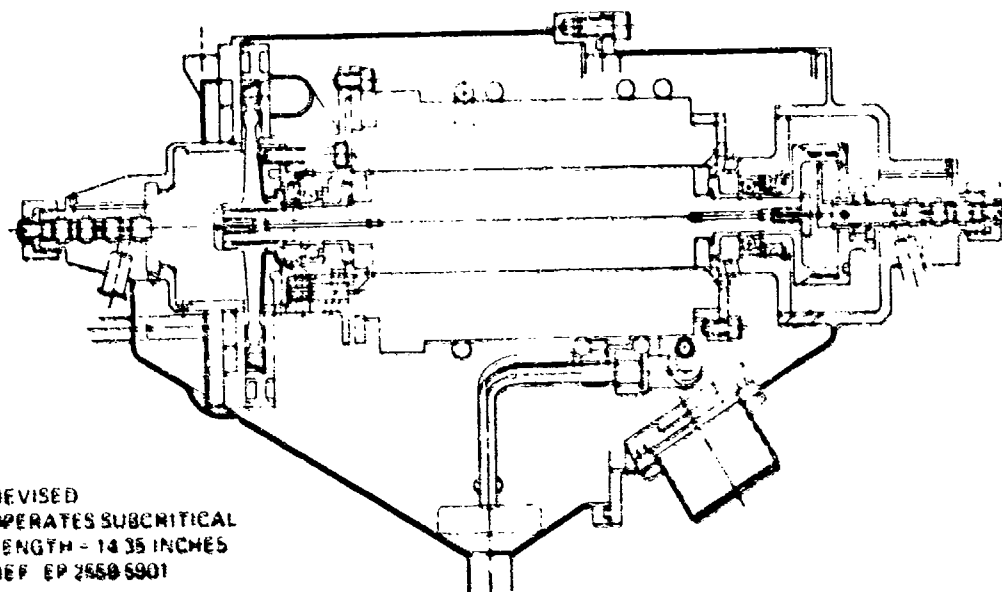


Figure III-3 Projected System Performance



SET NO. 1
OPERATES SUPERCRITICAL
LENGTH - 12 35 INCHES
REF EP 2559 1001



REVISED
OPERATES SUBCRITICAL
LENGTH - 14 35 INCHES
REF EP 2559 6901

Figure III-4 Set No. 1 and Revised CRU Configurations

Parasitic power reduction

Accessory power is considerably higher than desired and those areas where reduction is readily achievable should be investigated.

Startup

The Set No. 1 startup method involves retaining pressure in the accumulator from the shutdown and/or pressurizing as required to the desired level by the handpump. Both start pressure and start flow valves must be extremely leak tight. Other approaches, which may be simpler, e.g., start pump assisted starts, should also be investigated.

SECTION IV

SUMMARY

IV SUMMARY

This report is a summary of the development of a 1.5 KWe, 28 VDC organic Rankine cycle power plant. It specifically describes the degree of progress made between Set 1 and Set 2. Set 1 was described in Report ATR 1182 and delivered to USAMERDC at Ft. Belvoir in the first quarter of 1974. Set 2 is described in this report and was delivered in the first quarter of 1975.

Figure IV-1 is a photo of Set 2. Table IV-A summarizes its characteristics and Table IV-B is a summary of the 1.5 KW organic Rankine cycle modification benefit matrix. The Set is a low volume (~2' x 2' x 2'), low weight (212 lb), multifuel (demonstrated on MIL-T-5161 primary fuel and W-F-800 alternate fuel) machine that has had several improvements incorporated. Relative to Table IV-B these include all of Item 1.0, 2.0, 4.0, 5.0, 6.0, 7.0 and part of 8.0.

Except for battery start, the set is self-sufficient. Output power has been as high as 477 watts. The set has not achieved design power (1.5 KW) primarily due to heat losses and shunts within the machine, slightly lower than design turbine efficiency and lower pitot pump efficiency. Of these, the pitot pump predominates. A small effect in low output power is due to the regenerator effectiveness and heater efficiency being lower on Set 2 than that demonstrated on Set 1.

The lower pitot pump efficiency is attributed to changes in the pump housing and the pitot probe between Set 1 and Set 2. When designing the pump for Set 2, an approach thought to not functionally impact the pump performance was followed to reduce fabrication cost. This has proved to be detrimental.

Set 2 is a functional power plant. Its deficient output power needs correction through improvement in the performance of the components contributing most to the problem. Table IV-C summarizes these improvements and the resulting output power using actual test data presented in this report as a basis.

Other areas in need of further development include automatic startup and noise level, neither of which meet specification requirements although improvements have been made in both areas in progressing from Set 1 to Set 2.

Other areas where improvements have been made include control valves that are free from sticking, a significant reduction in parasitic power (approximately 76 watts), and an improved boost pump.

Set 2 is a significantly improved functional unit compared to Set 1 and represents a considerable step towards evolving a portable multifuel, 1.5 KWe, 28 VDC, silent power plant.



Figure IV-1 Set No. 2 on Test Stand

Table IV-A Power Plant Characteristics

Production Prototype Package	
Weight:	212 lb.
Volume:	7.7 cu. ft.
Performance:	Tests show potential for thermal efficiency of 10.4-13.9%
Durability:	In accord with specification
Operation:	1500 hrs. on CRU bearings 60 hrs. on accessories each Set 20 hrs. on hermetic system each Set Demonstrated multi-fuel capability Packaged controls demonstrated
Other:	Reduced gearbox noise (Set 2 lower than Set 1) Reduced start complexity (Set 2 less complex than Set 1) Reduced parasitic power (Set 2 lower than Set 1)

Table IV-B 1.5 KW Organic Rankine Cycle Modification - Benefit Matrix

MODIFICATION	COST		WEIGHT		EFFICIENCY		RELIABILITY		NOISE		Comments	
	Increase		Reduce		Increase		Reduce		Reduce			
	Reduce	Increase	Reduce	Increase	Reduce	Increase	Reduce	Increase	Reduce	Increase		
1.0 Eliminate												
1.1 Automatic starters	x	x	x	x	x	x	x	x	x	x		
1.2 Automatic valves	x	x	x	x	x	x	x	x	x	x		
1.3 Steam flow valve	x	x	x	x	x	x	x	x	x	x		
1.4 Steam旁通閥 (Bypass)	x	x	x	x	x	x	x	x	x	x		
1.5 Steam Pump	x	x	x	x	x	x	x	x	x	x		
1.6 Temperature Control Circuits	x	x	x	x	x	x	x	x	x	x		
1.7 Use three pressure switches to monitor combustion air temperature sensors	x	x	x	x	x	x	x	x	x	x		
1.8 New instruments	x	x	x	x	x	x	x	x	x	x		
2.0 Add dry sump pump	x	x	x	x	x	x	x	x	x	x		
2.1 Add Steam Pump	x	x	x	x	x	x	x	x	x	x		
2.2 Reinforcing flue side flues	x	x	x	x	x	x	x	x	x	x		
2.3 Reinforce fire tube flues	x	x	x	x	x	x	x	x	x	x		
2.4 Reinforce fire tube flues	x	x	x	x	x	x	x	x	x	x		
2.5 Reinforce fire tube flues	x	x	x	x	x	x	x	x	x	x		
2.6 Add flue end cap	x	x	x	x	x	x	x	x	x	x		
2.7 Add flue end cap	x	x	x	x	x	x	x	x	x	x		
2.8 Add flue end cap	x	x	x	x	x	x	x	x	x	x		
2.9 Reinforce flue ends	x	x	x	x	x	x	x	x	x	x		
2.10 Add automatic cleaning	x	x	x	x	x	x	x	x	x	x		
2.11 Add automatic cleaning	x	x	x	x	x	x	x	x	x	x		
2.12 Add flue end caps	x	x	x	x	x	x	x	x	x	x		
2.13 Reinforce flue ends	x	x	x	x	x	x	x	x	x	x		
2.14 Add automatic cleaning	x	x	x	x	x	x	x	x	x	x		
2.15 Reinforce flue ends	x	x	x	x	x	x	x	x	x	x		
2.16 Reinforce flue ends	x	x	x	x	x	x	x	x	x	x		

Table IV-C Improvements

Improvements	
Turbine:	Increase lap ratio to raise turbine efficiency from mid-50's to design point of 62%; requires no R&D.
Pitot Pump:	Increase efficiency by reducing drag, recirculation losses and housing effects through examination of variables experimentally.
Regenerator:	Lower effectiveness of Set 2 compared to Set 1 hypothesized due to sidewall leakage; design to eliminate.
Heater:	Lower η of Set 2 compared to Set 1 hypothesized due to manufacturing QC; improve and go to fin-tube design.
Performance Expectations	
Output Power	
At $\eta_t = .58$.35-.65 KW (net)
Plus reduced heat loss	.38-.68
Plus design regenerator effectiveness	.60-.85
Plus design pitot pump efficiency	1.1-1.43
Plus design heater efficiency	1.2-1.57
Plus increased fuel flow	>1.5 KW (net)
System thermal efficiency (based on HHV)	10.4-13.9%
Output power improvement would also be achieved in a variety of other ways including reduced parasitics, improved rectifier efficiency and increased generator performance.	

SECTION V
DESCRIPTION

V. DESCRIPTION

A general description is presented, followed by a description of how Set No. 2 differs from Set No. 1.

The Set uses a supercritical closed loop organic Rankine cycle with CP-25 as the working fluid. Figure V-1 shows a working fluid flow schematic and corresponding TS diagram.

The general overall mechanical arrangement of the Set is shown in Figure V-2 with some of the details in Figure V-3. All of the components are mounted to a common support plate which is shock mounted from the main support structure. The condenser regenerator, battery/instrument compartment, and condenser fan are located in the upper portion of the unit. The rest of the components are located in the lower section.

Protection of the unit from rough handling is provided by a tubular frame surrounding the unit. For further protection, including environmental conditions, covering and weather cap are provided. The weather cap is aluminum with a layer of sound absorption material bonded to the inner side. The upper cover is a fiberglass shroud while the lower covering consists of five panels of an aluminum/rubber honeycomb composite. These materials provide protection as well as reduce emitted noise.

Easy access to all interface points is provided though the Set is tightly packaged. Both the burner exhaust and cooling air flow merge in the unit and exit through the opening between the upper portion of the shroud and the weather cap. When operating in an enclosure where warm air exhaust is to be used as space heat, the burner exhaust can be separately ducted away.

Access to the riserator interface points is provided through the hinged front door. This area exposes the hand crank, hand pump, manual valves, fuel reservoir and fuel filter. The battery door is also hinged for access and battery replacement. Electrical and fuel hook-up points are accessible externally since these connectors protrude thru the recesses in the side panels. For maintenance purposes, all panels may be removed using a screwdriver.

A system schematic of Set No. 1 is shown in Figure V-4, and Figure V-5 illustrates the schematic for Set No. 2 along with identification of instrumentation. Figure V-6 is a functional schematic of the working fluid portion of the system. It can be seen that for Set No. 2, the accumulators, a valve, the start pressure valve, a check valve, the hand pump and the air compressor solenoid valve have been eliminated. Instead of a pressurized accumulator start, a start pump is used which reduces the start complexity considerably. Table V-A is a weight summary of Set 2.

The controller of Set 2 is slightly different to that of Set 1 due to the component changes and development improvements as the following list indicates:

<u>Set 1</u>	<u>Set 2</u>
Fixed inverter	Purchased
Start pressure valve	Eliminated
Temperature ready circuit	Eliminated

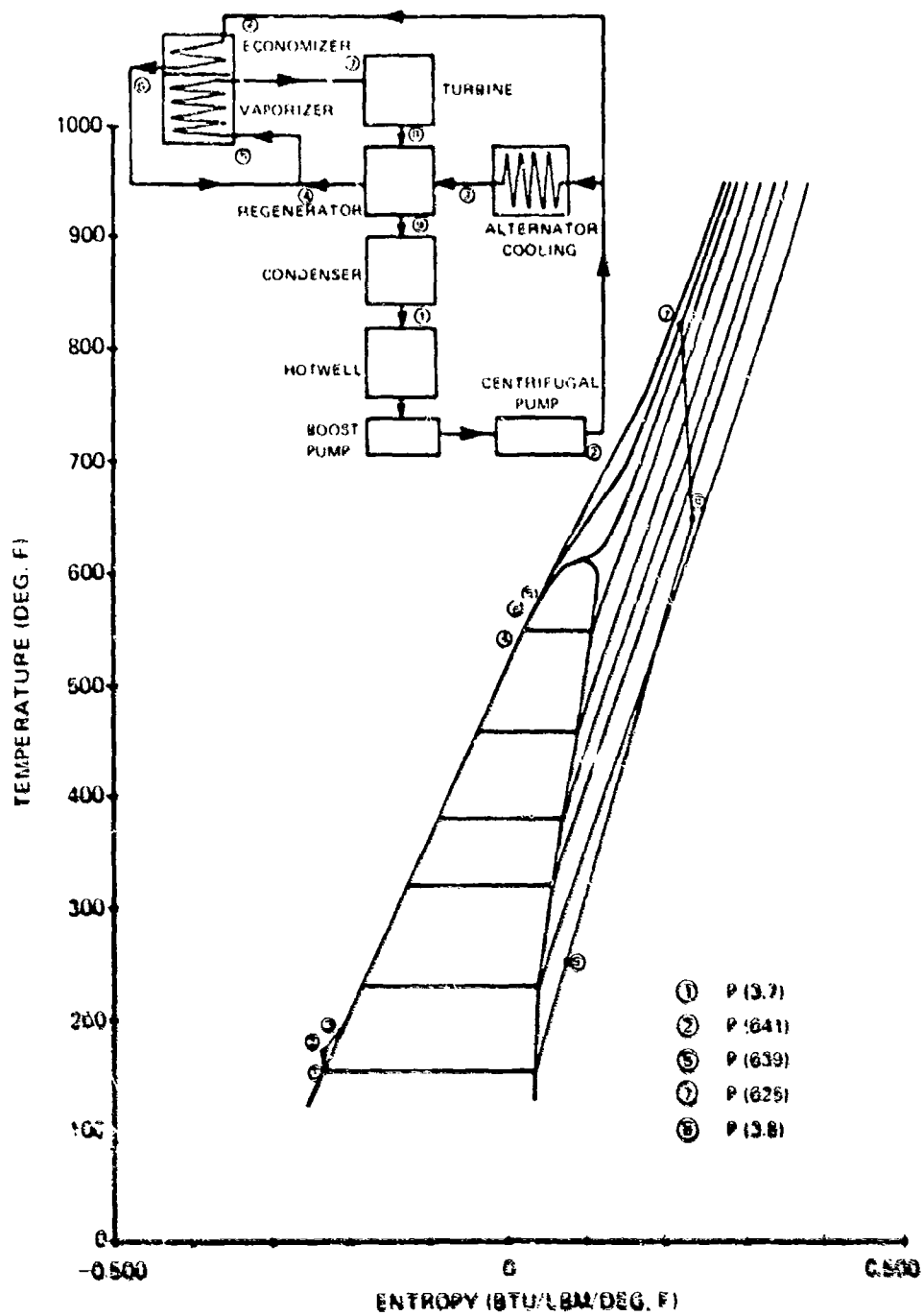
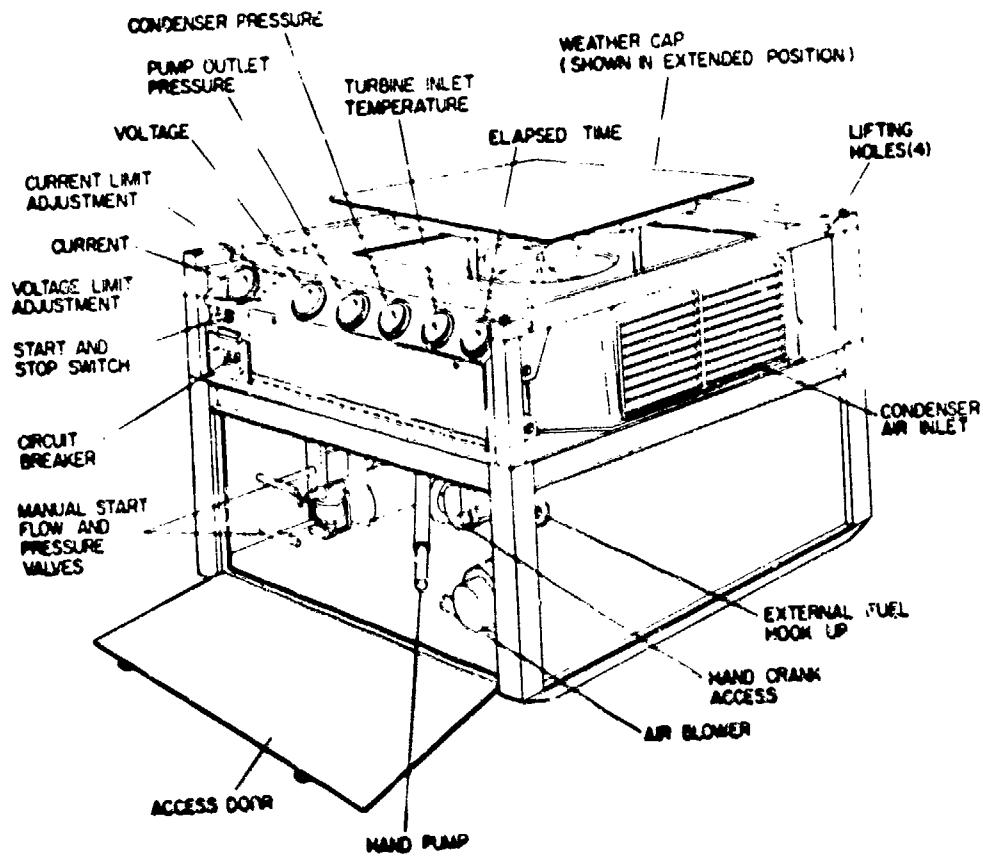


Figure V-1 Working Fluid Flow Schematic and T-S Diagram



A-6000

Figure V-2 Power Plant

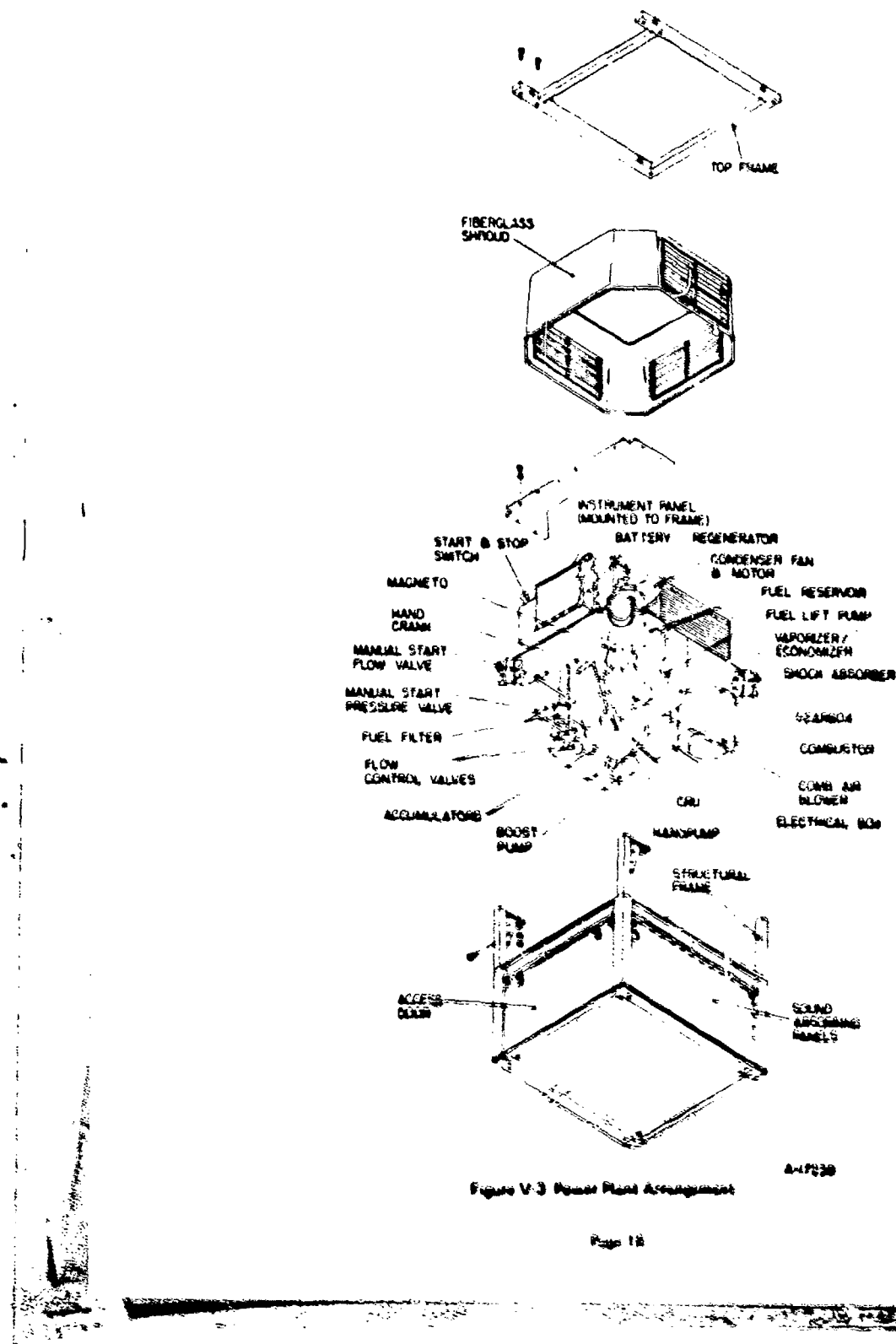
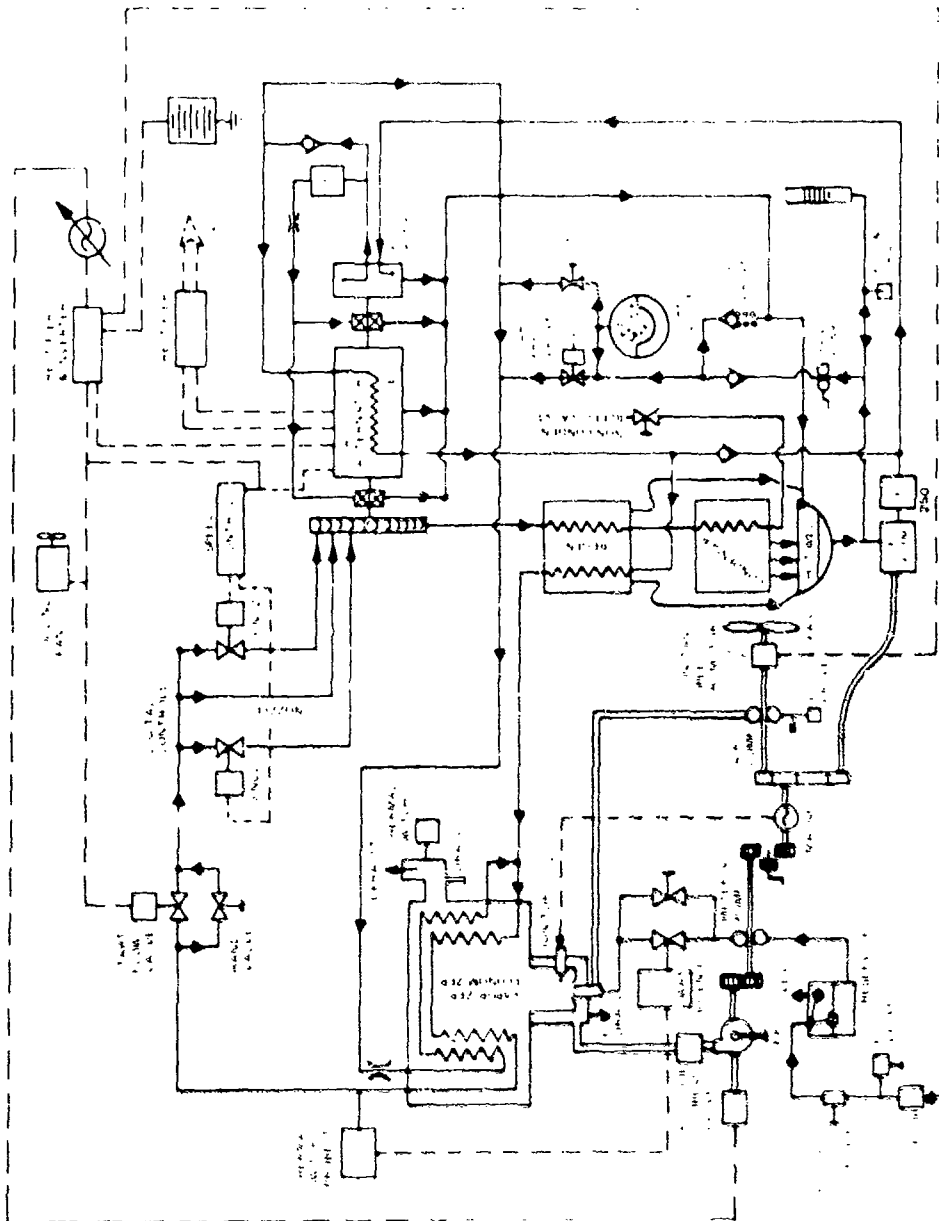


Figure V-3 Power Plant Arrangement

Page 18

Figure V.4. Set 1 System Schematic



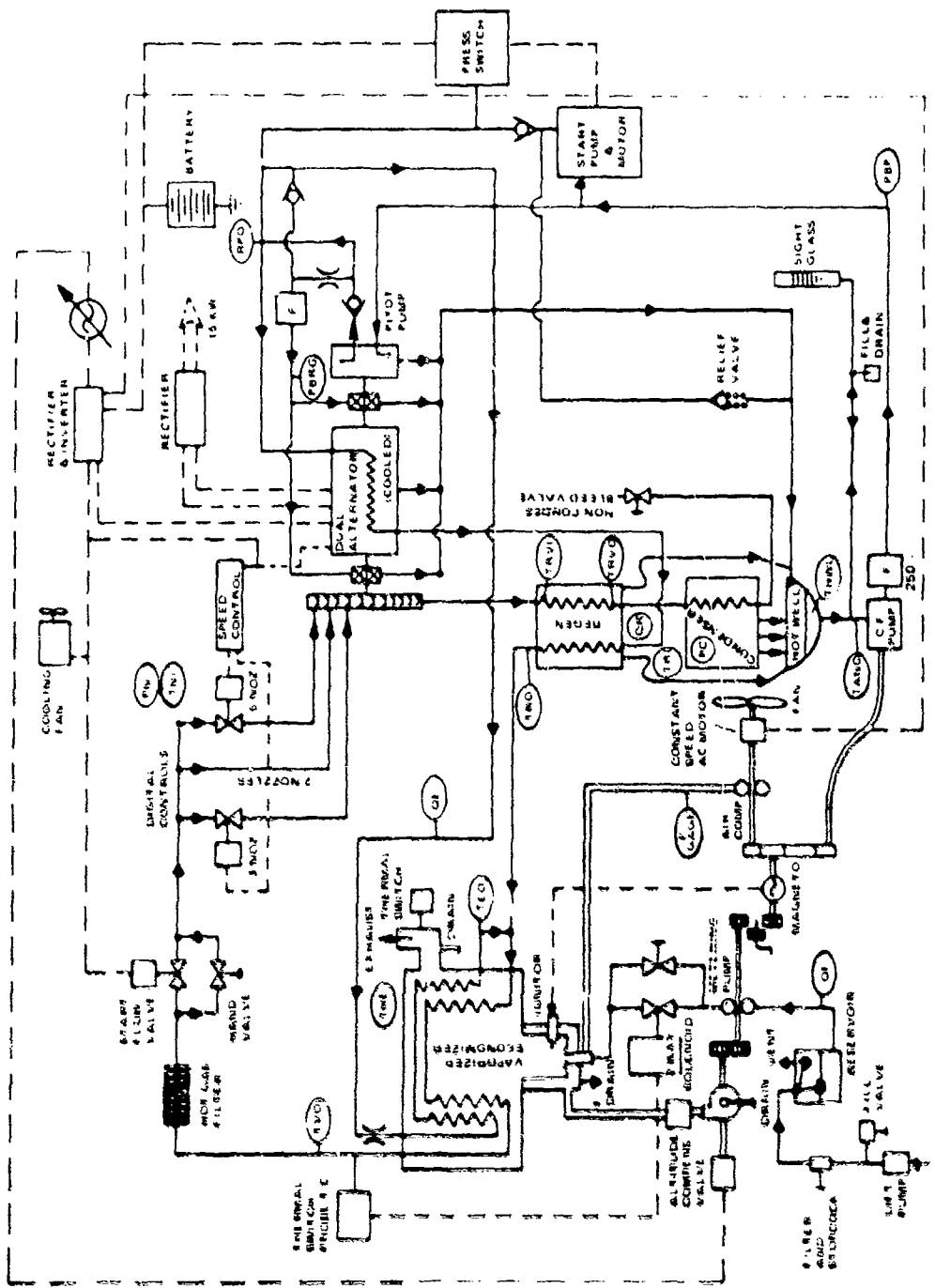


Figure V-5 Sier 2 System Schematic

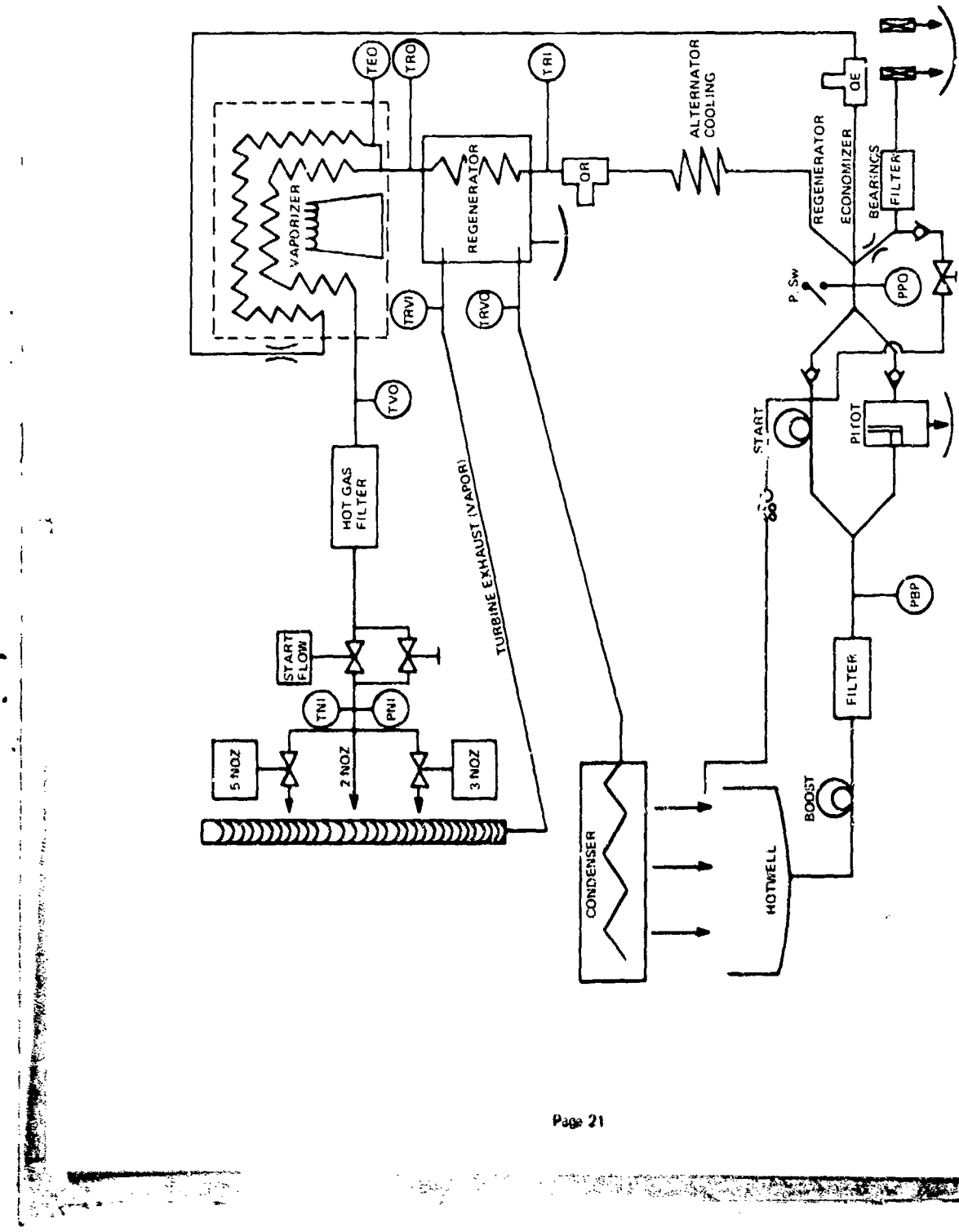


Figure V-6 1.5 KW MERRDC Functional Schematic

Table V-A Set 2 Weight Summary

Combustor Extension + Sight Tube	3.450 lb.
Hot Gas Filter	1.450 lb.
Shutoff & Control Solenoid Valve (S.B. 1.264 ea.)	3.795 lb.
Boost Pump (Gear Type)	1.812 lb.
Boost Pump Inlet & Outlet Plumbing + Fittings	0.700 lb.
Constant Frequency Fan	0.063 lb.
Condenser Overpressure Switch	0.512 lb.
Start Pump (.700), Motor (5.013), Coupling (3.000*)	0.713 lb.
Shutoff Hot Gas & Fill Hand Valves (1.000 ea.)	2.000 lb.
Battery and Gage Box	2.870 lb.
N-C Battery (9.637), Retainer (.250)	9.887 lb.
Constant Frequency Motor	6.575 lb.
Controller + Cover	9.188 lb.
Lift Pump, Fuel Sol. Valve, Bracket	2.000 lb.
Variable Frequency Blower, Motor, Mount Assy.	5.437 lb.
Magneto + Cable	3.000 lb.
Atomizing Air Compressor	2.938 lb.
Fuel Reservoir	0.563 lb.
Altitude Compensating Valve	0.375 lb.
Gages (.563 ea.)	3.380 lb.
Turbine-to-Regenerator Bellows	0.188 lb.
Combustor	1.250 lb.
Fuel Metering Pump, Coupling, Screws	0.300 lb.
Condenser Assy.	12.375 lb.
Fiberglass Cover (6.938), Weather Cap (2.500)	9.438 lb.
Regenerator	7.750 lb.
Panels (4 Sides + Bottom)	6.750 lb.
Heater	32.000 lb.
Accessory Gearbox (Lower)	5.100 lb.
Offset Gearbox (Upper*)	1.625 lb.
CRU (Noz. Plt. = 11.1, Aft Cover = 6.11, Bal. Assy. = 17.3	34.510 lb.
Frame, Shocks, Mount Plate	26.900 lb.
Miscellaneous*	2.706 lb.
 Total Dry Weight	209.600 lb.
 Total Wet Weight (2.4 lb. CP-25*)	212.000 lb.

* Estimates; all others are measured weights

Controller cooling fan	Eliminated
Solenoid air compressor valve	Eliminated
Accumulator underpressure	Eliminated
Eliminated	Start pump pressure switch
Eliminated	Start pump soft start circuit

The fixed inverter was purchased for Set 2 and mounted outside the controller, consequently, the cooling fan was eliminated due to lower controller heating. For the pump assisted start, the temperature ready, accumulator underpressure and the start pressure valve circuits were not necessary. The combustor was determined to operate satisfactorily at low fire without reduction in air compressor pressure, consequently, the solenoid valve was eliminated. A pressure switch was added to shut off the start pump after the pitot pump takes over. For startup, to prevent overriding the start pump magnetic drive, a soft start circuit was also added.

SECTION VI
COMPONENT DEVELOPMENT

VI. COMPONENT DEVELOPMENT

Development tests were performed on the constant frequency motor to reduce parasitic power, the noise output of the accessory components, the boost pump to improve cavitation sensitive characteristics, the pitot pump to develop a cheaper manufacturing process, the control valves to provide more reliable operation, and the CRU to develop a higher efficiency, more vibration free and less noise producing assembly.

Following is a discussion of each of these development items:

CONSTANT FREQUENCY MOTOR

The constant frequency circuit consists of motor, inverter, gearbox, cover, magneto, boost pump, air compressor and condenser fan. It was predicted to draw 210 watts and measured to be 360 watts. Without the cover, the power consumption was 346 watts, and the largest difference between this and predicted was due to the 1 phase motor being 43% efficient. A 3 phase motor and inverter were designed. The test data is shown in Figures VI-1 and VI-2. In the operating region, the motor runs at 65% efficiency for an input power requirement of 270 watts.

When compared to the 1 phase motor/inverter, a power savings of about 76 watts is achieved and a start relay and capacitor are eliminated.

NOISE

The noise level of Set No. 1 was excessive. This was largely due to the vibration of the turbine rotating assembly inducing resonances in the hotwell fore and aft shells in which it is mounted. A variety of tests were conducted (at MERDC) using Set No. 1 as a test bed to separate out the excessive from the non-excessive noise producing components so that an improvement could be made with Set No. 2.

Audible noise spectrum data was taken with the constant frequency motor and associated accessories operating and then with the turbine and variable frequency circuit running. This data is shown in Figure VI-3, the analysis of which is summarized below:

GEARBOX NOISE

CALCULATING FREQUENCIES:

- (1) All fundamental constant speed motor gear mesh frequencies are about 3507.7 Hz, and the sum of gear mesh frequencies are about 7015.4 Hz.
- (2) The magnetomotive force wave frequencies from the electric motor are 1556.5 Hz, 1686.5 Hz, and 1826.5 Hz.
- (3) Line frequency and its first harmonics are 60 Hz and 120 Hz.
- (4) Rotor unbalance frequency is 57.5 Hz.

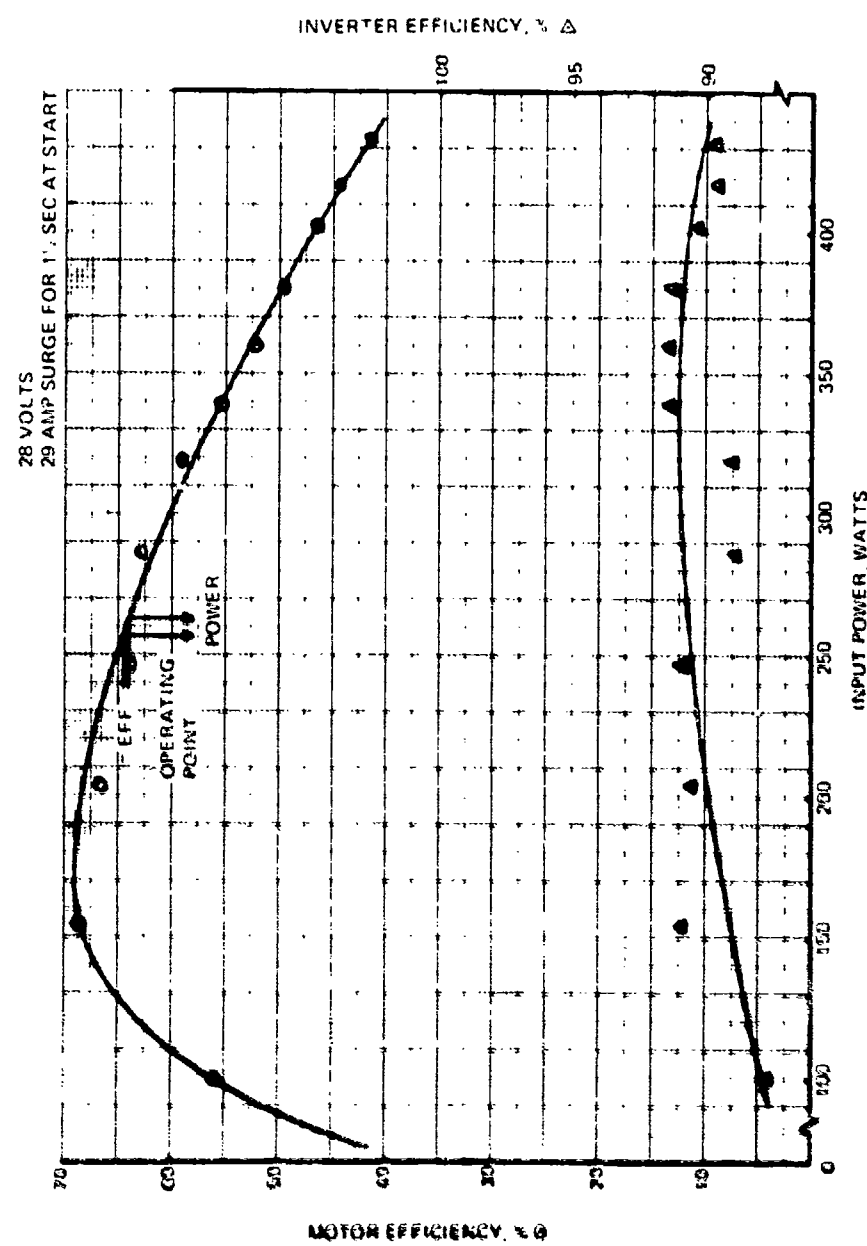


Figure VI-1-3 - Phase Motor

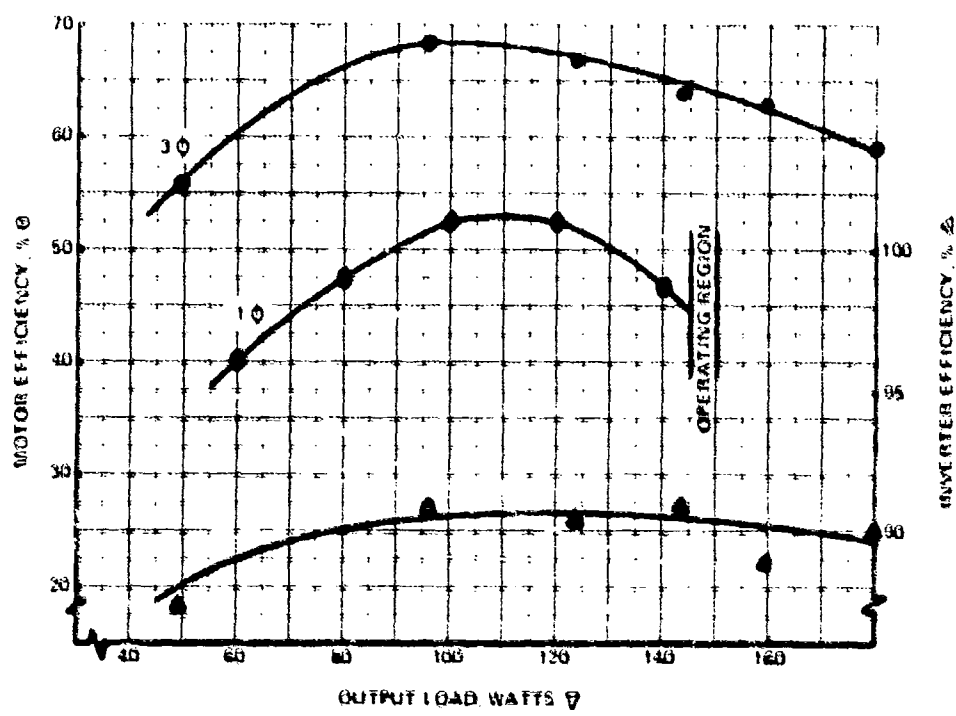
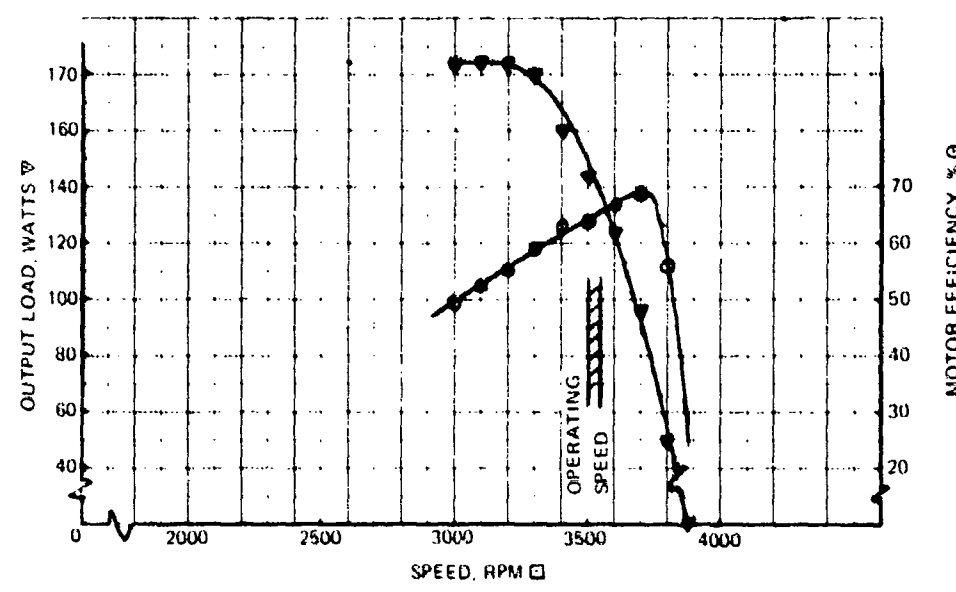


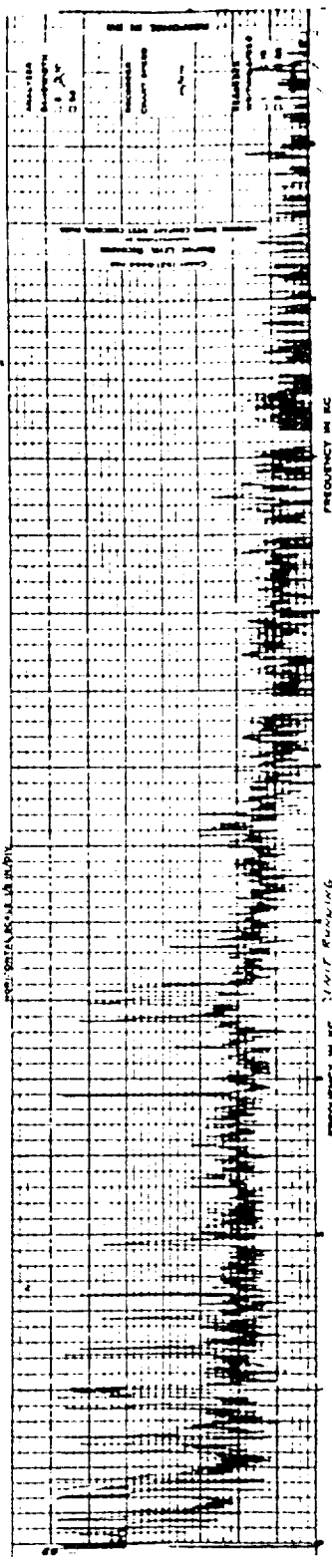
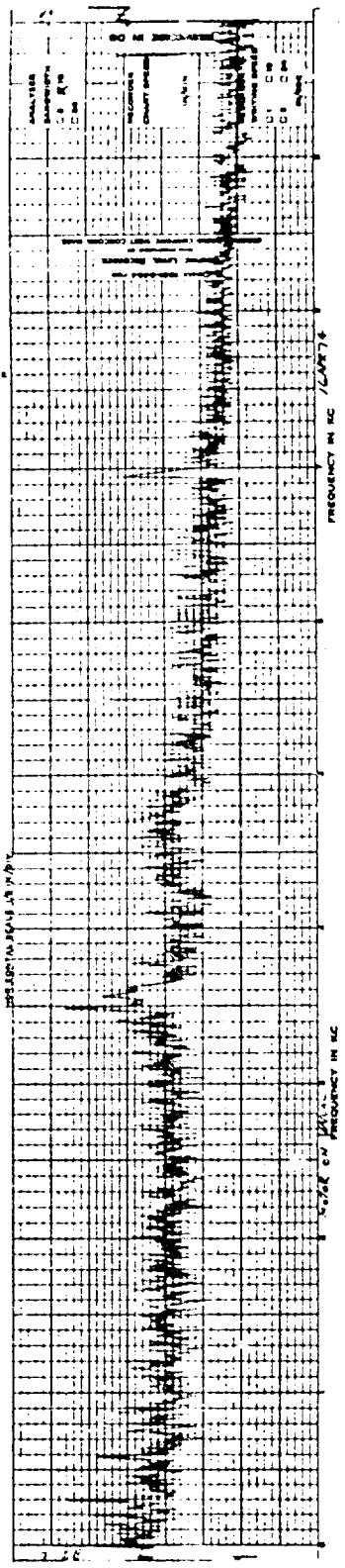
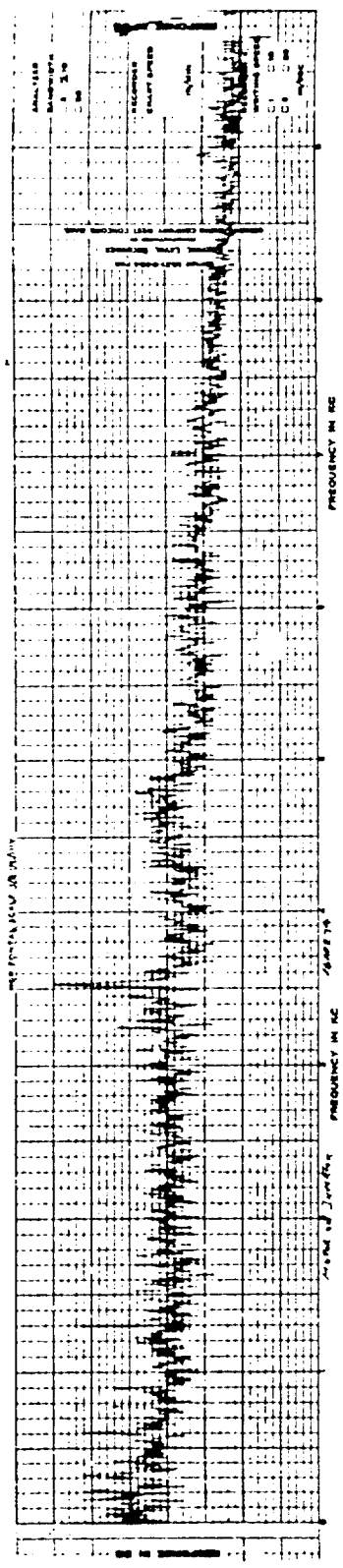
Figure VI-2-3 - Power Motor Performance

AUDIBLE NOISES SPECTRUM ANALYSIS

הנִזְקָנָה בְּבֵית־הַמִּלְחָמָה

卷之三

intercepted lecture in one section or two hours in another section.



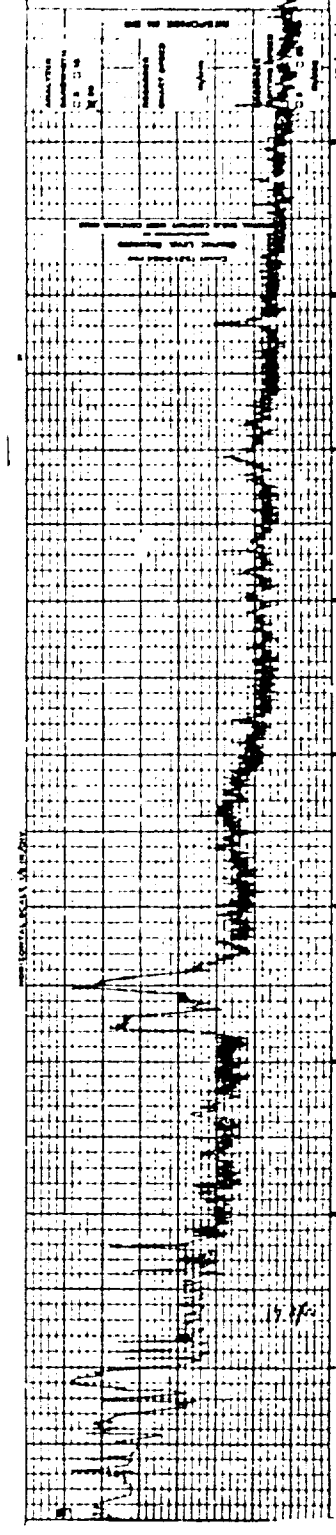
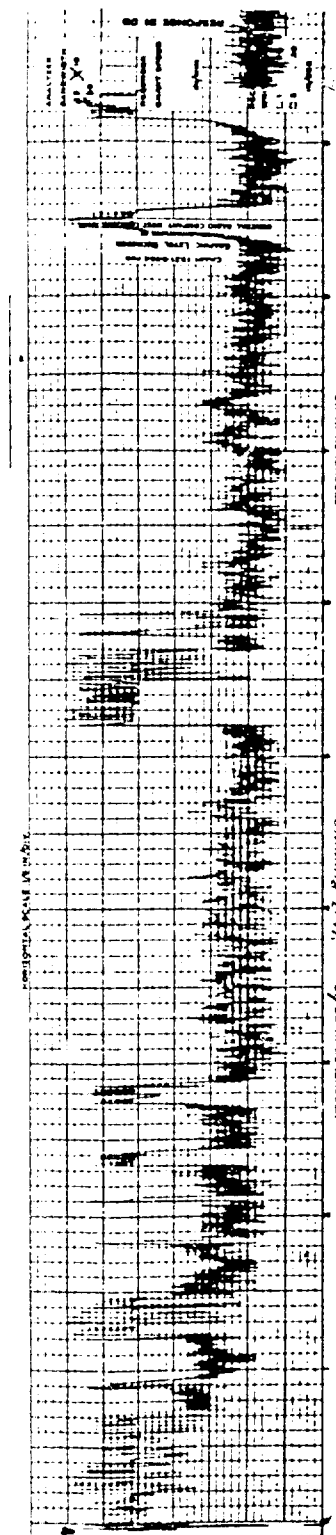
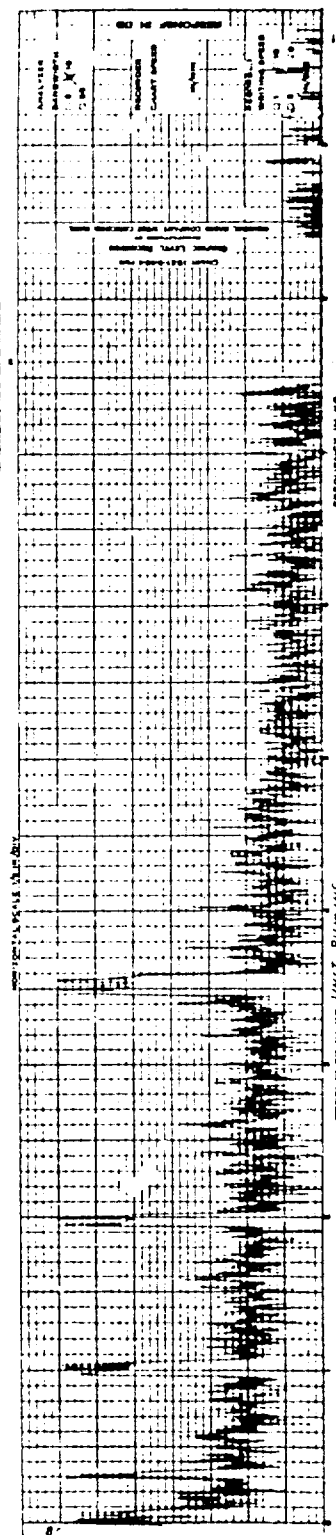
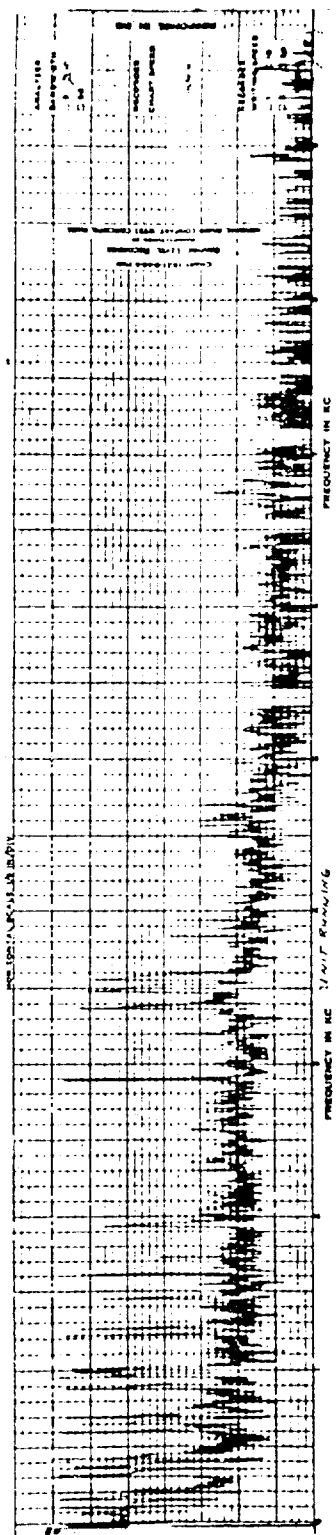
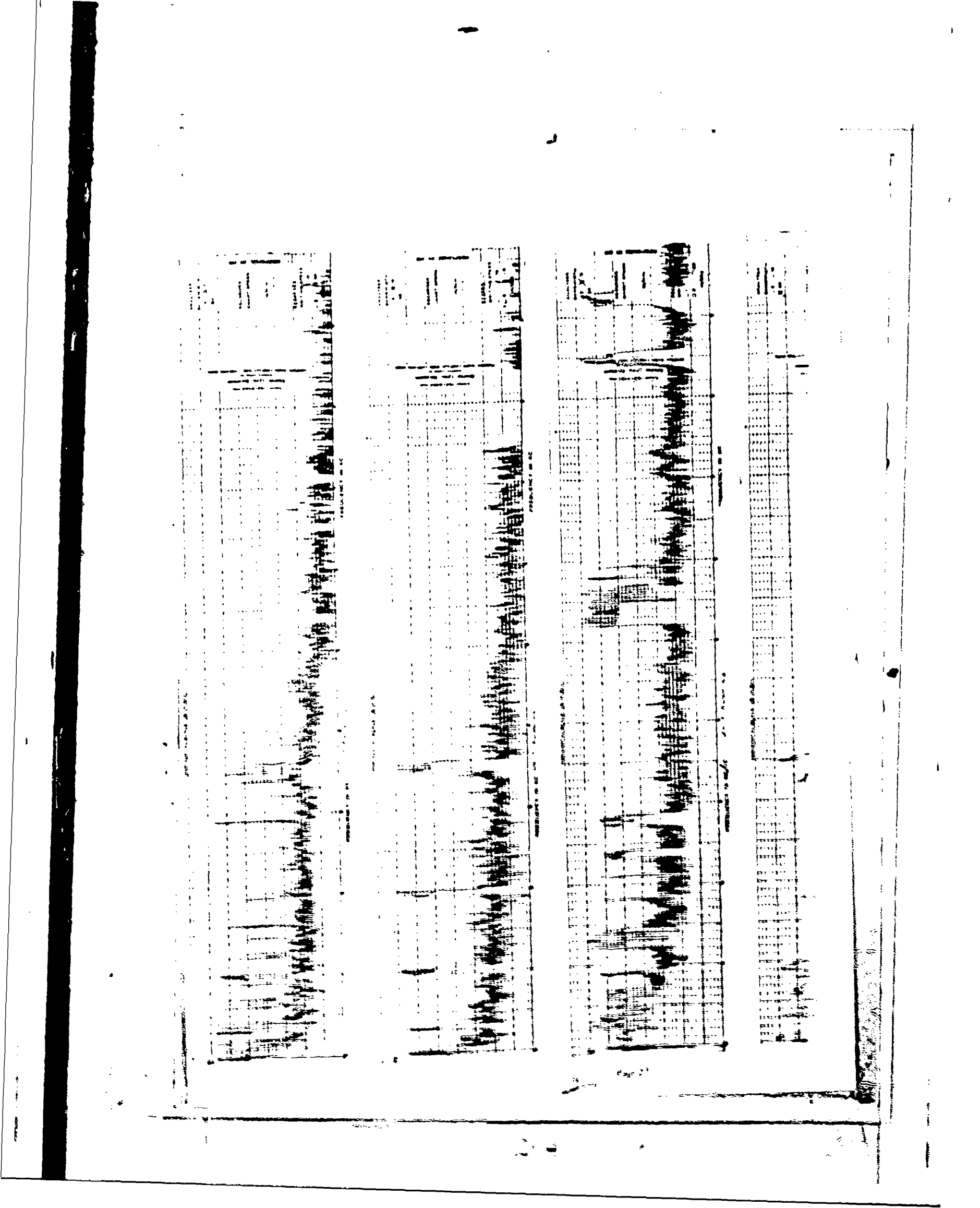
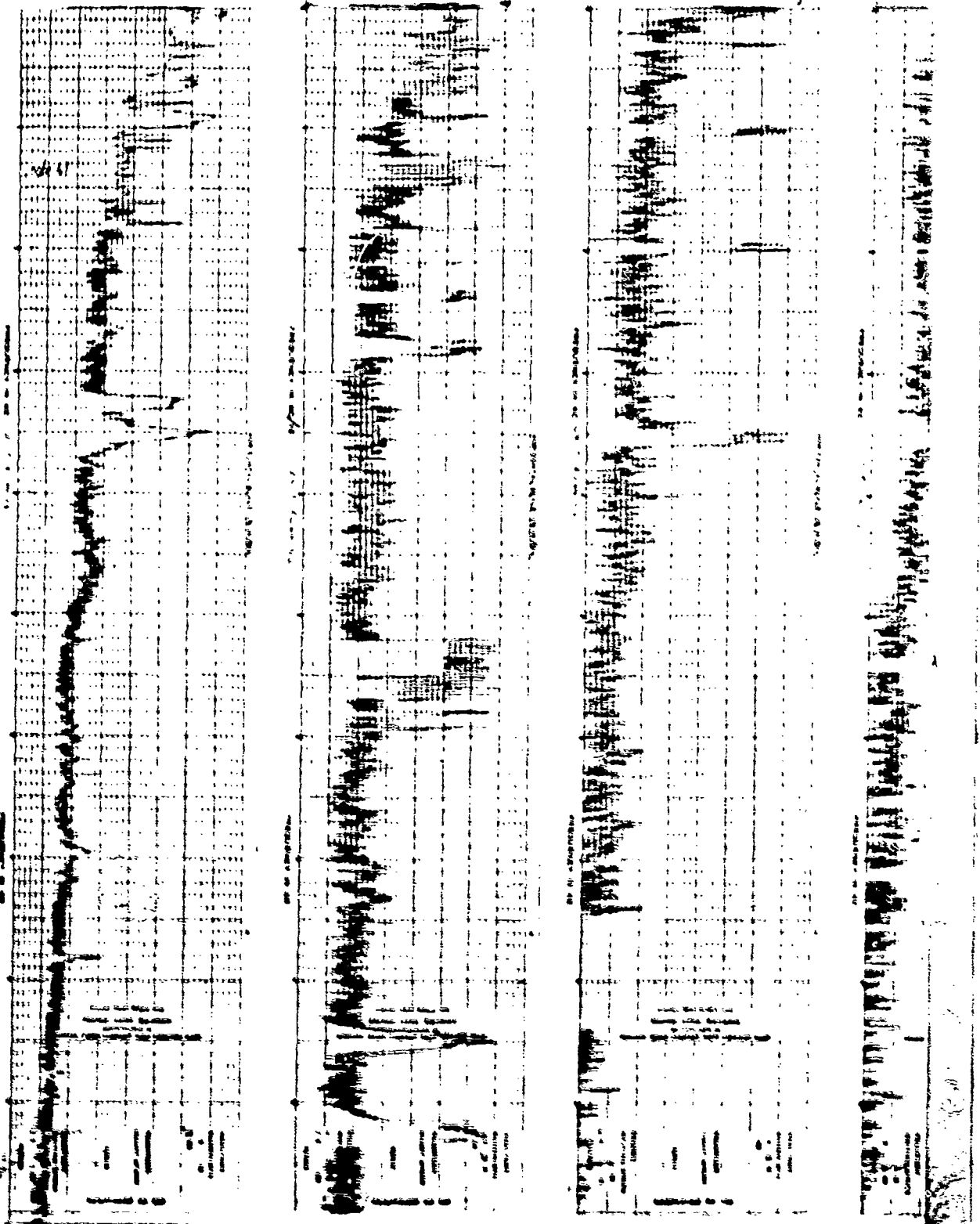


Figure VI-3 Audible Noise Spectrum Analysis

1940-1941
1941-1942
1942-1943
1943-1944
1944-1945
1945-1946
1946-1947
1947-1948
1948-1949
1949-1950
1950-1951
1951-1952
1952-1953
1953-1954
1954-1955
1955-1956
1956-1957
1957-1958
1958-1959
1959-1960
1960-1961
1961-1962
1962-1963
1963-1964
1964-1965
1965-1966
1966-1967
1967-1968
1968-1969
1969-1970
1970-1971
1971-1972
1972-1973
1973-1974
1974-1975
1975-1976
1976-1977
1977-1978
1978-1979
1979-1980
1980-1981
1981-1982
1982-1983
1983-1984
1984-1985
1985-1986
1986-1987
1987-1988
1988-1989
1989-1990
1990-1991
1991-1992
1992-1993
1993-1994
1994-1995
1995-1996
1996-1997
1997-1998
1998-1999
1999-2000
2000-2001
2001-2002
2002-2003
2003-2004
2004-2005
2005-2006
2006-2007
2007-2008
2008-2009
2009-2010
2010-2011
2011-2012
2012-2013
2013-2014
2014-2015
2015-2016
2016-2017
2017-2018
2018-2019
2019-2020
2020-2021
2021-2022
2022-2023
2023-2024
2024-2025
2025-2026
2026-2027
2027-2028
2028-2029
2029-2030
2030-2031
2031-2032
2032-2033
2033-2034
2034-2035
2035-2036
2036-2037
2037-2038
2038-2039
2039-2040
2040-2041
2041-2042
2042-2043
2043-2044
2044-2045
2045-2046
2046-2047
2047-2048
2048-2049
2049-2050
2050-2051
2051-2052
2052-2053
2053-2054
2054-2055
2055-2056
2056-2057
2057-2058
2058-2059
2059-2060
2060-2061
2061-2062
2062-2063
2063-2064
2064-2065
2065-2066
2066-2067
2067-2068
2068-2069
2069-2070
2070-2071
2071-2072
2072-2073
2073-2074
2074-2075
2075-2076
2076-2077
2077-2078
2078-2079
2079-2080
2080-2081
2081-2082
2082-2083
2083-2084
2084-2085
2085-2086
2086-2087
2087-2088
2088-2089
2089-2090
2090-2091
2091-2092
2092-2093
2093-2094
2094-2095
2095-2096
2096-2097
2097-2098
2098-2099
2099-20100





3

FIVE MOST PROMINENT FREQUENCIES FROM BEARINGS ARE LISTED BELOW:

- (5) Irregularity of a rolling element or the case = 23 Hz.
- (6) Fundamental rotational frequency of unbalance or eccentricity = 57.5 Hz.
- (7) Ball spin frequency = 110.4 Hz; 220.8 Hz.
- (8) Rough spot on inner race frequency = 310.5 Hz.
- (9) Rough spot on outer race frequency = 207 Hz.

NOISE FREQUENCIES IDENTIFICATION FROM TEST DATA:

Five frequencies with high noise level in two sets of noise spectrum were identified and shown in the following table.

From these data, it is evident that the gear meshes caused the major noise in the motor gear system. A redesign of the gear train should substantially reduce the total gear motor noise.

Inverter Drive	Variac Drive	Cause Associated with Frequencies
3510 (80 d.B.)	3490 (76 d.B.)	(1) Gear Mesh (4 gears at the same frequency).
200 (72 d.B.)	200 (69 d.B.)	(9) Rough Spot on Outer Race
310 (72 d.B.)	300 (76 d.B.)	(8) Rough Spot on Inner Race
600 (72 d.B.)	590 (68 d.B.)	(9) First Harmonics
160 (72 d.B.)	130 (66 d.B.)	(3) (4) (6) (7)

IMPROVEMENTS IN GEAR NOISE REDUCTION:

- (1) Helical types have the advantage of maintaining more than two teeth in contact during operation. Because of this, it is possible to get as much as 12 d.B.A. reduction in noise by using them instead of spur gears.
- (2) The finest possible pitch should be selected for the given load condition. This increases the amount of tooth overlap; the higher tooth overlap produces a smoother transfer of load, reducing dynamic oscillation of the gear mesh. This also will produce a higher mesh frequency; however, higher frequencies are easier to damp and easier to isolate than low frequencies.
- (3) The lowest possible pressure angle also can make gears tend to be quieter, because the transverse overlap ratio is higher.
- (4) For only one direction gear drive, recess-action gears can provide a further reduction in noise.
- (5) Gear noise at the mesh can be reduced by designing so that the total overlap ratio is an integral number of teeth. (Tests have shown that if the ratio is exactly 2.0, the smoothest transfer of load is obtained.)
- (6) Higher AGMA quality level (12 or better) gives smooth operation.
- (7) A non-integral gear ratio should be selected to prevent a tooth on the pinion from contacting periodically the same teeth on the mating gear.

Based upon these results, alternative offset (constant frequency) gearbox designs were made. Simultaneously, accelerometers were attached to selected locations on Set No. 1 and tested as follows:

<u>Channel</u>	<u>Location</u>	<u>Test Condition</u>
1	Aft CRU can, longitudinal	Constant f motor running
1	Right front frame, vertical	Constant f motor running
4	Aft CRU can, vertical	Constant f motor running
5	Mount plate, vertical	Constant f motor running
6	Offset gearbox, vertical	Constant f motor running
1	Aft CRU can, longitudinal	Turbine running
6	Mounting plate, vertical	Turbine running
4	Aft CRU can, vertical	Turbine running

Figures VI 4, 5, 6 and 7 are representative plots of this data. Its analysis is summarized below:

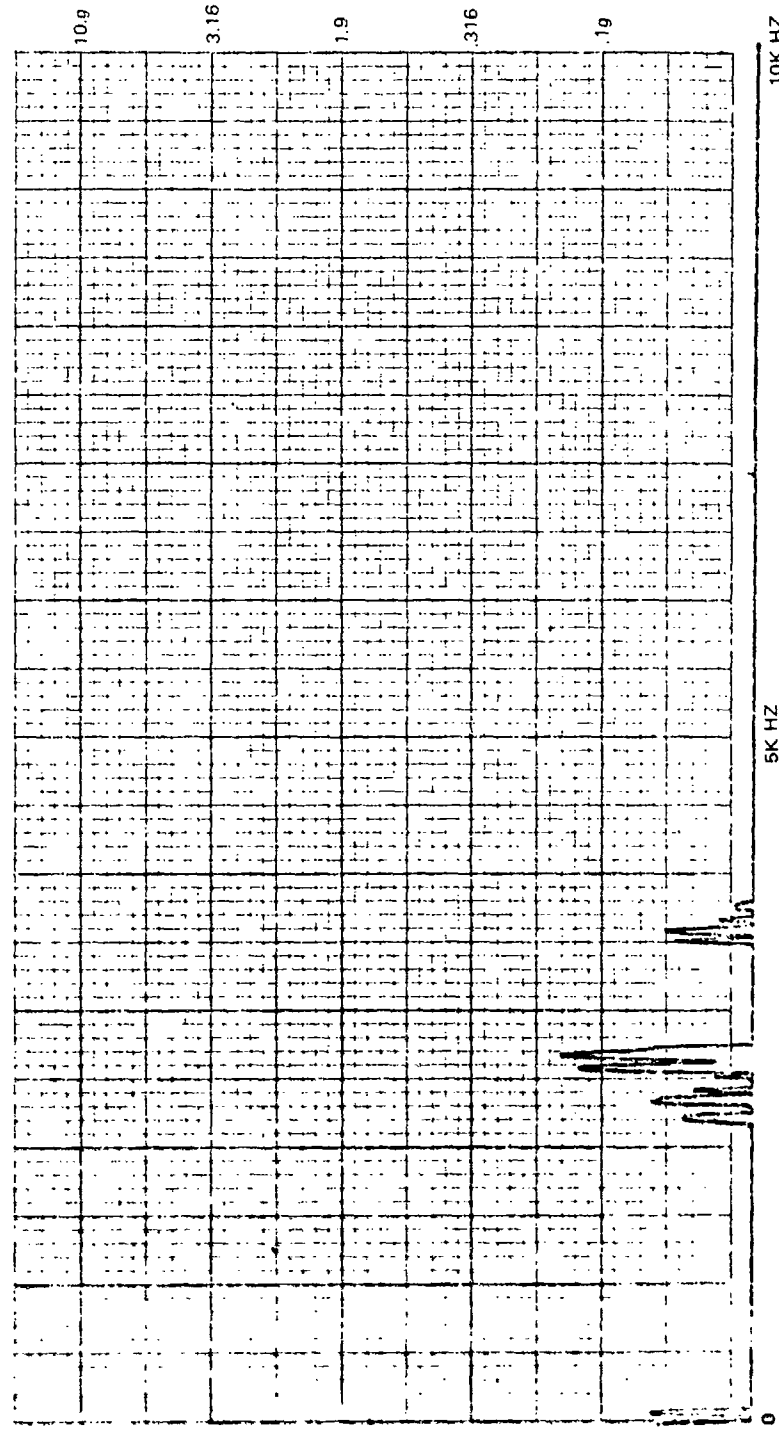


Figure VI-4 Channel No. 1 AFT CAN Longitudinal Constant Speed Motor Running

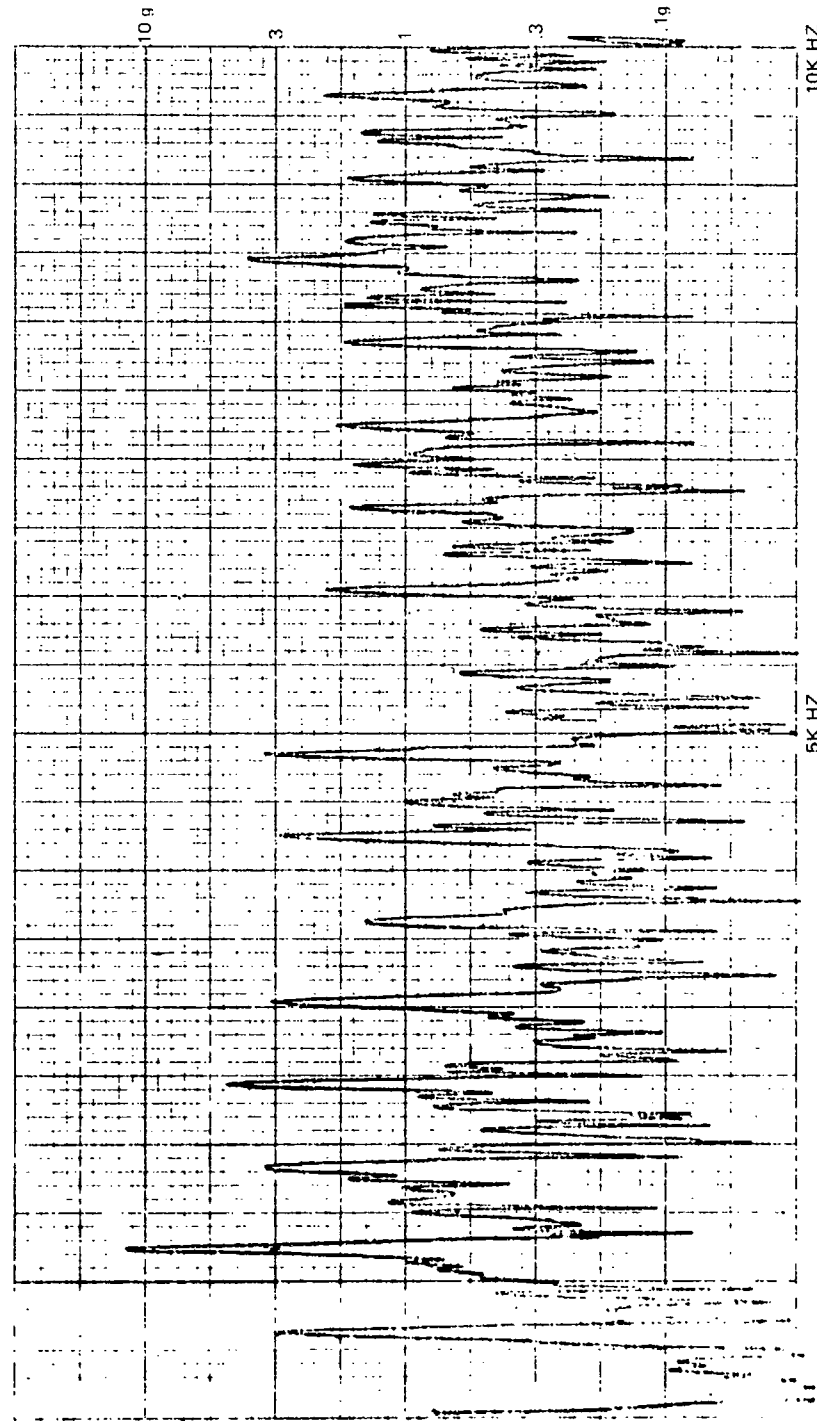


Figure VI-5 Channel No. 1 AFT CAN longitudinal Turbine Running

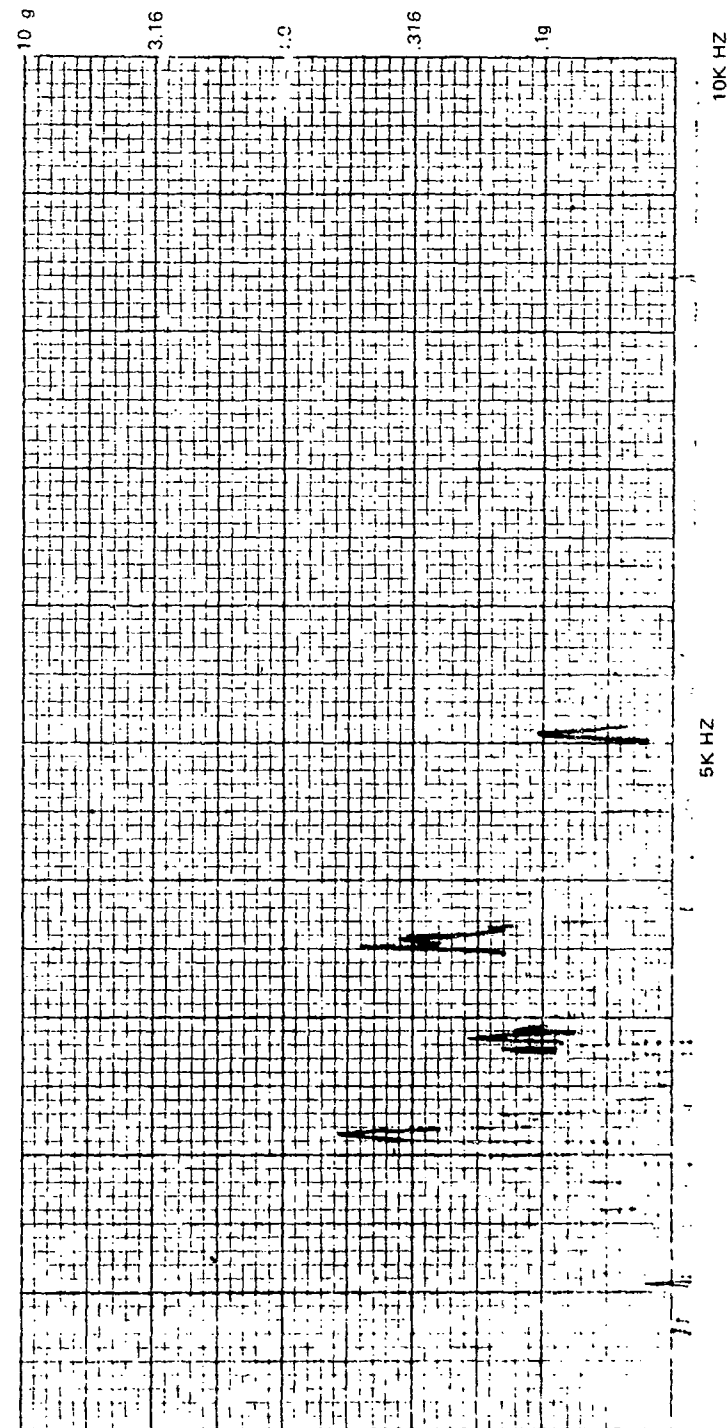
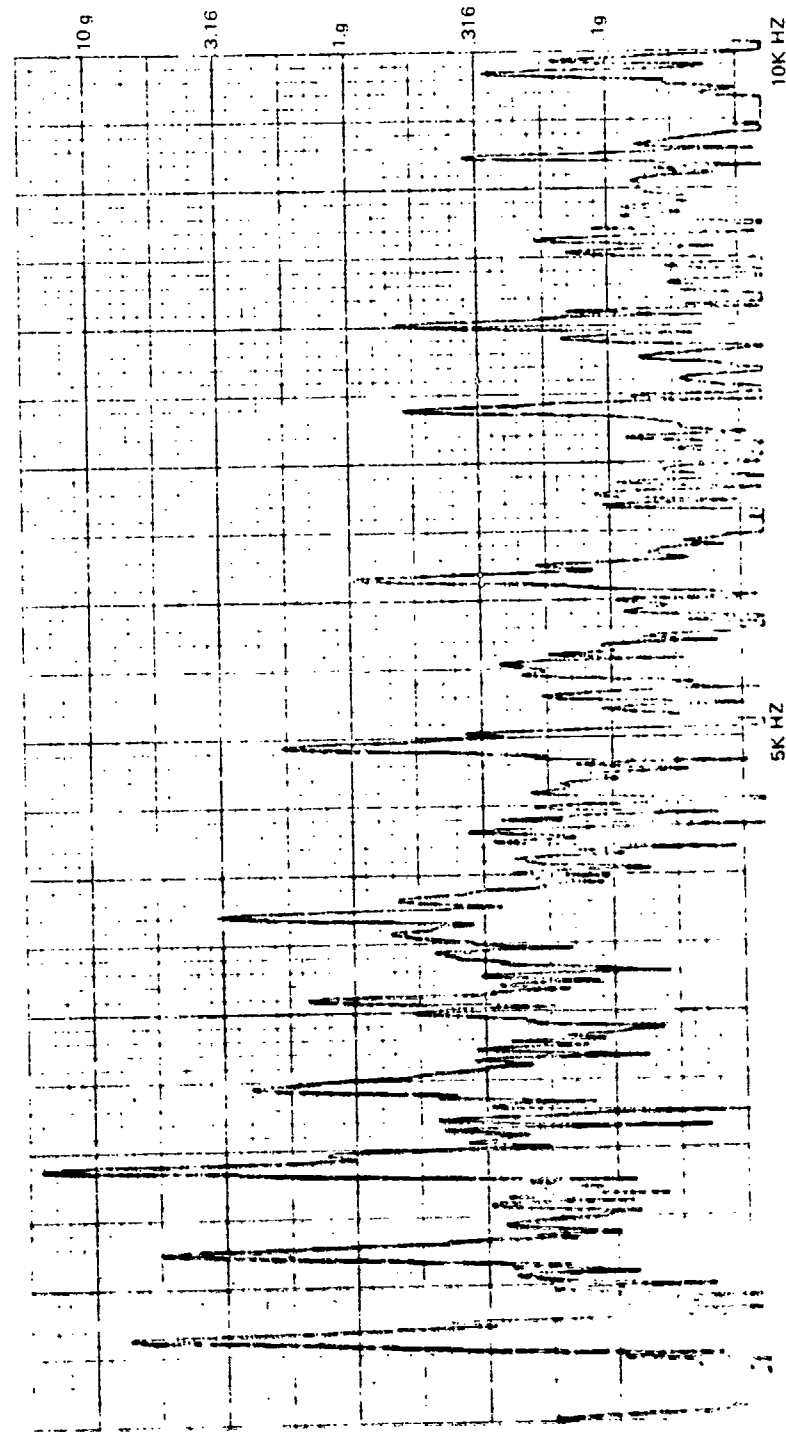


Figure VI-6 Channel No. 5 Mounting Plate Vertical Constant Speed Motor Running



Page 33

Figure VI-7 Channel No. 5 Mounting Plate Vertical Turbine Running

CPU NOISE

CALCULATING FREQUENCIES:

- (1) Roto/unbalance frequency = 625 Hz (37,500 RPM).
- (2) Element train passage or cage frequency = 260 Hz.
- (3) Ball spin and waviness frequency = 1247 Hz, 2494 Hz, 3741 Hz, and 4988 Hz.
- (4) Rough spot on inner race frequency = 3287 Hz.
- (5) Rough spot on outer race frequency = 2340 Hz.
- (6) Variable contact compliance vibration frequency = 2340 Hz, 4680 Hz, and 7020 Hz.
- (7) Flexural vibration of the outer ring caused by inner ring waviness of lower order = 1250 Hz, 1875 Hz, 2500 Hz, 3125 Hz, and 3750 Hz.

FREQUENCIES IDENTIFICATION:

Vibration data of Channel No. 5 was used to identify vibratory mechanisms. The following table shows the result.

<u>Frequency (Hz)</u>	<u>"G" Level</u>	<u>Cause Associated with Frequencies</u>
620	7.4	(1)
1250	5.5	(3) (7)
1870	17.0	(7)
2450	2.5	(3) (7)
3100	1.5	(7)
3720	3.1	(3) (7)
4940	1.9	(3) (7)

DISCUSSION:

- A) From these data, it is evident that the rotor unbalance, ball waviness, and inner ring waviness of different orders caused the major vibration in this rotor-bearing system.
- B) The blade passing frequency is above the data cut-off ($>10K$ Hz).
- C) Random type vibration is negligible.

IMPROVEMENTS:

- A) Better rotor balance (flexural rotor balance may be needed) gives smooth operation.
- B) An increase in the number of balls results in a reduced vibration level generated from ring and balls waviness. For example, the change of nine balls to eleven balls could reduce the correlative vibration level by 10%.

- C) Axial load and alignment of the bearing should be carefully designed and checked; the loose balls passing the unload zone or insufficient land height creates additional vibration.

It should be noted that this data was taken with the turbine operating at 37,500 RPM. Based upon these test results, the following changes were implemented to the CRU to reduce imbalance induced vibrations:

<u>Type Nozzle</u>	<u>Forward Can</u>	<u>Aft Can</u>	<u>Bending Criticals</u>
EP2559-1228 Used on Set 1	Stainless Steel .032 thick	Aluminum .032 thick	32 Krpm, pump hsg. 48 Krpm, no pump
EP2559-1228A Used on Set 2	Stainless Steel .075 thick	Stainless Steel .075 thick	65 Krpm, pump hsg. both ends

It should be noted that the noise emitted from Set 1 is significantly greater than the specification. The major contributor is the CRU noise. The changes that were implemented for Set 2 were based upon analysis of the data from Set 1 and were limited to those items that could be readily implemented to qualitatively reduce noise. A significant reduction in the component noise levels have been made. When performance testing Set 2, no measurements of noise level were made. To the naked ear, the noise level of Set 2 has been reduced significantly over that of Set 1. Although improved, the CRU hotwell shell still appears to be acting as an amplifier such that the Set is not sufficiently quiet to meet the specification. The improvements need to be carried further to reduce noise to an acceptable level.

Since the hotwell shell was responding to the rotating assembly imbalance, a significant reduction in the amount of imbalance would also help to reduce noise. Consideration was given to both improved low speed balancing and balancing at speed. For Set 2, the low speed (~2000 rpm) balancing was improved from 0.002 to 0.0002 in-oz imbalance. Though not employed, further improvement would be made by balancing at speed at this sensitivity.

OFFSET GEARBOX

Four gearbox design approaches were considered as presented in Table VI-A. The Berg sprocket belt driven gearbox is shown as an example in Figure VI-8. Each gearbox was installed in Set No. 1 and tested with a microphone located at the center of the condenser louvers 3 foot from the Set on each side. The following data are attached:

Table VI-B Gear and Belt Data

Figure VI-9 Gear and Belt dBt Plot (worst case)

Table VI-C Belt Data

Figure VI-10 Belt dBt Plot (worst case)

Table VI-D Berg Data

Figure VI-11 Berg dBt Plot (worst case)

Table VI-A Gearbox Design Approaches

Type	Gear	No. Teeth	Pitch dia.	Speed (rpm)
Spur (Set 1)	1	61	1.906	3450
	2	42	1.312	5010
	3	46	1.437	4575
	4	75	2.344	2806
Belt Drive	1	18	1.375	3450
	2	12	.764	5117
	4	22	1.401	2820
Berg Drive	1	22	1.162	3450
	2	15	.812	5057
	4	28	1.462	2710
Helical	1	85	1.906	3450
	2	60	1.348	4887
	3	66	1.480	4443
	4	105	2.358	2792

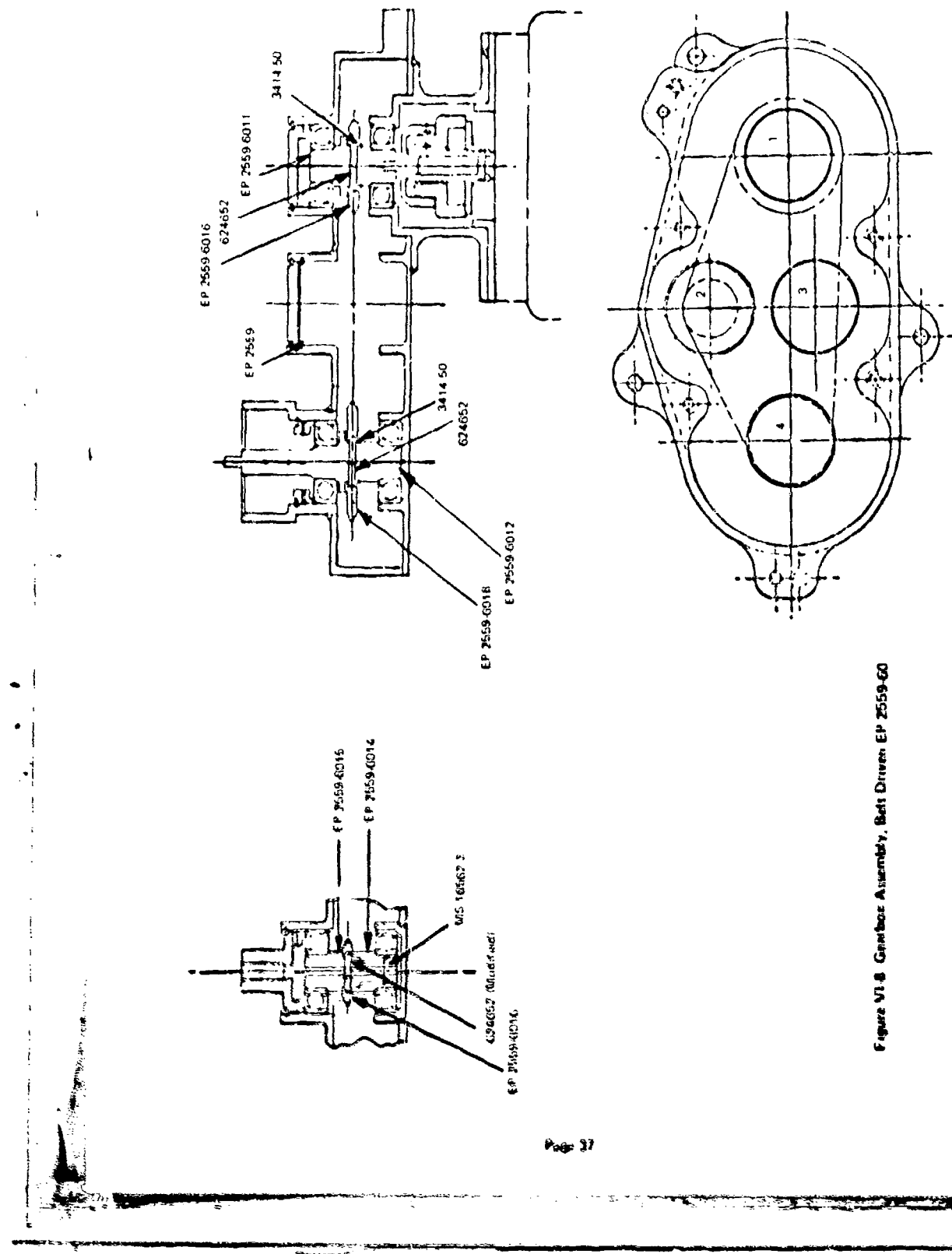
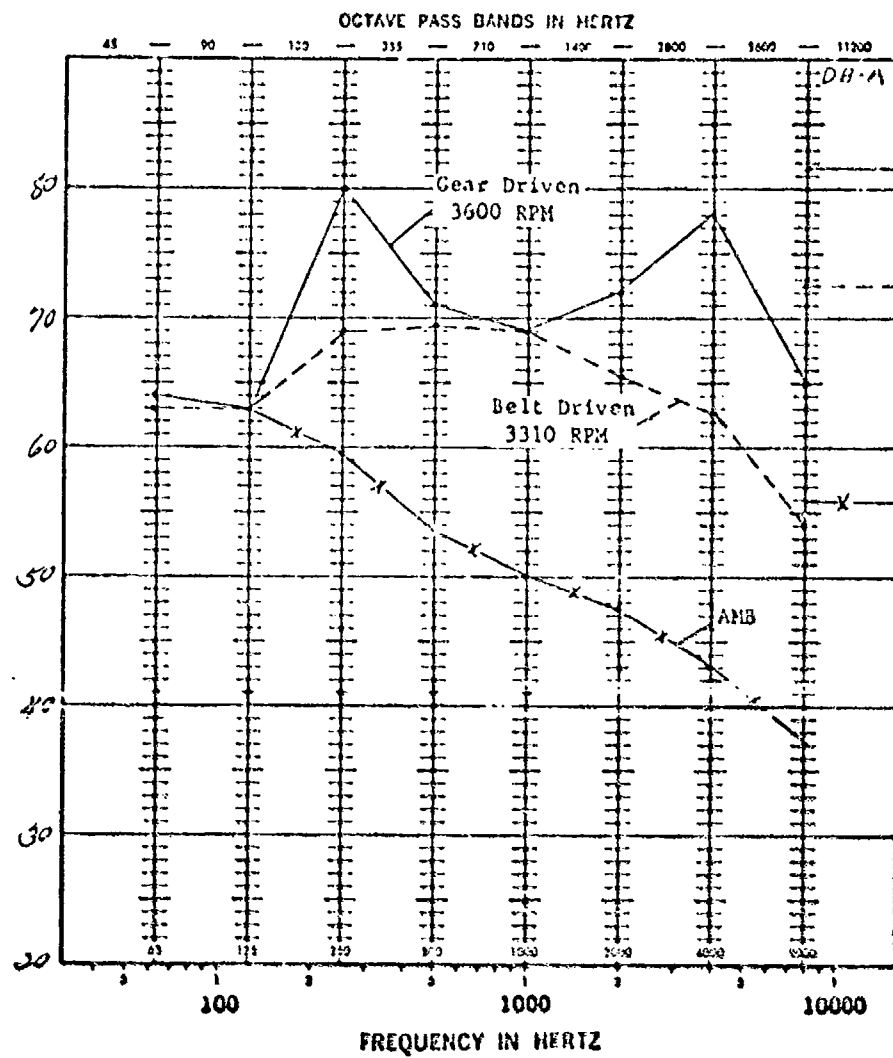


Figure VI-8 Grindstone Assembly. Bed: Diorite EP 2559-60

Tables VI-8, Gear and Spurit Data

TEST AND EVALUATION DIVISION		TEST NO.	
U. S. ARMY MOBILITY EQUIPMENT RESEARCH AND		SHEET	OF
DEVELOPMENT CENTER		DATE	668 AUG 74
FORT BELVOIR, VIRGINIA 22060		JOB NO.	T-74-32
AUDIO ACQ/SIG TEST		RECODER	JACKIE GUY
OCEANIC BAND SOUND PRESSURE LEVELS		OBSERVER	W. VAUTIER
DA RE C-662 MICROBAR			R. HILL
CONSTANT SPEED ACCESSORY DRIVE			
1. SKULL BARKING			
EFFECT			
AFGR. SIGN. - STRAND			
MODEL NO.			
SERIAL NO.			
P.R.F.			

EXHIBIT FORM 2B



Position #2
Back

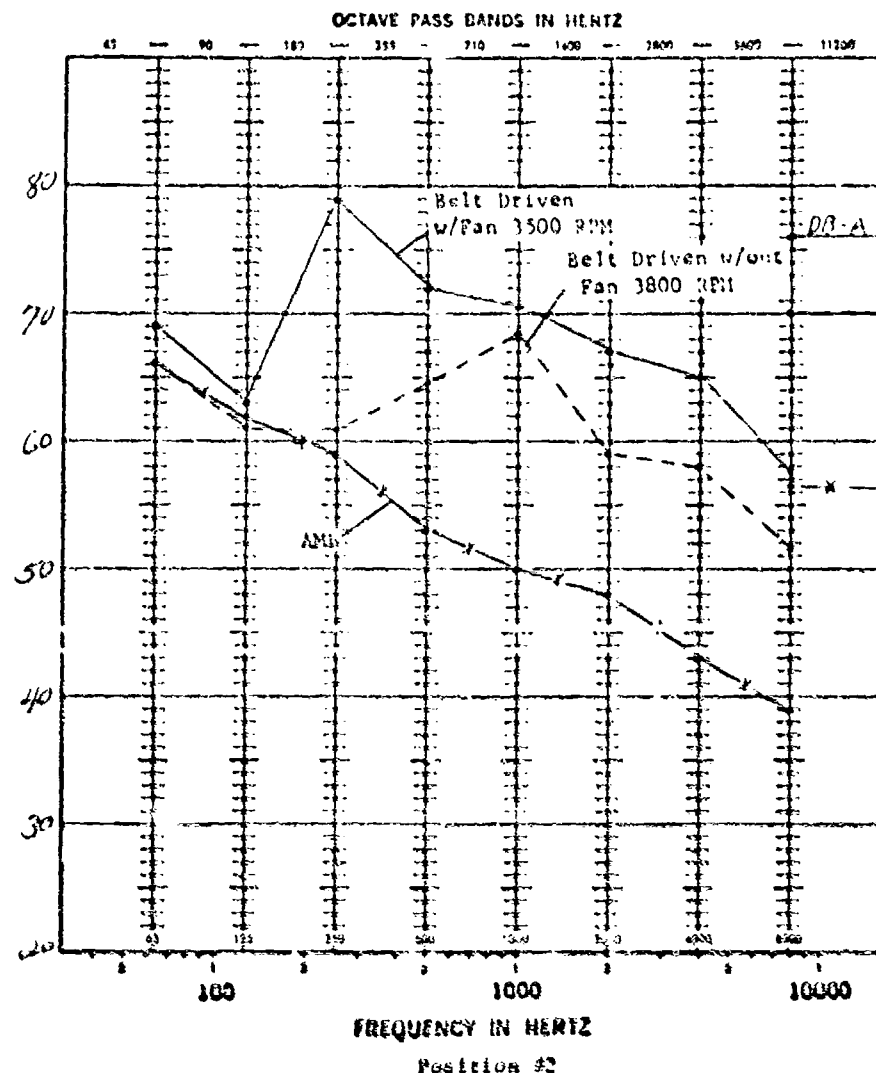
1.5 KW Rankine
Mfg. Sundstrand
Test Conducted:
6 & 8 Aug 74

Figure VI-9 Gear and Belt d-f Plot (Warts Case)

Table VI-C Bell Data

TEST AND EVALUATION DIVISION U. S. ARMY MOBILITY EQUIPMENT RESEARCH AND DEVELOPMENT CENTER FORT BELVOIR, VIRGINIA 22060		TEST NO. _____ SHEET _____ OF _____ DATE 14 JUN 72 JOB NO. T-21-39
TESTING DEVICE SC-42 PRESSURE LEVELS DR. R.C. C. MICHENER		RECORDER J. NICKELLS OBSERVER W. L. ALATOR
TEST	TEST NUMBER	MICROPHONE LOCATED CENTER LINE AT 1 FOOT FROM TEST POINT
NUMBER	NUMBER	1 2 3 4 5 6 7 8 9 10 11 12 13 14 15 16 17
1	1	0.0 0.0 0.0 0.0 0.0 0.0 0.0 0.0 0.0 0.0 0.0 0.0 0.0 0.0 0.0 0.0 0.0
2	2	0.0 0.0 0.0 0.0 0.0 0.0 0.0 0.0 0.0 0.0 0.0 0.0 0.0 0.0 0.0 0.0 0.0
3	3	0.0 0.0 0.0 0.0 0.0 0.0 0.0 0.0 0.0 0.0 0.0 0.0 0.0 0.0 0.0 0.0 0.0
4	4	0.0 0.0 0.0 0.0 0.0 0.0 0.0 0.0 0.0 0.0 0.0 0.0 0.0 0.0 0.0 0.0 0.0
5	5	0.0 0.0 0.0 0.0 0.0 0.0 0.0 0.0 0.0 0.0 0.0 0.0 0.0 0.0 0.0 0.0 0.0
6	6	0.0 0.0 0.0 0.0 0.0 0.0 0.0 0.0 0.0 0.0 0.0 0.0 0.0 0.0 0.0 0.0 0.0
7	7	0.0 0.0 0.0 0.0 0.0 0.0 0.0 0.0 0.0 0.0 0.0 0.0 0.0 0.0 0.0 0.0 0.0
8	8	0.0 0.0 0.0 0.0 0.0 0.0 0.0 0.0 0.0 0.0 0.0 0.0 0.0 0.0 0.0 0.0 0.0
9	9	0.0 0.0 0.0 0.0 0.0 0.0 0.0 0.0 0.0 0.0 0.0 0.0 0.0 0.0 0.0 0.0 0.0
10	10	0.0 0.0 0.0 0.0 0.0 0.0 0.0 0.0 0.0 0.0 0.0 0.0 0.0 0.0 0.0 0.0 0.0
11	11	0.0 0.0 0.0 0.0 0.0 0.0 0.0 0.0 0.0 0.0 0.0 0.0 0.0 0.0 0.0 0.0 0.0
12	12	0.0 0.0 0.0 0.0 0.0 0.0 0.0 0.0 0.0 0.0 0.0 0.0 0.0 0.0 0.0 0.0 0.0
13	13	0.0 0.0 0.0 0.0 0.0 0.0 0.0 0.0 0.0 0.0 0.0 0.0 0.0 0.0 0.0 0.0 0.0
14	14	0.0 0.0 0.0 0.0 0.0 0.0 0.0 0.0 0.0 0.0 0.0 0.0 0.0 0.0 0.0 0.0 0.0
15	15	0.0 0.0 0.0 0.0 0.0 0.0 0.0 0.0 0.0 0.0 0.0 0.0 0.0 0.0 0.0 0.0 0.0
16	16	0.0 0.0 0.0 0.0 0.0 0.0 0.0 0.0 0.0 0.0 0.0 0.0 0.0 0.0 0.0 0.0 0.0
17	17	0.0 0.0 0.0 0.0 0.0 0.0 0.0 0.0 0.0 0.0 0.0 0.0 0.0 0.0 0.0 0.0 0.0
A-C	TEST 213 1222	1 2 3 4 5 6 7 8 9 10 11 12 13 14 15 16 17
B-A	TEST 223 1260 745 725	1 2 3 4 5 6 7 8 9 10 11 12 13 14 15 16 17

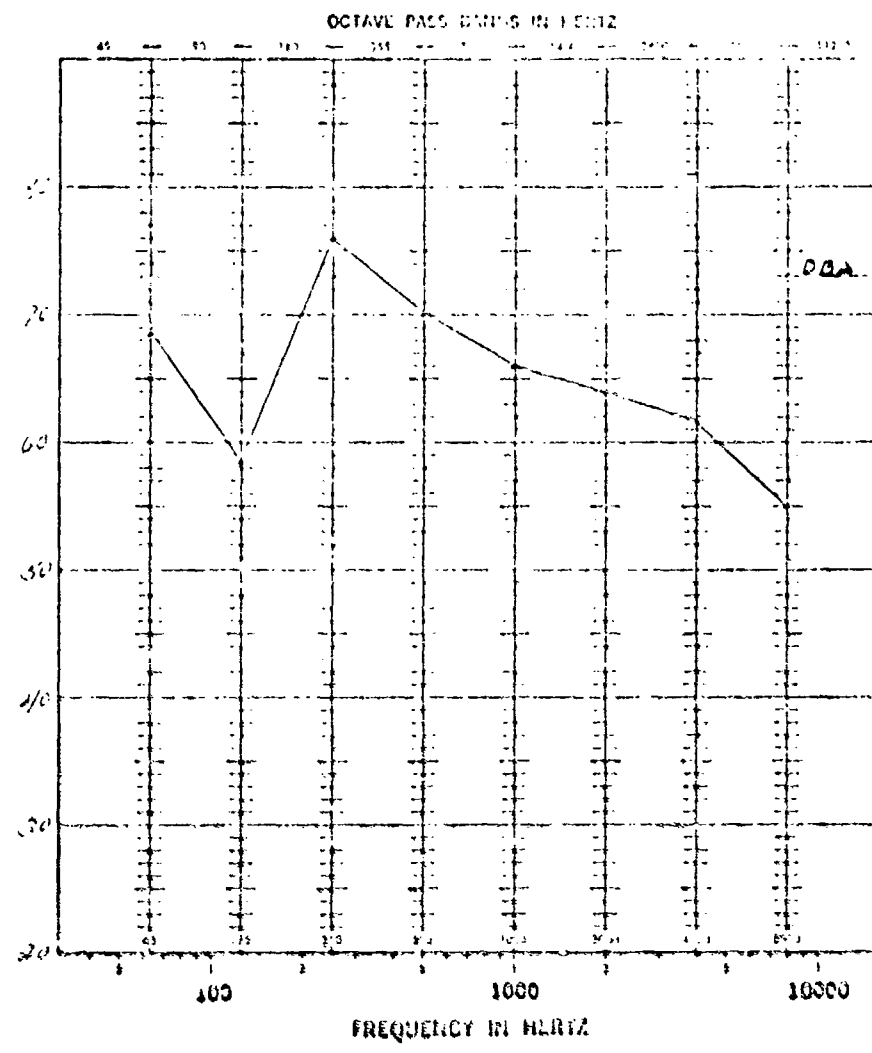
SFDP Form 28
16 Jun 72



1.5 KW Rankine
N.E.P. Subflood
Test conducted 14 Aug 74

Figure VI-16. Belt Drive Power (Waves Cured)

Table VI-D Test Data



Position : 4

Control Panel
1.5 KW Function
w/soft start
By Sanderson
Test Conducted
21 Oct 74

Figure VI-11 Borg-Chat Plot (Worst Case)

Table VI-E Helical Data

Figure VI-12 Helical db-f Plot (worst case)

From these tables and figures, Table VI-F (summary of the peak db for each location and ranked from (1) the quietest to (4) the noisiest), and Table VI-G (summary of the selection tradeoff), the selection of the Berg version was made. This gearbox is shown in Figure VI-13.

While limited noise data was taken on the variable speed gearbox, the levels were considerably lower than for any of the above. It is also buried in the lower compartment of the Set and no improvement in noise was attempted although, based upon the desirable results of the constant frequency offset gearbox, significant improvement could be made.

CRU (COMBINED ROTATING UNIT)

The redesigned CRU is shown in Figure VI-14. Because the turbine balance assembly is installed in the hotwell which is made of thin gauge material for minimal weight, it is capable of acute vibration. Simultaneous with the relocation of the pitot pump from the forward to aft end of the assembly, the turbine wheel overhang was reduced.

Critical speeds were determined by an analysis which includes the gyroscopic effects and the spring mounts (bearings) for any spin to whirl ratio. Also a normalized mode shape of the shaft deflection is given for each critical speed.

Utilizing a spin to whirl ratio of 1.0 (synchronous whirl) and bearing stiffnesses of 250,000 lb/in for each bearing, the first three critical speeds were calculated for seven configurations. Table VI-H shows critical speeds and mode shapes for each configuration.

In order to push the critical speeds out of the operating range either increasing the shaft thickness (new bearings) or decreasing the length of the overhang could be incorporated. If 0.2 inch is removed from the turbine overhang end and 0.25 inch removed from the pump overhang end, the critical speed is pushed up to 58,000 rpm (Configuration 6). With a titanium pump housing the critical speed is 63,000 rpm (Configuration 7).

Configuration 7 was selected with a slightly smaller pump overhang so that the bending critical speeds at both turbine and pump end are 65,000 rpm. This is 18% above the 55,000 rpm operating speed and is considered sufficient, though in the long run slightly more margin is desirable. The turboalternator is shown in Figure VI-15.

After this redesigned CRU was fabricated, a series of development tests were conducted using gaseous dry nitrogen as the test gas. With the redesigned nozzle plate (EP2659-1228A) in the as-received condition, stall torques were measured and compared to the original (Set No. 1) nozzle plate and the test plate (flat plate) used as a basis for establishing the nozzle spacing. This data is shown in Tables VI-I and VI-J which revealed poor performance. Consideration was given to possible manufacturing error so the drawing and hardware were examined for possible discrepancies, e.g., nozzle overlap, nozzle-blade gas impingement, nozzle profile, and blade-diffuser impingement. Multi-size layouts and shadowgraph tracings of the hardware were made which indicated that the new nozzle plate is dimensionally as accurate as the previous ones. One possible improvement would have been slightly greater nozzle-to-blade height lap ratio. A series of spin, flow, and acceleration tests were made; data shown in Table VI-K. The conclusion from this testing is that the as-received

Table VI-E Helical Data

ITEM		TEST AND EVALUATION DIVISION		TEST NO.		SHEET		OF	
I.S. KEY RANKING U/		U. S. ARMY MOBILITY EQUIPMENT RESEARCH AND DEVELOPMENT CENTER		DATE		17 OCT 74			
HEARCA G-GEAR B.C.E.		FORT BELVOIR, VIRGINIA 22060		JOB NO.		T-24 - 35			
MFGR. SUNDSTRAND		AUDIO NOISE TEST		RECORDER T. M. K. G. S.					
MODEL NO.		OCTAVE BAND SOUND PRESSURE LEVELS		OBSERVER R. L. J.					
SERIAL NO.		DB RE C. 000 2 MILICBAR							
REF:									
INST. ♦		TEST SITE: LAR AREA BLDG. 323 MICROPHONE LOCATED CENTER OF LOUDERS, LEFT-FRONT POSITION							
END									
TEST									
STAN.									
COC.									
OCOTAVE BAND									
CHARTS									
TEST									
NO.									
1									
2									
3									
4									
5									
6									
7									
8									
9									
10									
11									
12									
13									
14									
15									
16									
17									
NOTES:									

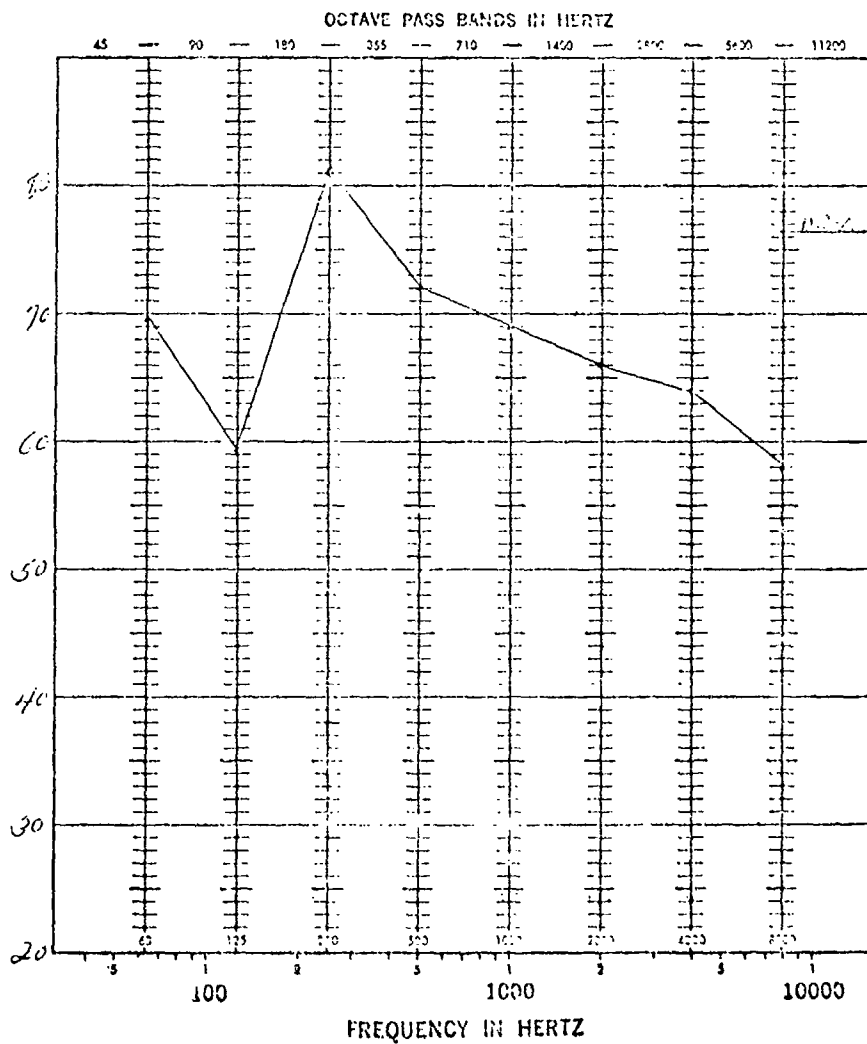


Figure VI-12 Helical db-f Plot (Worst Case)

Table VI-F Data Summary

Octave Center Hz		Right Side	Rear	Left Side	Control Panel	Avg.	Rank
63	Belt Drive	66.0	69.0	69.0	67.0	67.75	4
	Berg Drive	61.5	59.0	57.0	68.5	61.50	1
	Helical Gear	61.0	61.5	58.0	69.5	62.50	2
	Spur Gear	65.0	64.0	66.0	65.0	65.0	3
125	Belt Drive	63.0	63.0	63.0	64.0	63.25	3
	Berg Drive	60.5	60.5	60.0	58.5	59.875	1
	Helical Gear	60.0	61.5	61.5	59.5	60.625	2
	Spur Gear	63.0	63.0	64.0	63.0	63.25	3
250	Belt Drive	71.0	79.0	73.0	74.0	74.25	3
	Berg Drive	72.0	74.5	72.0	76.0	73.625	1
	Helical Gear	72.0	78.0	72.5	81.5	76.0	4
	Spur Gear	72.0	80.0	70.0	74.5	74.125	2
500	Belt Drive	70.0	72.0	70.0	68.0	70.0	2
	Berg Drive	70.5	71.0	71.0	70.0	70.625	3
	Helical Gear	71.0	72.0	72.0	72.0	71.75	4
	Spur Gear	69.0	71.0	68.5	67.5	69.0	1
1000	Belt Drive	68.0	70.5	69.5	67.0	68.75	2
	Berg Drive	69.5	70.0	69.0	66.0	68.625	1
	Helical Gear	70.5	72.0	70.0	69.0	70.375	3
	Spur Gear	67.5	69.0	70.5	68.0	68.75	2
2000	Belt Drive	64.0	67.0	67.0	64.0	65.5	1
	Berg Drive	67.0	68.0	66.5	64.0	66.375	2
	Helical Gear	70.5	71.0	69.0	66.0	69.125	3
	Spur Gear	72.0	72.0	71.5	67.0	70.625	4
4000	Belt Drive	62.0	65.0	66.0	62.5	63.875	1
	Berg Drive	64.5	66.5	65.0	61.5	64.375	2
	Helical Gear	67.5	69.0	67.0	64.0	66.875	3
	Spur Gear	82.0	78.0	74.5	71.0	76.375	4
8000	Belt Drive	54.5	57.5	58.0	55.0	56.25	1
	Berg Drive	58.5	60.5	58.5	55.0	58.2	2
	Helical Gear	61.0	63.0	61.0	58.0	60.75	3
	Spur Gear	63.5	65.0	65.0	61.0	63.625	4
A.P	Belt Drive	76.0	80.5	78.5	77.0	78.0	2
	Berg Drive	77.0	78.0	76.5	78.0	77.375	1
	Helical Gear	78.0	81.0	78.0	82.0	79.75	3
	Spur Gear	83.0	83.0	80.0	78.0	81.0	4
D.B.A	Belt Drive	72.0	76.0	74.5	72.5	73.75	1
	Berg Drive	74.0	75.5	74.0	73.0	74.125	2
	Helical Gear	76.0	78.0	75.5	76.5	76.5	3
	Spur Gear	83.0	81.5	78.5	75.0	79.5	4

Table VI-G Selection Tradeoff

<u>63-8000 Hz</u>	<u>Belt</u>	<u>Berg</u>	<u>Helical</u>	<u>Spur</u>
Times 1st	11	14	2	8
Times 2nd	11	12	10	2
Times 3rd	5	6	12	9
Times 4th	5	0	8	13
	32	32	32	32
<u>A-P</u>				
Times 1st	2	2	0	0
Times 2nd	1	2	1	1
Times 3rd	1	0	3	0
Times 4th	0	0	0	3
	4	4	4	4
<u>DB-A</u>				
Times 1st	2	2	0	0
Times 2nd	2	2	0	0
Times 3rd	0	0	3	1
Times 4th	0	0	1	3
	4	4	4	4
Pwr. Consumption (watts)	280	262½	246	252-270
(Taken on #1 Unit)				
Selection				
Based on lowest noise		X		
Based on lowest power			X	

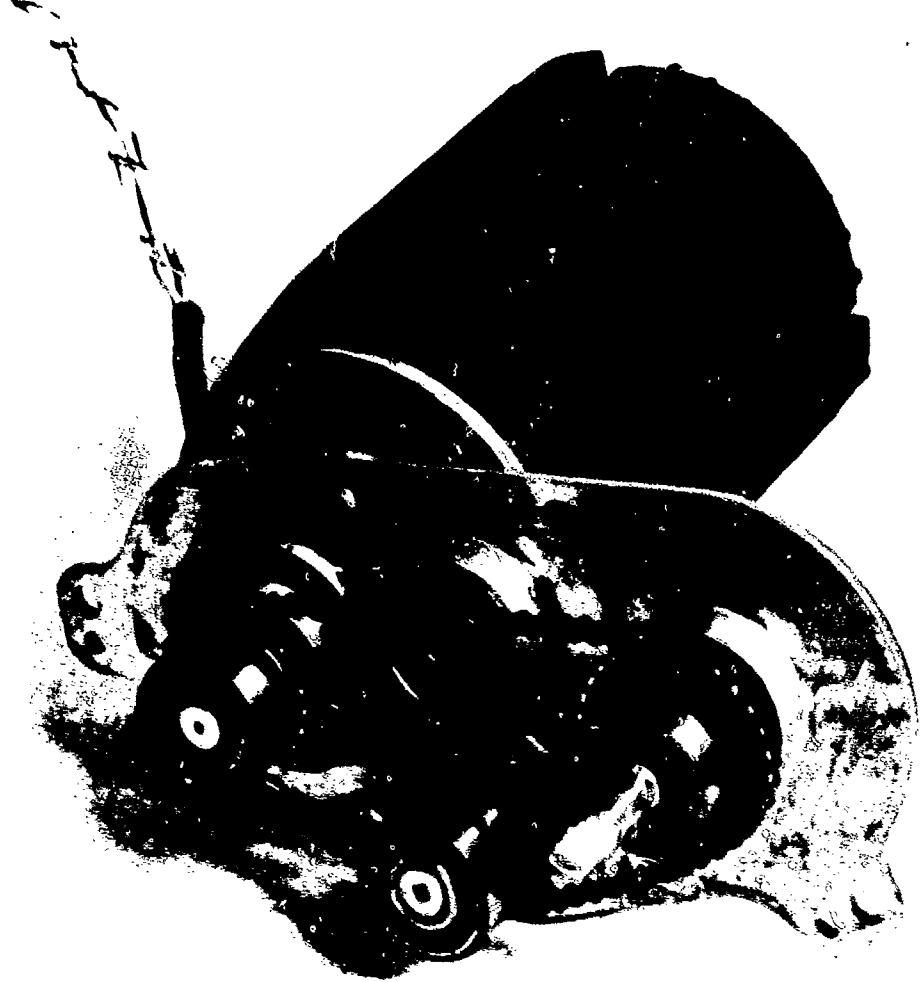
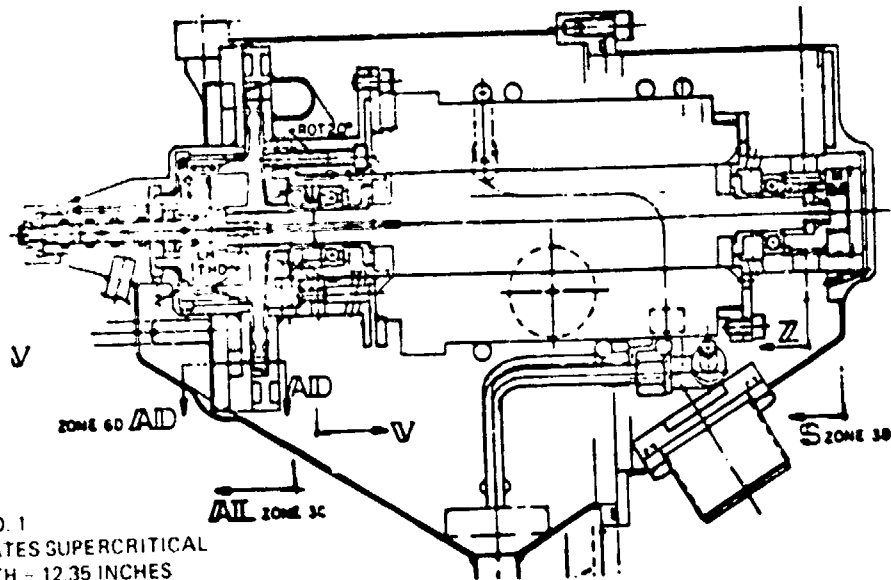
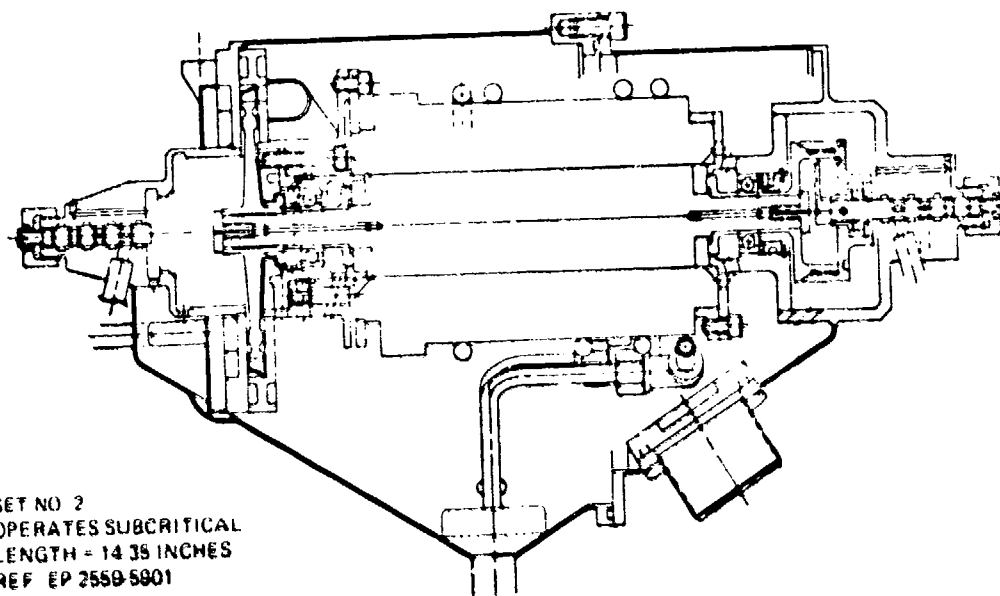


Figure VI-13 Constant Frequency Motor and Offset Gearbox



SET NO. 1
OPERATES SUPERCRITICAL
LENGTH = 12.35 INCHES
REF: EP 2559 1001

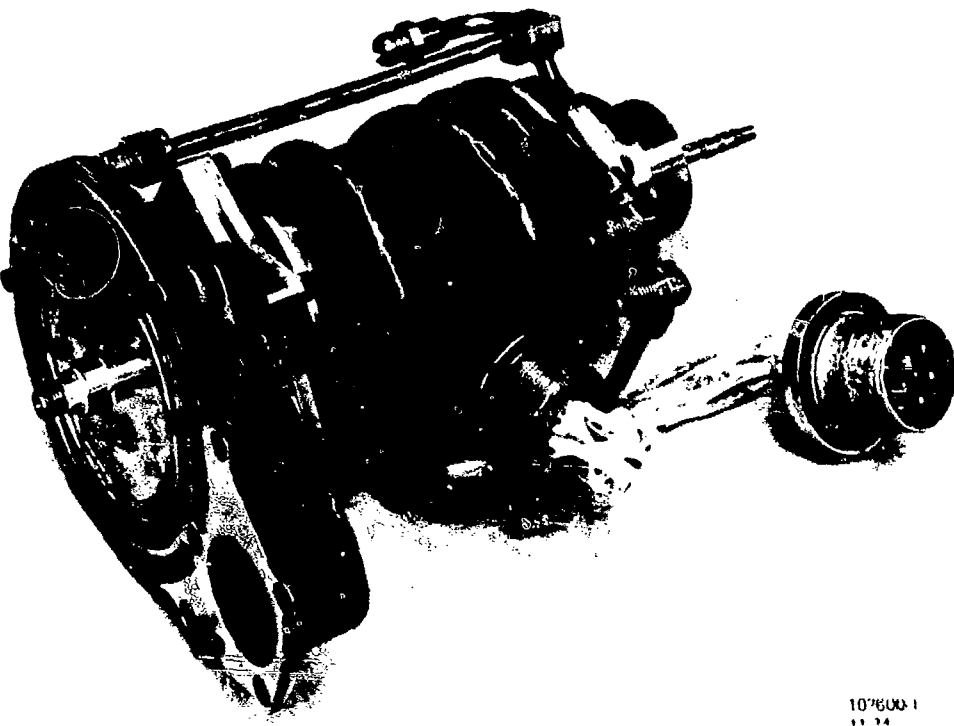


SET NO. 2
OPERATES SUBCRITICAL
LENGTH = 14 38 INCHES
REF: EP 2559 5801

Figure VI-1d Set No. 1 and No. 2 CRU Configurations

Table VI-H Turboalternator Pump Rotating Shaft Critical Speed Configuration Analysis

Configuration	Critical Speeds		
	1st	2nd	3rd
1. Original shaft	29,500 RPM	71,000 RPM	169,000 RPM
2. Aft Pitot Pump hsg. with stub on wheel (steel hsg.)	47,500	49,500	75,000
3. Aft pitot pump hsg. with stub on wheel (titanium hsg.)	49,000	53,500	74,500
4. Aft pitot pump hsg. no stub (steel hsg.)	48,000	57,500	77,000
5. Aft pitot pump hsg. no stub (titanium hsg.)	53,000	58,000	76,000
6. Modified - .2" at turbine overhang .25" at pump overhang (steel hsg.)	58,000	63,000	89,000
7. Modified same as 6, only (titanium hsg.)	63,000	65,000	87,500



102600-1
11-24

Figure VI-15 Turbo Alternator Pump Assembly

Table VI-I Summary of Stall Torque & Spinup Data

Nozzle Plate	No. Noz.	PNI (PSIG)	Tq (in lb)	w (lb/sec.)	Ax. Cl.	PNI @ 55K	Comments
Original (Wide Spaced) EP 2559 1228	9	1350	12	.094	.034		
		1250	10.5	.033	.034		
		850	7	.061	.034		
		1250	13	.069	.020	660 @ 52000	Flows may be questionable?
		830	8	.045	.020		
		1350	13	.093	.010		
		1250	12	.088	.010		
		850	8	.061	.010		
	4	1310	7	.035	.020		
		1250	6.5	.034	.020		
		850	4	.024	.020		
Flat Plate (Close Spaced) EP 2559 1270	10	1250	16.5	.110	.020	400 @ 57000	
		800	10.1	.068	.020		
	7	1200	11.3	.074	.020	480 @ 50,500	
		850	7.5	.049	.020		
	5	1215	8.2	.052	.020	580 @ 56,000	
Latest (A) (Close Speed) EP2559 1228A	10	1350	11.5	.094	.020	750 @ 60,000	(Run 203) with 204 PP Hsg
		1200	9.5	.082	.020		
		850	6	.058	.020		
	7	1350	7	.063	.020	800 @ 54,000	(205)
	003 CRU	1200	6	.056	.020		
002 Exh. Hsg		850	4	.040	.020		
5 17 74							

Table VI-J Nondimensional* Stall Torque Data Using GN₂ (Des. PR = 529 @ AR = 25)

Noz. Plate	No. Noz.	Meas. A.R.	Pin (PSIA)	PR.	r calc.	r meas.	%	Calc in r meas.	%	C _d
New EP2559 1228A	10	26.6	1365	84	.6582	.6196	78	6045	77	
			1395	94.5	.6585	.5382	81	5901	80	.81 .93
			1265	115	.6690	.5727	85	5668	84	
	7	25.4	1365	88	.6677	.4816	70	4199	64	
	5	26.1	1370	90	.6512	.5720	88	6788	104	
			1365	182	.6738	.5802	87	4023	104	
	10	12.6	1265	76	.6831	.6376	92	7168	134	
	7	12.45	1215	78	.6947	.6496	93	7260	105	
	5	12.4	1230	81	.6842	.6681	98	7298	107	
Original EP2559 1320	9	17.2	1365	84	.6675	.6397	81	6466	82	
	4	18.54	1326	96	.6580	.643	126	7624	116	Questionable data

$$\cdot r = \frac{t_2 g t_3}{\rho C_D P_3}$$

Table VI-1. CRU Test Data

Table VI-K CRU Test Data (Cont.)

nozzle plate was not adequately clean and installing flush parts to clean the nozzles was sufficient to enable predicted performance to be achieved. There was still a discrepancy between measured and calculated flow through the nozzles so after brass plugs were installed in place of the steel plugs to minimize leakage that might escape through the flush ports. The resulting non-dimensionless data is shown in Table VI-L and Figure VI-16 from which it can be seen that reasonable correlation to prediction exists.

VALVES

Three hot gas solenoid valves are used in the Set, one shutoff and two control valves. Two designs were tested, one designated AG56C-21 and the other GA-17310. Both are pilot actuated valves with the former being significantly smaller, lighter in weight and more leak tight than the latter. This valve is used in Set No. 1 and often experienced sticking. They were replaced with the GA-17310 valves which cycled well (except at low voltage conditions).

For Set No. 2 both valves were modified. The AG56C-21 internal clearance was increased. The GA-17310 valve was modified for a Hastelloy 25 seat and a Stellite 6 hard facing over 17-4 PH poppet for better internal leakage and long term endurance. The solenoids of both were also increased in size for higher pull-in power at lower voltage.

The GA-17310 valves are used in Set No. 2 and have performed flawlessly during testing.

PITOT PUMP

The Set No. 1 pitot probe (EP2559-1148) operated at 28% efficiency (reference Figure VII-9), and was internally milled and externally shaped by hand. In an effort to reduce the cost of manufacturing the Set No. 2 pitot probe (EP2559-5969) was stamped internally and milled to shape externally with minimum hand finishing. This accounts for the more simplified shape of this probe. Rig tests showed little difference in performance between the long and short nose versions of a given configuration so the Set No. 2 probe was made with the short nose. Little difference was intuitively expected in efficiency.

BOOST PUMP

The boost pump (Micropump Model 10-90-316-961) supplied with Set No. 1 included a 2 fluted inducer. The pump showed difficulty in priming and operating at a low NPSH. It was concluded that an improved pump would be desirable.

For Set No. 2, two other configuration pumps were tested. One was a Micropump Model 10-90-316-961 modified with a single flute. This pump experienced less difficulty in priming and was able to pump its rated capacity down to 9.5 psia where the pump lost prime.

The other configuration pump tested was Micropump Model 12-00-303-763 gear pump modified with an oversized (3/8" diameter) inlet. No difficulty was experienced in priming under very low conditions of NPSH and the pump exceeded capacity requirements in both head rise and flow. The pump was tested under simulated conditions in the hotwell with CP-25 as the working fluid down to NPSH = 0.73 psia and an inlet head of 4.5 inches. The pump performed satisfactorily under these conditions and was able to execute a series of starts and stops without losing prime. The pump characteristics are shown in Figure VI-17.

Table VI-L Data Summary, Brass Flush Port Fittings

GN₂ Accel Data	<u>2 Noz</u>	<u>3+2 Noz</u>	<u>5+2 Noz</u>
Speed (Krpm)	35	50	50
P R	382	232	166
T meas (ft lb)	.218	.301	.411
T Pred (ft-lb)	.171	.313	.445
meas (lb/sec)	.017	.049	.071
pred (lb/sec)	.017	.039	.057
meas	.587	.288	.275
pred	.574	.358	.342
pred	.448	.373	.370
GN₂ Stall Data	<u>PNI (Pre)</u>	<u>T (Pre)</u>	<u>PNI (Post)</u>
2 Noz	840	2	1060
	1190	3	
5 Noz	650	3.5	1060
	1240	7.4 - 8.3	6
7 Noz	660	4.75	1018
	1200	10.4	
10 Noz	650	7	1000
	1150	14	12.5
GN₂ No Load Spin Data			
Pre Brass	: 390 PSIG @ 50.5 Krpm		
	500 PSIG @ 61.5 Krpm		
Post Brass	: 480 PSIG @ 57 Krpm		

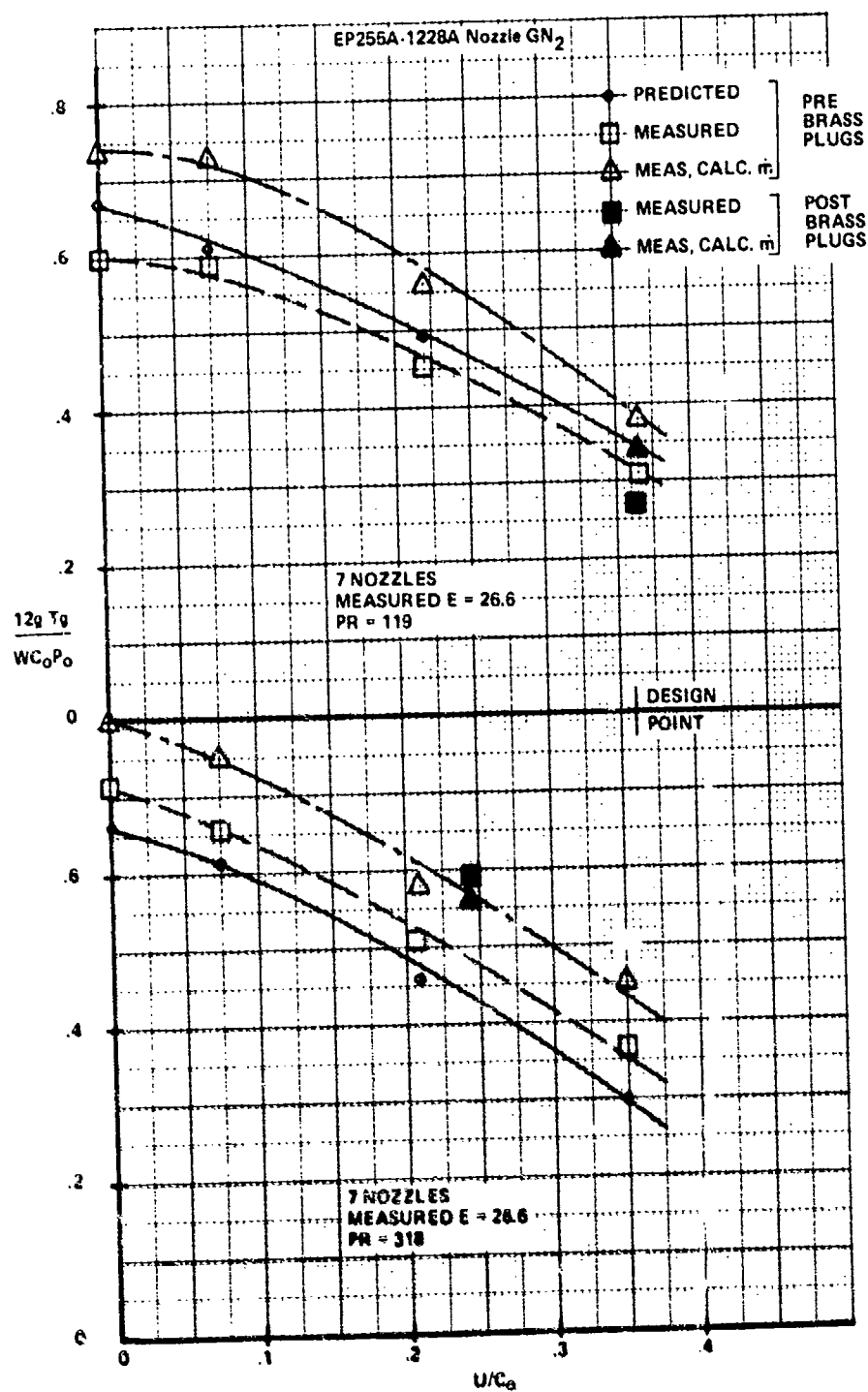


Fig. 46 V1-V3. Non-dimensional Torque vs. Speed

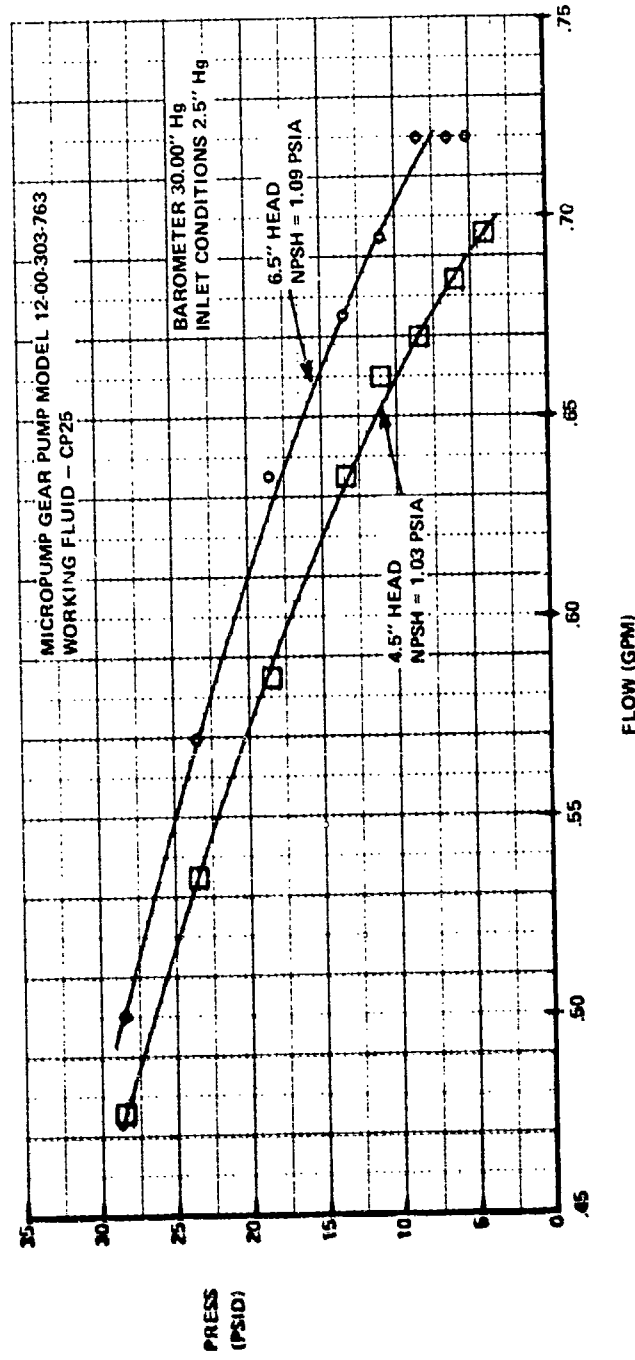


Figure VI-17 Pressure vs. Flow

There are conditions in the set where the NPSH could be on the order of the height of the fluid over the inlet of the pump. The worst case occurs at shutdown or during a load reduction where the condenser fan cools the condensate to a temperature below that of the fluid in the hotwell. Under this condition the saturated fluid in the hotwell will boil. To ascertain the capability of the 12-00-303-763 modified configuration pump to continue to pump, this condition was simulated using water in a bell-jar and pulling vacuum until a rolling boil occurred. Visually, it was observed that pumping continued.

It was decided if even a slight amount of subcooling could be done between the hotwell and the inlet of the pump, that some positive margin in pumping characteristics could be maintained. A calculation at a 160°F hotwell temperature and 100°F air temperature surrounding the 3 inch + transfer tube indicated that by finning the tube, 2°F of subcool could be induced.

The cooling fins and the as-described modified gearpump were selected for Set No. 2.

START APPROACH

The Set No. 1 start approach depends upon an accurate measurement of the heater fluid temperature to trigger the opening of the shutoff and control valves. With the accumulators in the system to absorb the expanding fluid backflowing from the heater, system pressure would build up as the temperature increased. When the temperature and pressure are in the vicinity of the design point, the valves are signaled to open and the turbine would accelerate to control speed in a matter of seconds.

The heater outlet is at the high point and so the control thermocouple was placed at the outlet under the hypothesis that the hotter fluid would migrate there. The result was that with the valves closed during the heatup period, the thermocouple was not sufficiently buried in the heater to be exposed to the maximum temperature of the fluid. Overheating of the fluid during startup could occur and was prevented by premature manual actuation of the valves to expose the thermocouple to flowing fluid. Only then did it accurately register the temperature. To rectify this condition for a satisfactory automatic start approach for Set No. 2, the following was considered:

- Construct new heater with buried temperature sensors.
- Sense heater inlet to pick up the temperature of the fluid backflowing out during heatup.
- Cycling the start flow valve to intermittently expose the outlet thermocouple to hot fluid.
- Use pressure as an indication of the start signal.
- Bootstrap or assisted bootstrap start of which there are a variety of techniques.

Any of these approaches required a change to the controller. Additionally, an important consideration was the differences in complexities between the various methods.

Tests were conducted at MERDC on Set No. 1 modified for a start pump assisted bootstrap start. These were not fully automatic starts but were manually assisted. This data is presented in Figures VI-18, VI-19, and VI-20. These simulated starts are acceptable. A plot of pump pressure (pilot pump against that used on Set No. 1) vs. speed (Figure VI-21) implies that the pilot pump will overcome the start pump at about 115 psi and 21,000 rpm.

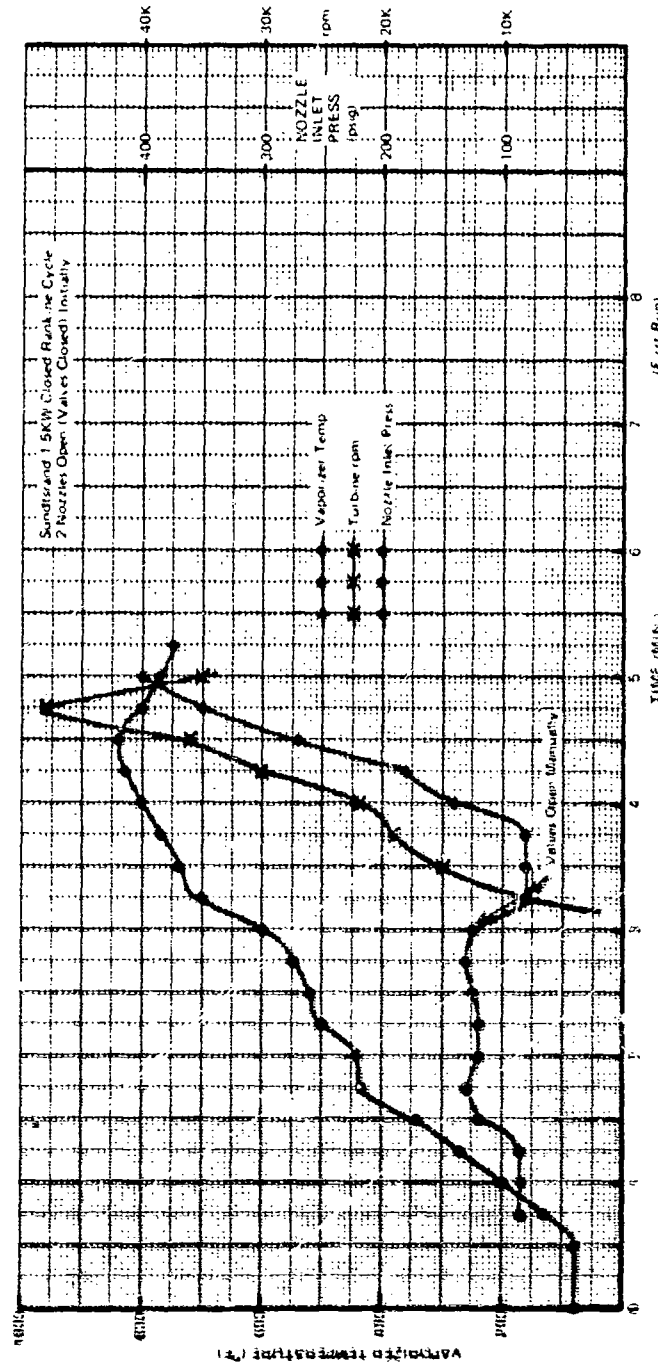


Figure VI.1B System Parameters on Startup

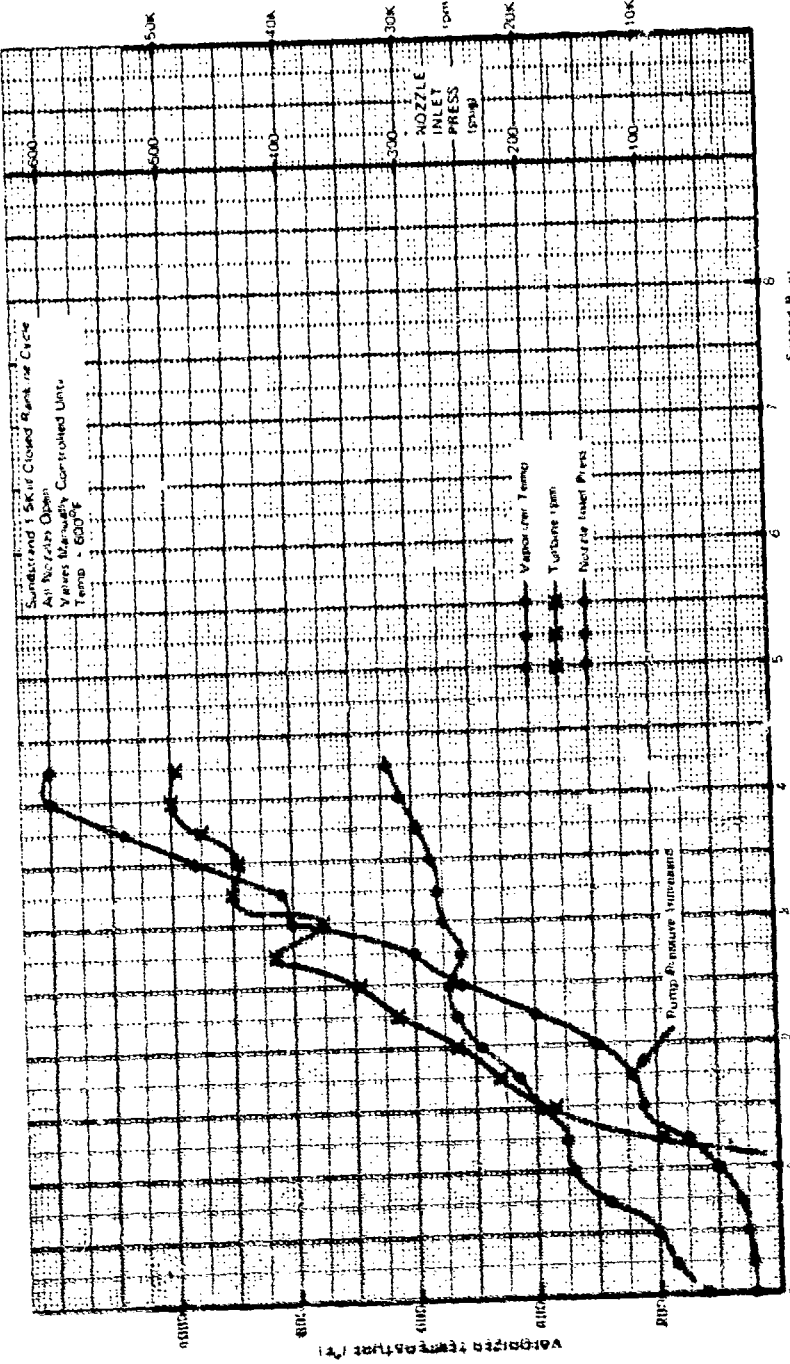


Figure VI-19 System Parameters on Startup

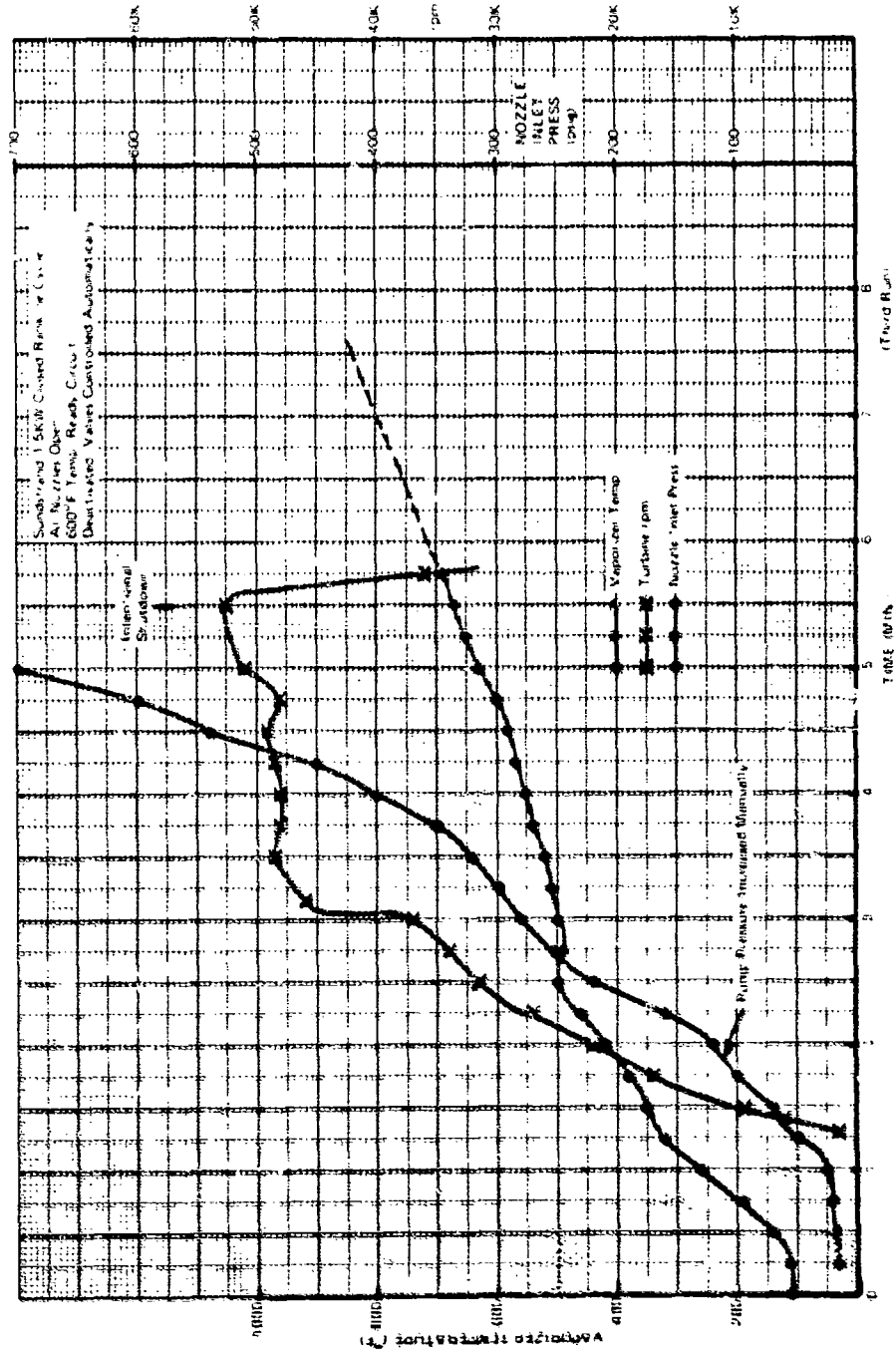


Figure VI.20 System Parameters on Startup

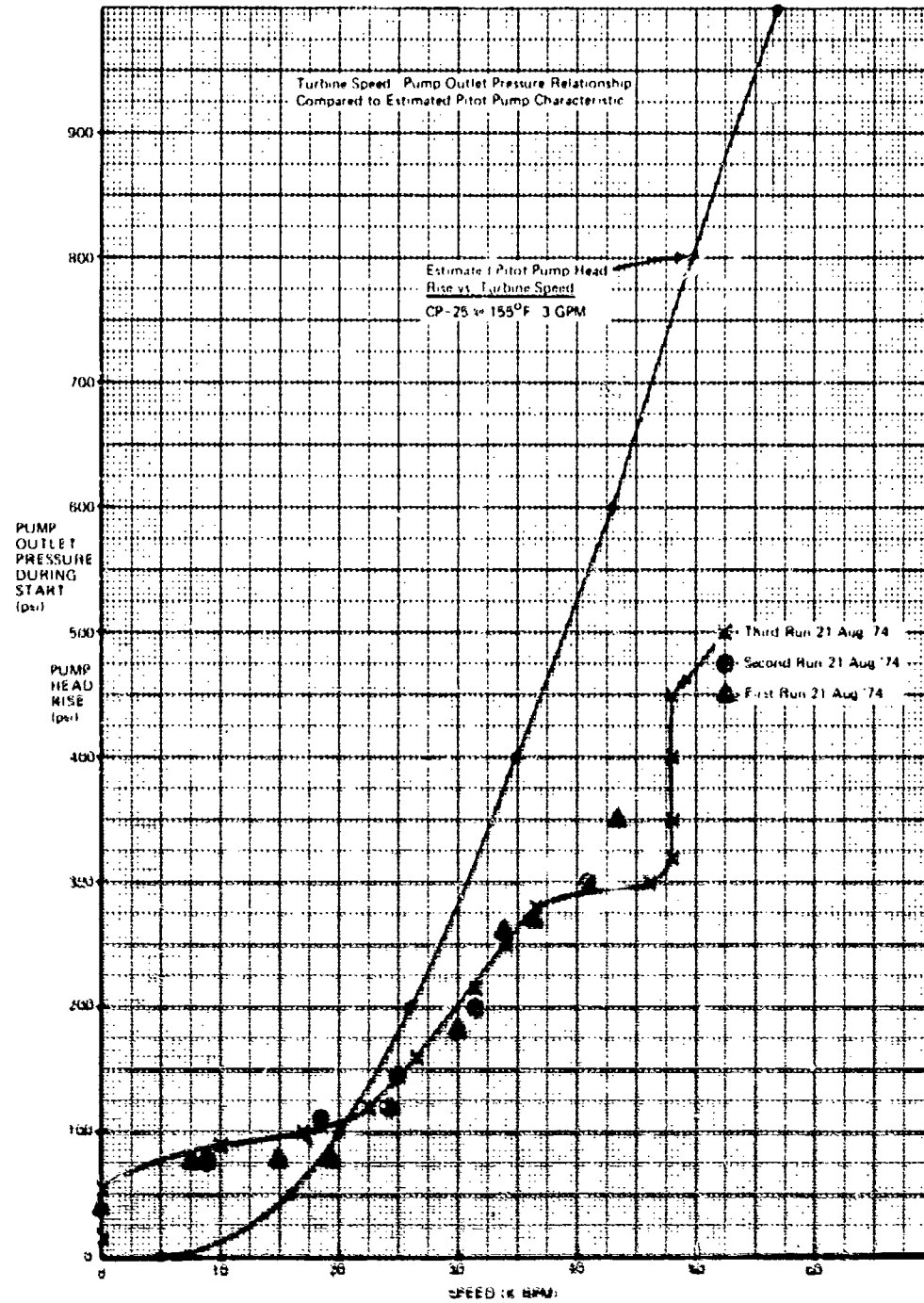


Figure VI-31 1.5MW GPC Breathing Start

These tests provided justification to switch to a start pump assisted start approach using a pump with sufficient margin to provide the required pressure at 10 nozzles worth of flow. A calculated flow value of about 0.1 gpm as a minimum would be necessary to be provided by the start pump.

Two Wankel rotor pumps were tested; data is presented in Figures VI-22 and VI-23. At the risk of being oversized, the P260 pump was selected due to the marginal head rise of the P193A1 pump. The finished hermetic assembly is shown in Figure VI-24.

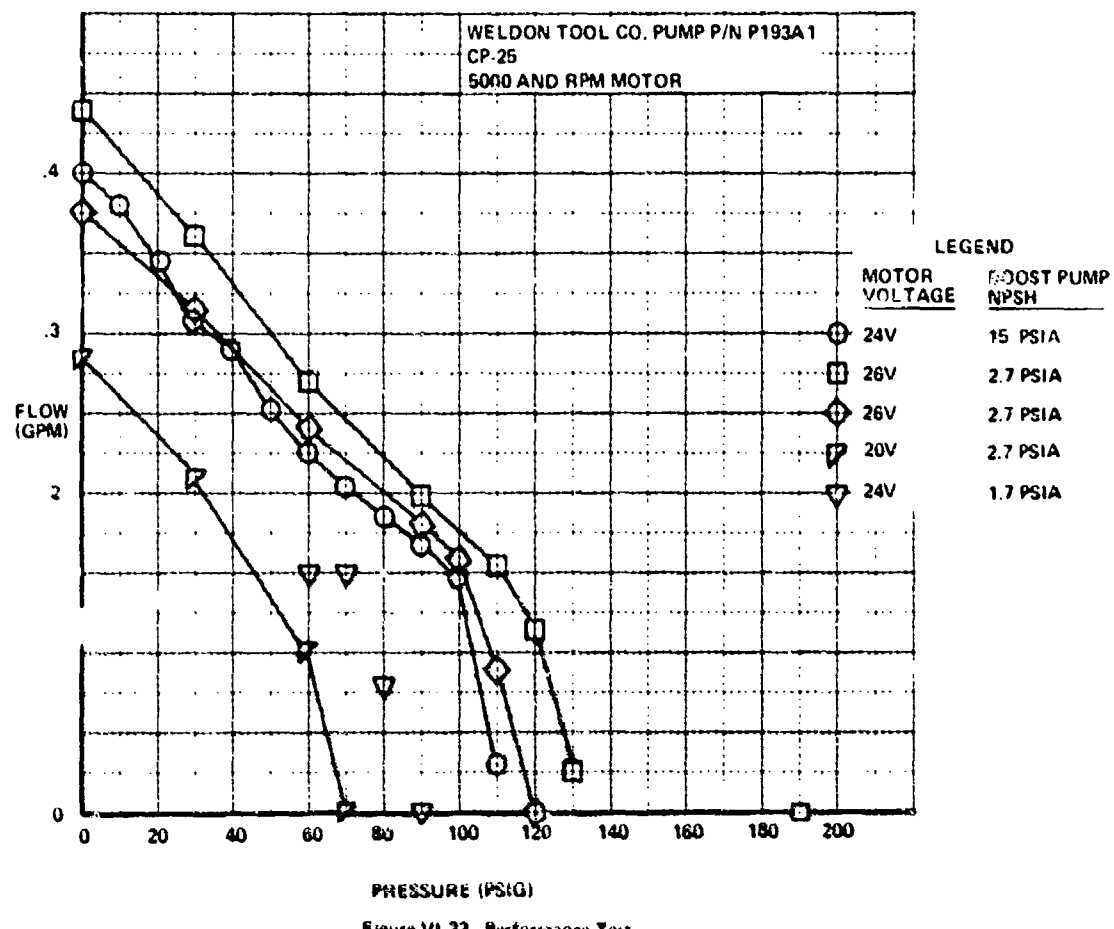


Figure VI-22 Performance Test

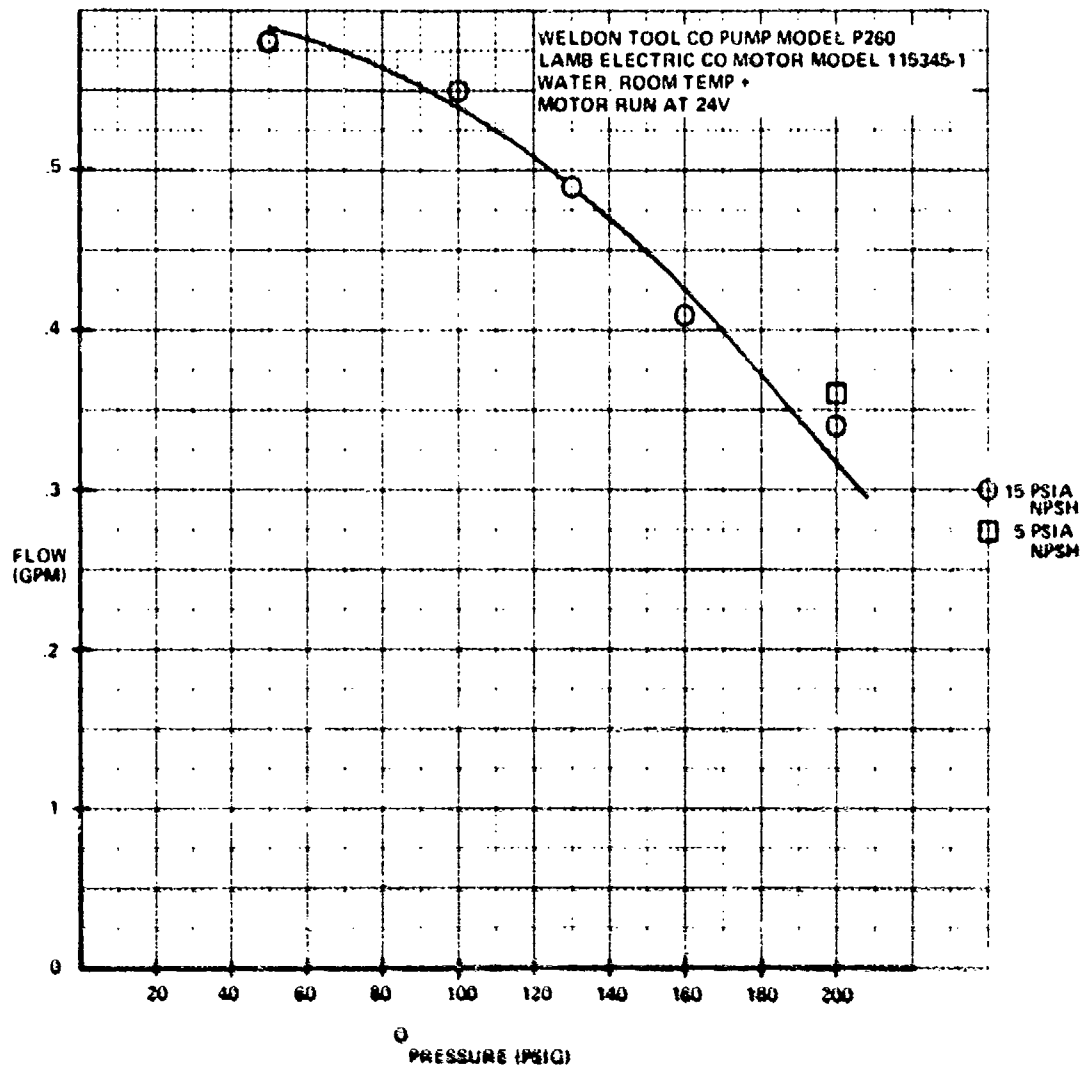


Figure VI 23 Performance Curve

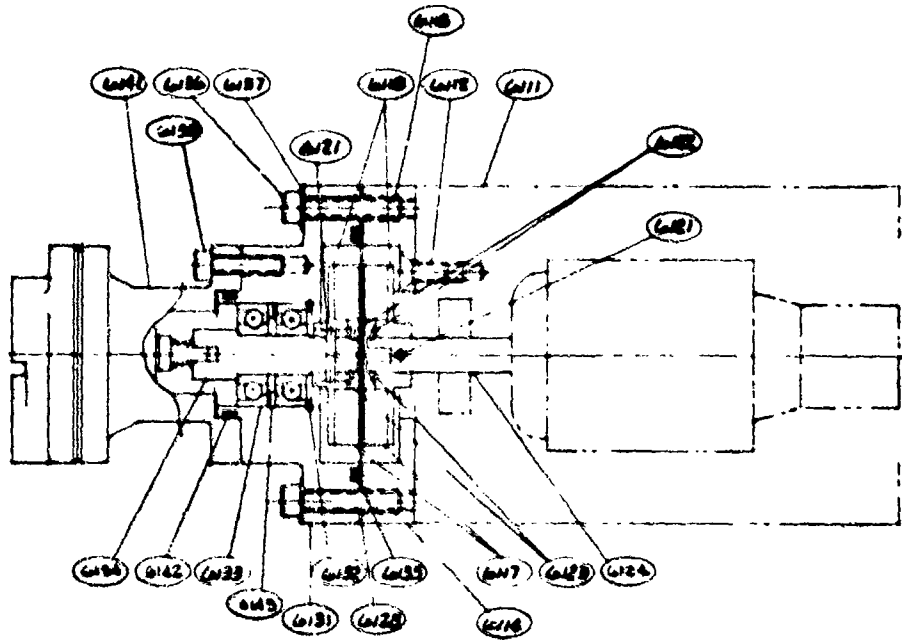


Figure VI-34 Start Pump, Coupling, Motor Assembly
Ref EP 25594101

SECTION VII
SYSTEM DEVELOPMENT

VII. SYSTEM DEVELOPMENT

Unit No. 2 was tested as a complete packaged system except that the control box was not installed and an external power supply was used to operate the start pump and several parasitic loads. Figures VII-1 through VII-5 are various views of the 2' x 2' x 2' system.

Thirty (30) tests were conducted at Sundstrand and sixteen (16) conducted at USAMERDC laboratories which form the basis of knowledge about the system at this writing. Throughout the test program several changes were made to improve operation. Figure VII-6 is a schematic which represents Sundstrand post Run 017 tests while Figure VII-7 is an update illustrating changes made at USAMERDC (most of these changes were made prior to 6-20-75).

Test data is illustrated in Table VII-A (Sundstrand tests) with data analysis illustrated in Table VII-B. Table VII-C lists data and analysis conducted on the Set at USAMERDC. The results of these tests indicate that the Set is not producing the required amount of output power. The following discussion elaborates on this result.

The changes made between Figures VII-6 and VII-7 were an attempt to isolate possible heat shunts to ascertain any effect on output power. These included the following:

Two of four condenser drains capped to induce the condensate to drain through two active drains.

Hand valve installed in the one of two active drains which dumps condensate into the hotwell close to the exhaust housing.

The regenerator condensate drain closest to the regenerator vapor inlet port had a hand valve installed.

The effect of these with and without the valves open did not materialize in any obvious change to the output power. In addition, the hotwell was modified so that condensate would drain through the main hotwell into a modified hotwell. This also had no noticeable change in output power. Other differences between Figures VII-6 and VII-7 are immediately downstream of the start and pitot pumps to gain knowledge about automatic start characteristics.

STEADY STATE OPERATION

Figure VII-8 summarizes the original design point performance. Review of the Tables VII-A, B, and C indicates that the data falls into two categories:

Data at greater than design turbine inlet pressure (P_{NI})

Data at greater than design turbine outlet pressure ($P_C + \Delta P \approx P_C + .3$)

This partly, but not fully, explains the low power. Other contributing areas are summarized as follows:



Figure VII-1 Set No. 2 on Test Stand

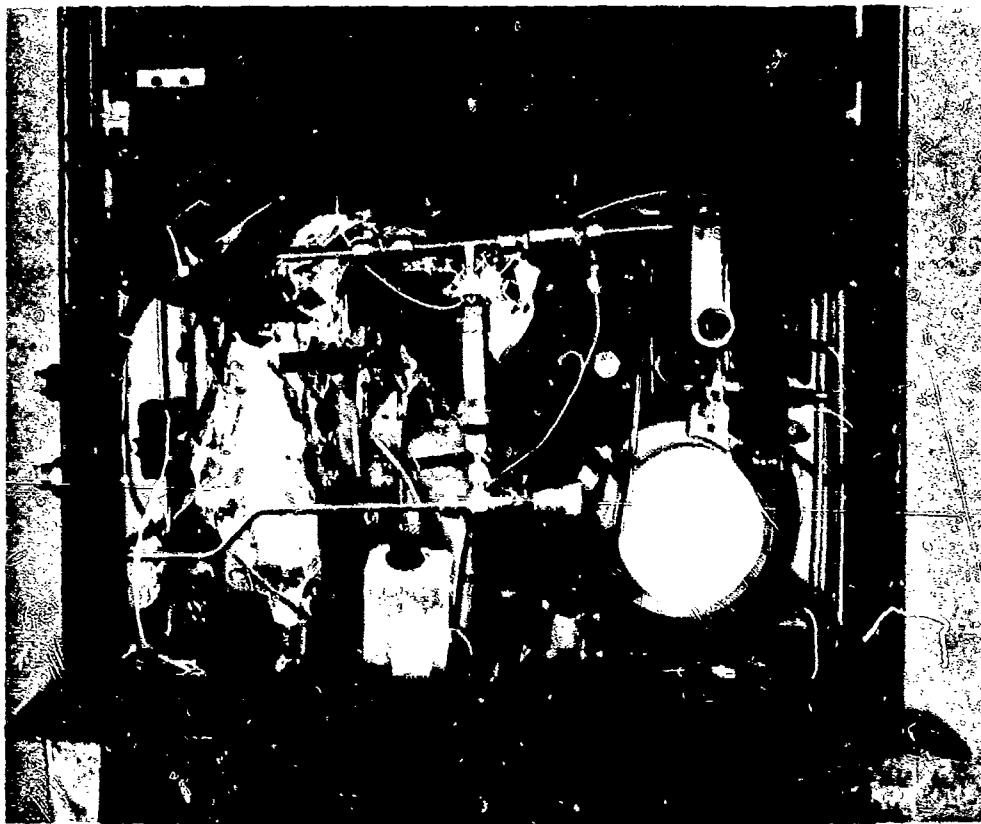


Figure VII-2 Set No. 2 Front Door Open

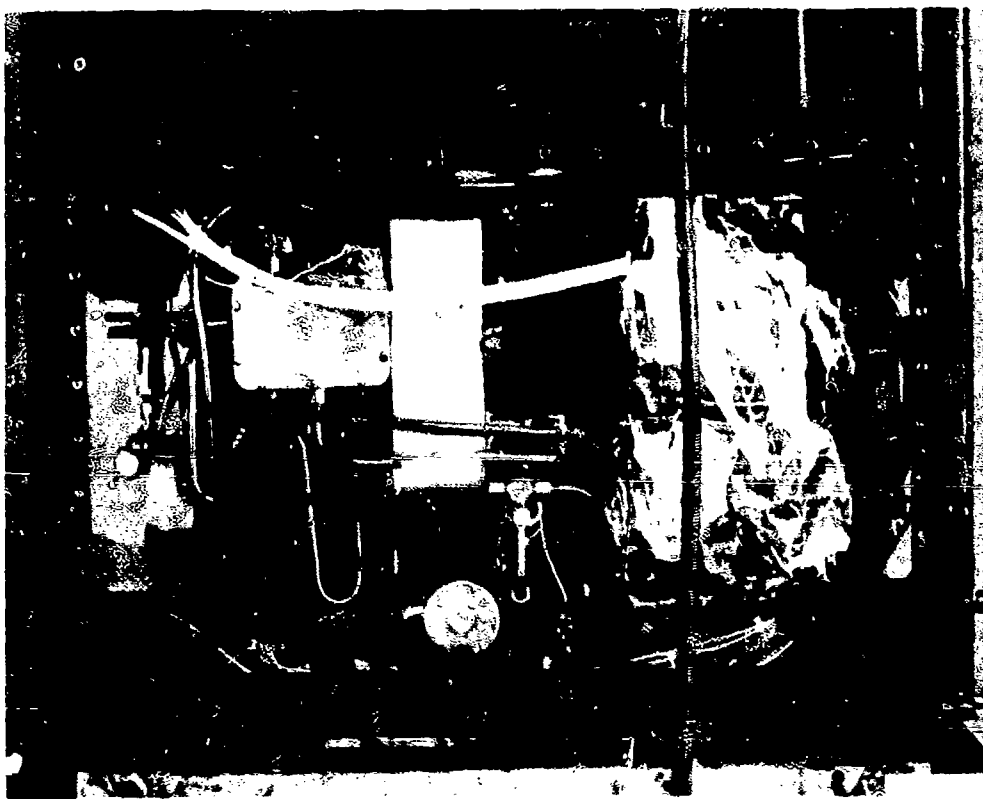


Figure VII-3 Set No. 2 Right Side Panel Removed

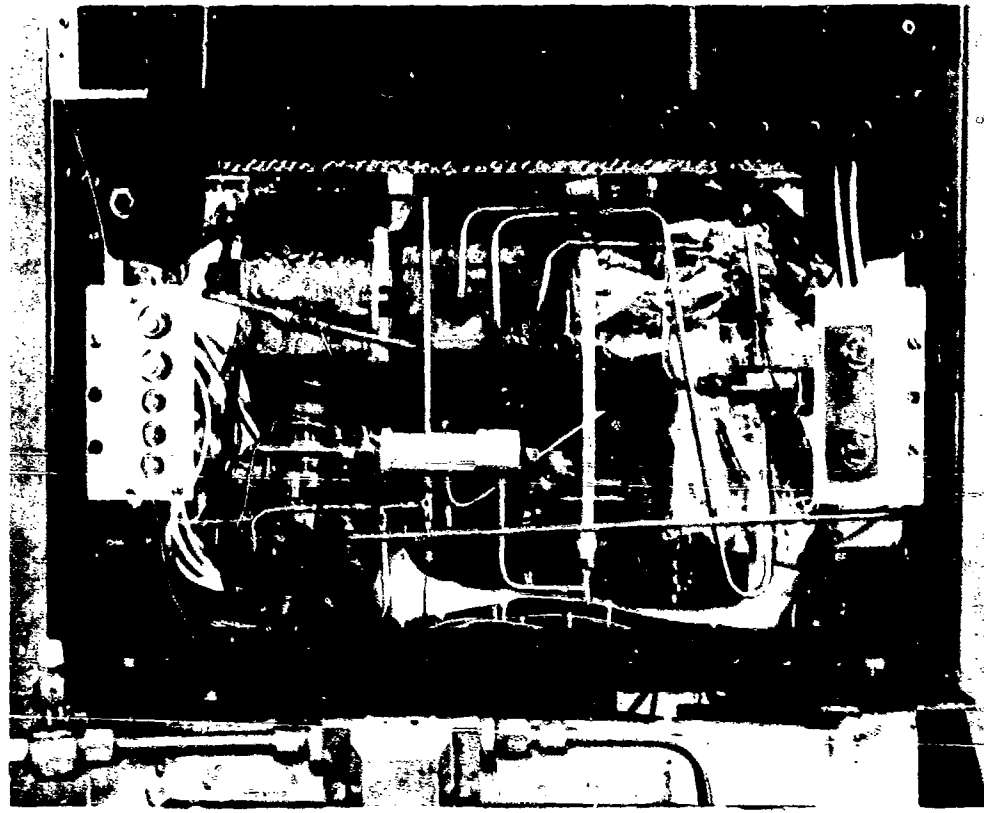


Figure VII-4 Set No. 2 Left Side Panel Removed

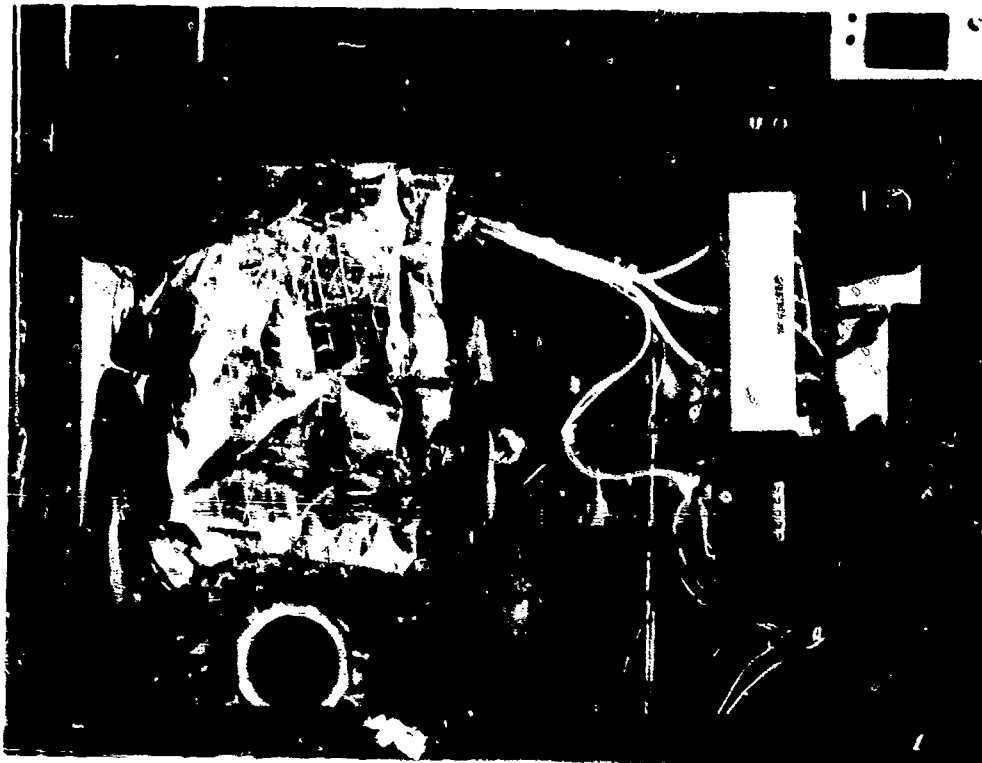


Figure VII-5 Set No. 2 Back Panel Itemized

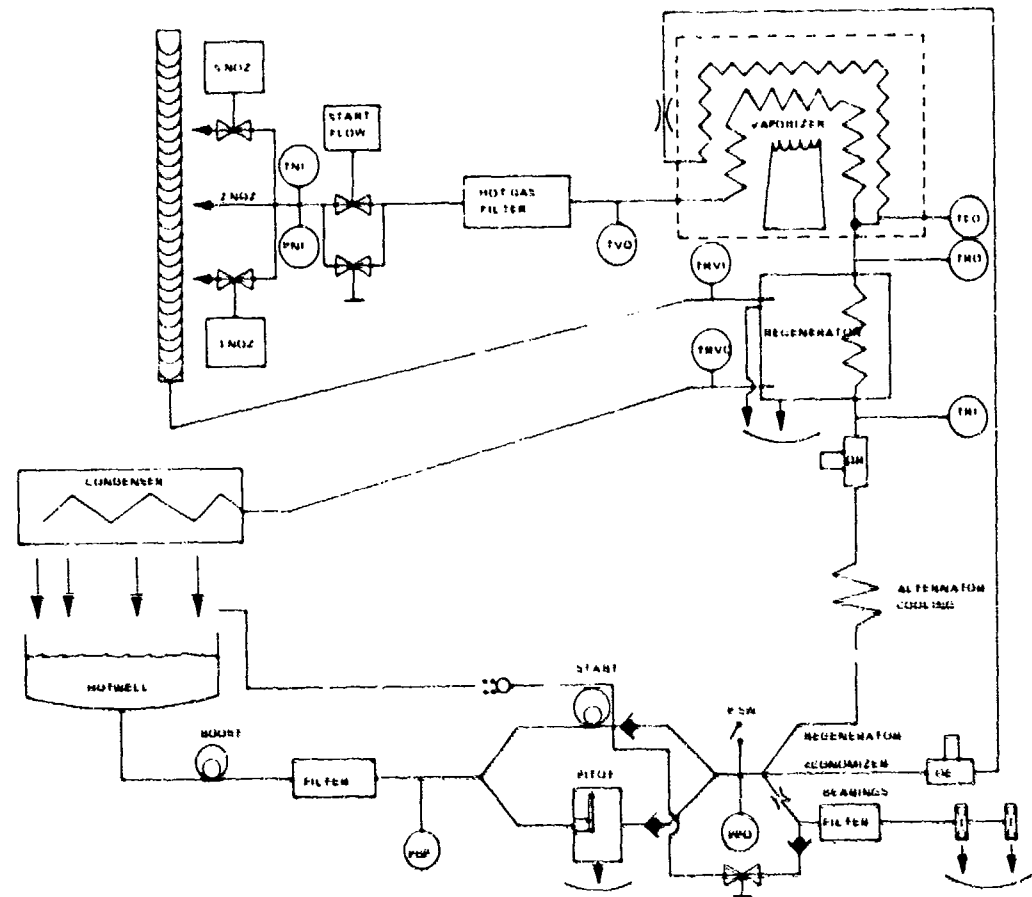


Figure VII-6 1.5 KW MERDC Functional Schematic (Post Run 017)

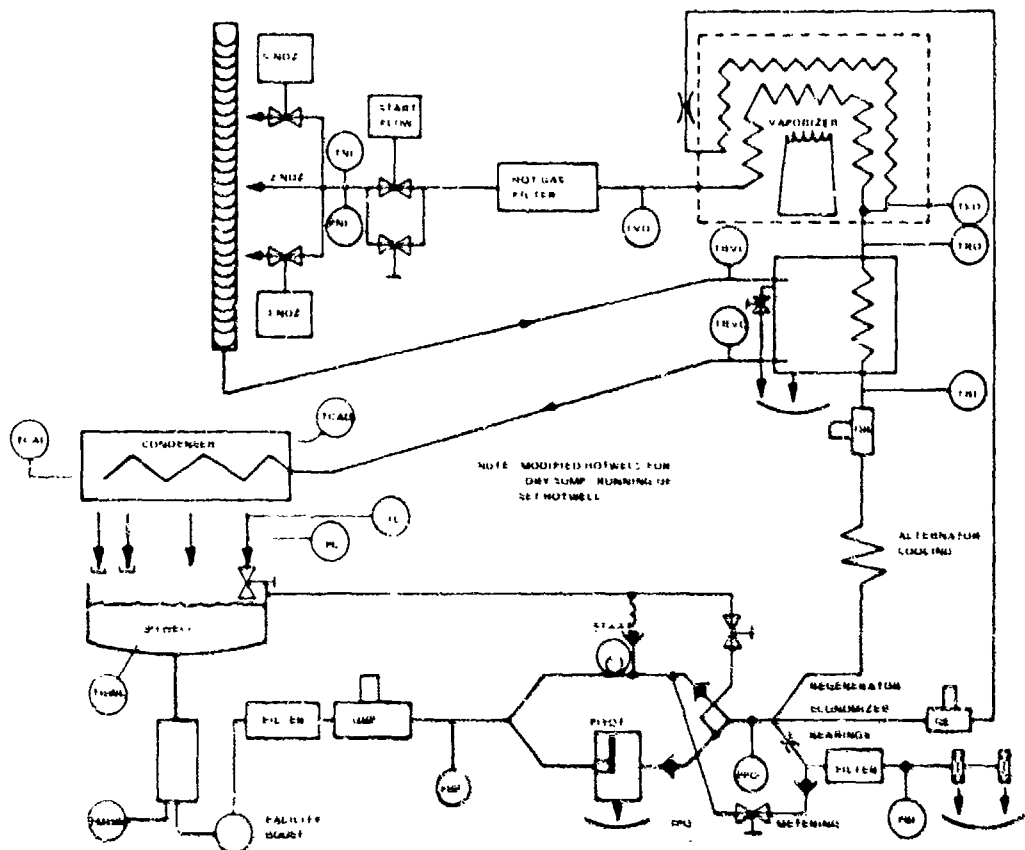


Figure VII-7 1.5 KW Closed Rankine Cycle Functional Schematic

Vista Vista VITA Sunbeam and Test Data, Set No. 2

Table VII-A. Success and Test Data. See No. 2 (Cont.)

Table VII-A. Sundari and Test Data, Set No. 2 (Cont.)

Table 271-A. Standard Test Data, Set No. 2 (Cont.)

THE VILLAGE IN KARACHI DISTRICTS 205

Table VIIC. Test Data Reduction Statistics and 95% Confidence Intervals for the Rankine Cycle. Serial No. 2

Table VIII-C Test Data Reduction Summary for 5 KW Closed Rankine Cycle, Serial No. 2 (Cont.)

Table VI-C Test Data Reduction Summary 1.5 kW Closed Rankine Cycle Serial No 2 (Cont.)

OPENDS 1.5 BAR ODC R_MOTORIA 5-21-75 CASE 1
 IN EFF 0.62614E-00 0.39000E-00 0.18000E-00 0.90000E-00 0.10700E-00 0.65500E-01
 OUT EFF 0.37301E-00 0.16000E-00 0.72000E-02 0.16500E-00 0.13300E-02 0.20000E-01
 DPL VAR 0.13001E-02 0.56000E-01 0.62000E-03 0.12000E-04 0.37100E-01 0.0
 PUMP FR 0.10000E-01 0.64000E-00 0.10000E-01 0.48000E-00 0.60994E-01 0.18900E-05
 INH FUEL 0.20120E-05 0.10000E-00 0.15000E-02 0.33000E-04 0.28100E-00 0.16750E-02
 FLUID CODE 0.30000E-01 0.31000E-05

STATE POINT	PRESSURE(PA)	TEMPERATURE(K)	ENTHALPY(J/KGK)
VAP OUT	0.62000E-03	0.82460E-03	0.31532E-03
TH IN	0.61500E-03	0.82433E-03	0.31532E-03
REGEN VAP IN	0.30222E-01	0.64800E-03	0.24312E-03
COND IN	0.37172E-01	0.24700E-03	0.65690E-02
PUMP IN	0.37100E-01	0.15490E-03	-0.13297E-03
ALT IN	0.64210E-03	0.16740E-03	-0.12627E-03
REGEN LIQ IN	0.63580E-03	0.18210E-03	-0.11994E-03
REGEN LIQ OUT	0.63390E-03	0.55940E-03	0.89141E-02
ECON OUT	0.63180E-01	0.52330E-03	0.62958E-02
VAP IN	0.63180E-03	0.55555E-03	0.86952E-02
CRU EFF	0.42614E-00	0.31172E-01	0. RELEASED 0. ASSIMILATED 0. REJECTED 0. SYSTEM EFF 0.16542E-01
FUEL FLOW TH/HR	0.17430E-01		PUMP EFF 0.35000E-00

ECON. IN TEMP. (F) = 0.6261672E-03 ECON. OUT TEMP. (F) = 0.2641286E-03

Figure VII.8 Original Design Point Performance

1923 Oct 26

	(1) Set 1	(2) Set 2	(3) Design Pt.
Heater efficiency	.88	.82 - .84	.88
Regenerator effectiveness	.80	.69 - .74	.855
Pitot pump efficiency	.28	.121 - .165	.35
Turbine Efficiency	.31	(1) (2) (3)	.62
Heat Shunts	Not considered ?	0	

The quality of the data on Set 2 exceeds that on Set 1. Nonetheless, it appears that heater and regenerator performance is down slightly. This may be due to manufacturing QC for the heater and either core to housing fit and/or slightly undersize for the regenerator. These can be controlled at the design level and do not represent an R & D effort.

The expectation for 23% pitot pump efficiency for Set 2 was based upon the data obtained for Set 1. This is shown in Figure VII-9 along with a plot of Set 2 pitot pump power consumption. The Set 2 pitot probe was designed to be more cost effective than that of Set 1. These differences are elaborated upon in the improvements section.

The turbine performance of Set 1 was low primarily due to the separation distance between the nozzles. The efficiency of the turbine of Set 2 was investigated in several ways. The data of Tables VII-B and VII-C shows turbine efficiencies based on shaft power (calculated from measured output power + rectifier and generator losses + parasitic losses + bearing and rotor windage losses) and enthalpy (based on measured turbine inlet temperature and pressure). These range from 27.6 to 59.6% with the lower efficiencies occurring at higher than design turbine back pressure.

Figure VII-10 is a recording of Run 030 from which the slope of the accelerating and decelerating portions of turbine speed trace was used to determine shaft power and predicted turbine efficiency. This data is summarized in Table VII-D from which the following is evident:

Measured in and predicted in CP 25 agree

Calculated shaft loss and that based on output power generally agree

Calculated η_t based on acceleration/deceleration analysis agrees with the average η_t calculated from output power considering that flow to the turbine is cycling from 5 to 2 nozzles to maintain turbine speed at 55 ± 1 Krpm. Thus the turbine appears to be operating close to predicted though the speed trace scale makes qualit + analysis difficult.

Turbine efficiency depends upon inlet conditions, exit conditions and degree of admission. As shown in Table VII-D, the partial admission effect is significant (2 noz vs. 5 noz η_t).

A further analysis was performed to determine if heat loss in the nozzle housing was contributing to low power output. Figure VII-11 is a sketch illustrating possible heat flow paths. The following data points were selected because they represent a wide range of turbine inlet and outlet conditions

<u>Run</u>	<u>Conditions</u>
030-1	Nozzles liquid level below turbine housing Design point turbine outlet conditions

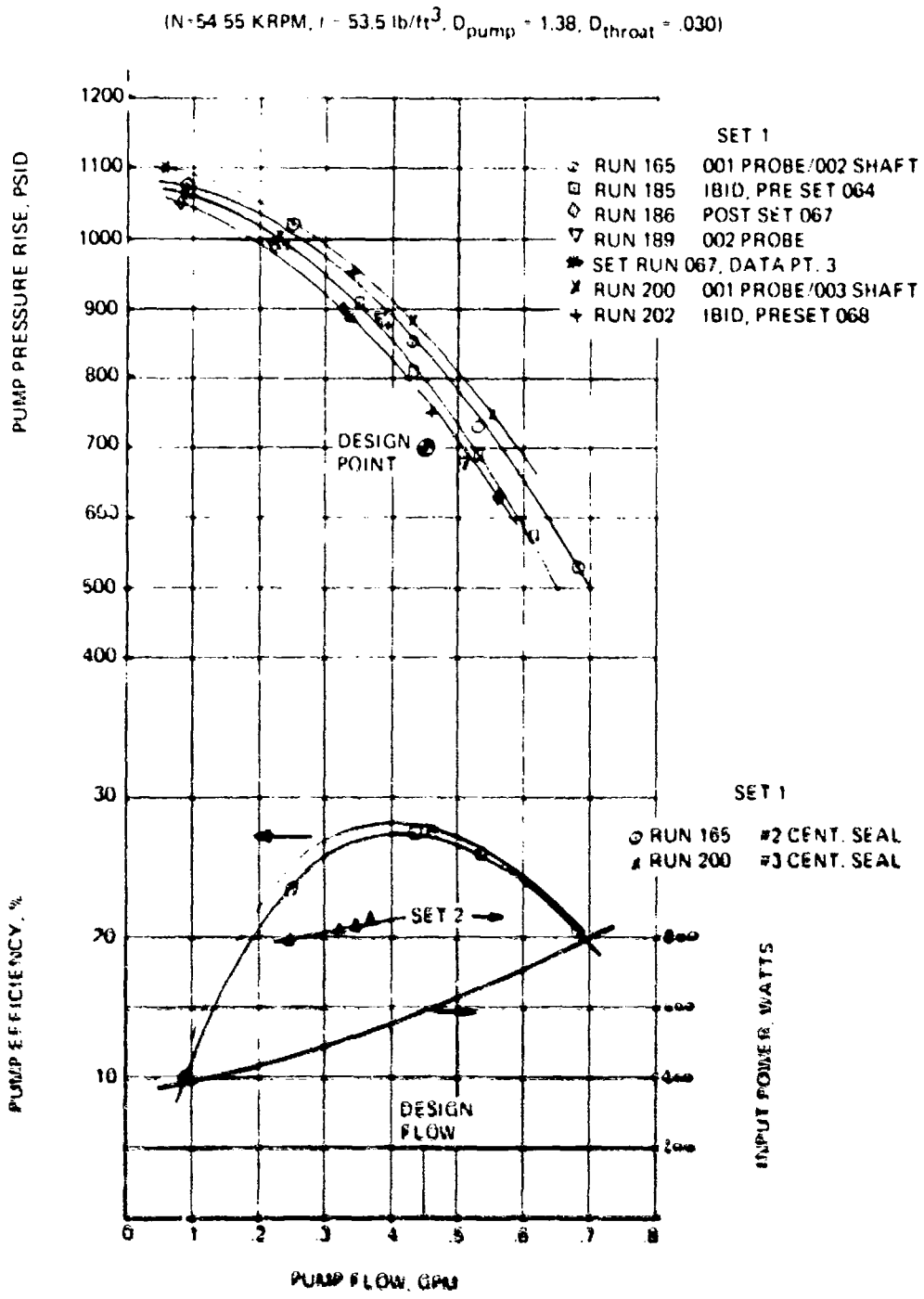
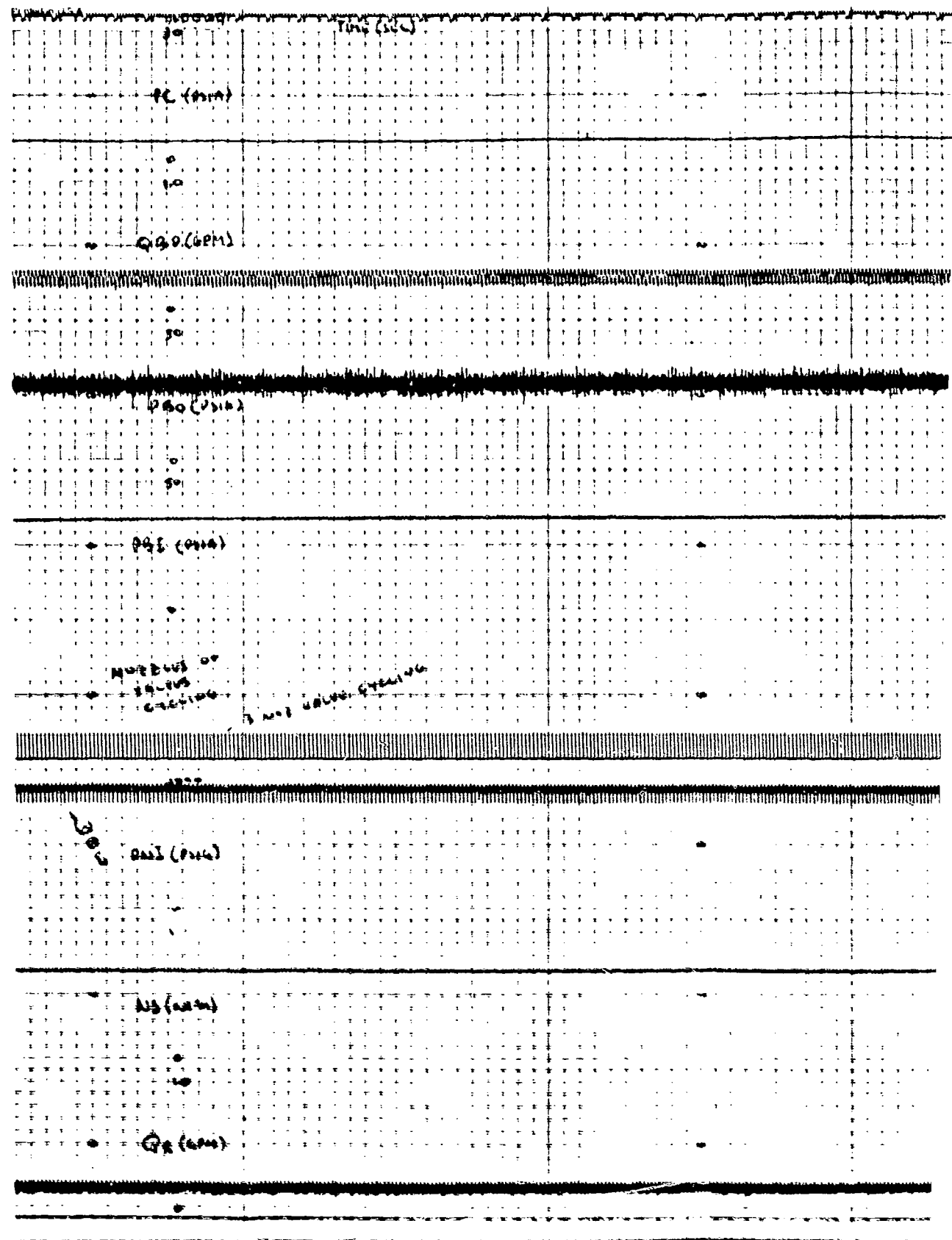


Figure VII-9. Pump Pump Output & Performance Characteristics



GENERAL ACCUMULATIONS

9

١٢

2

1

1

卷之三

1

•

11

Figure VI-10 Bus Q30 Results

	VOC	
	WEL(GeII)	
	TBC(-P)	
	TBC(+)a	
	TBC(+)b	
	TBC(+)c	
	TBC(+)d	
	TBC(+)e	
	TBC(+)f	

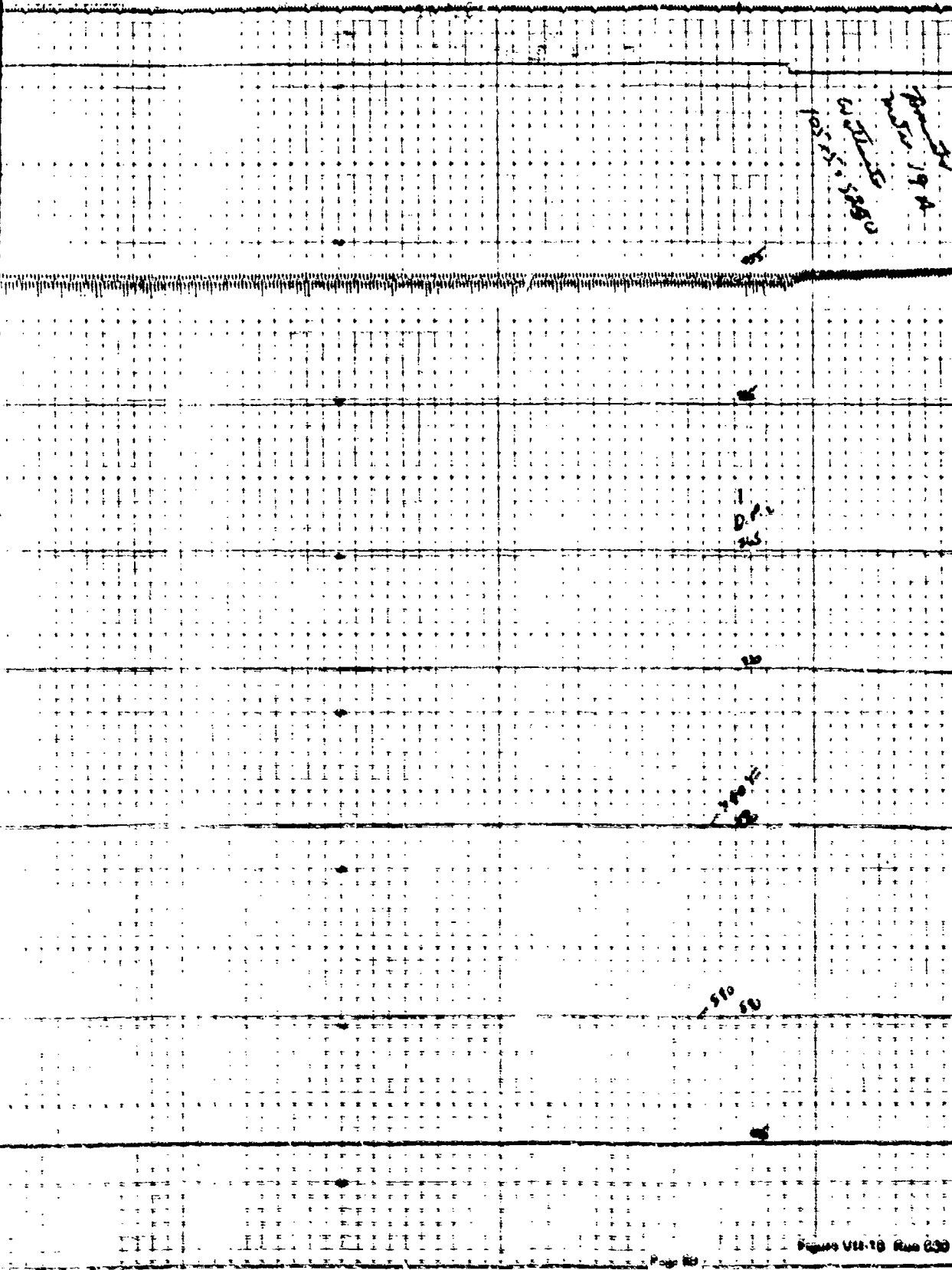


Figure VI-19. Run 630 Recording Case 1

Table VII D Turbine Performance

Data Point	030 DP1	030 DP2	028 DP1	028 DP2	028 DP1	028 DP2
TNI	840	840	830	774	812	812
(I) Accel	1.72	1.358	1.661	.453	1.137	943
(II) Decel	94	1.137	1.115	1.316	1.2	1.13
I_A/I_D	2.66	2.495	2.776	1.771	2.337	2.074
Pin (5)	994	924	954	904	984	864
Pin (2)	959	944	1004	874	904	884
m (5) (E19)	.0342	.0318	.03276	.03194	03076	03007
m (2) (E19)	.0147	.01443	.01541	.01372	01397	01367
(m) av (E19)	.0244	.0231	.0242	.02283	0224	0219
(m) meas.	.0284	.0292	0363
Shaft loss w	1558	1680	2010	1301	1700	1496
Shaft loss (*) w	1600	1515	1700	1819	1864	1863
Pex psid	3.6	5.0	2.7	4.9	3.1	3.8
HP (5) meas.	3.60	3.44	4.15	2.14	3.25	2.82
HP (5) E19	3.61	3.18	3.53	2.93	3.17	3.03
HP (2) meas.	1.26	1.26	1.710	678	1.25	1.03
HP (2) E19	1.17	1.08	1.30	877	1.12	1.03
η_t (5) E19	579	583	570	581	574	581
η_t (2) E19	44	423	45	404	445	435
Avg Pred (*)	572	49	385	455	479	50

NOTES

- (*) From Table 7.2
- (5) Indicate 5 nozzles active
- (2) Indicate 2 nozzles active
- (E19) is computer performance program designation

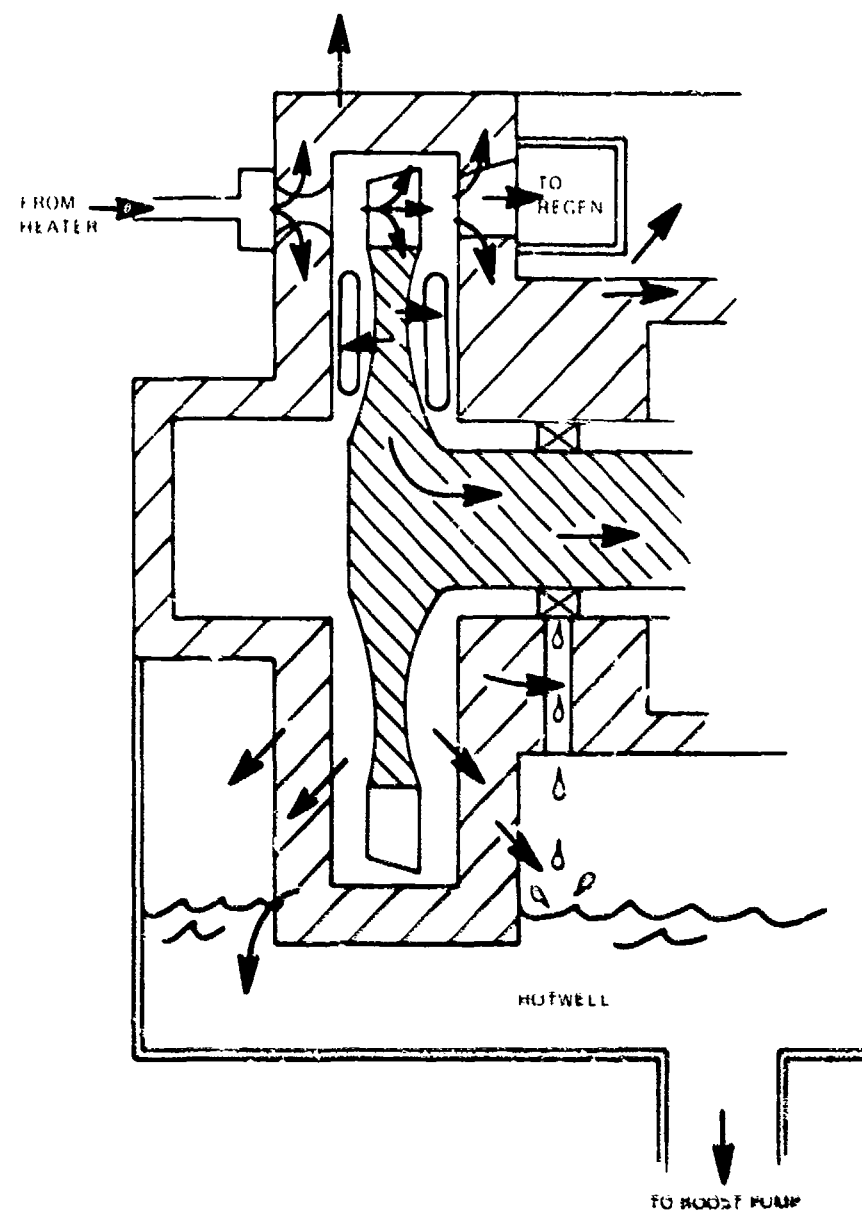


Figure VII-11. Turbine Heat Flux Model

028 2 Hotwell liquid level contacting turbine housing
Design point turbine outlet conditions

16 5 Hotwell liquid level = 0, flow through into modified
& hotwell (holding tank attached to bottom of hotwell)
16 7 Design point turbine inlet condition

The objective of the analysis was to determine turbine efficiency using test data and considering heat losses, to determine why the regenerator vapor inlet temperature is 30-60°F lower than it should be and why the different hotwell liquid levels did not make a sizeable change in output power. It is worth noting that Set 2 has produced up to 477 watts net output power, but for all the tests on the average, net output power is close to zero.

Three heat transfer analyses were conducted - the wet, partially dry, and dry cases to simulate the following conditions respectively (1) hotwell liquid level contacting the nozzle plate, (2) hotwell liquid level below the nozzle plate with the bearing drainage flowing down the face of the plate and (3) no liquid in the hotwell with the bearing drainage not contacting the face of the plate. Note that lab experiments imply the bearing drainage flows down the face of the plate. Table VII E is a summary of this analysis for Run 030 1 which indicates that the wet case has approximately twice the heat loss as the dry case, and the predominant loss is the heat flow to the wheel. Table VII F uses these heat flows and applies them to the various tests to determine which case best represents each test, how the predicted regenerator vapor inlet temperature (TRVI) compares to that measured and what the real turbine efficiency is factoring in heat losses. The asterisks in Table VII F indicate the cases which typify each test run by choosing the case that most clearly matches measured TRVI. For example, the partially dry case best describes Run 030 1 since the calculated TRVI is only 12°F lower than that measured. The heat loss at the inlet of the turbine is small but is a factor. The corresponding turbine efficiencies compare well with the data of Tables VII B, C, and D. The turbine efficiency of Run 016 is low due to the very high back pressure. As the design point is approached, the turbine efficiency becomes higher and approaches that of Run 030 1.

From this, a prediction is made of the expected output power with the correct design turbine conditions and what may be expected if the performance of certain components is improved. For this analysis, it is assumed that design point conditions are achieved at the inlet and exit of the turbine (by reducing non condensable leaks into the low pressure side of the system) and that heat losses can be reduced to the dry case. Additionally, the generator and rectifier losses are taken as the worst possible case (would be lower using TRW data, reference Figure VII 12) and parasitics are taken as the highest measured (range = 466-605 watts). It is further assumed that the reduction in heat loss in the wheel only improves shaft power indirectly through greater regeneration and the ability of the system to support greater mass flow.

Thus, the results of this analysis, presented in Table VII G, are conservative and imply the following:

With a 58 ft. 650 watts is the maximum power that can be expected out of Set 2 at design point conditions.

The effect of heat loss is not significant.

The pitot pump is the greatest contributor to low output power.

Table VII-E Heat Loss Summary (Run 030-1)

	<u>Wet</u>	<u>Partially Dry</u>	<u>Dry</u>
Inlet Gas \rightarrow Inlet Hsg. (Q_L , in)	509	398	342
Exh. Gas \rightarrow Exh. Hsg. (Q_L , exh)	119	71	38
Hot Gas \rightarrow Wheel (Q_L)	2397	1158	308
Disc Friction (Df)	670	670	670
Pumping (P)	<u>125</u>	<u>125</u>	<u>125</u>
Total Loss from Exhaust	3820 B/hr	2422 B/hr	1484 B/hr

Run 030 conditions

\dot{m} = 77.3 lb/hr
 T_{NI} = 840°F
 P_{NI} = 974 psia
 P_e = 3.6 - 4.0 psia

Scavenging Loss(s) = 410 B/hr

Table VII-F Effect of Heat Loss on Performance
(Prediction of Regenerator Vapor Tin and η_T)

HEAT BALANCE $m h_1 - Q_{Lm} - G_L D_f - P S = m h_3$												
$\frac{h_2 - h_1}{m} \frac{Q_{Lm}}{m} = \frac{h_4 - h_3}{m} \frac{Q_{Leak}}{m}$												
RESULTS												
RUN	CASE	h_2	h_1	h_3	h_4	T_1	T_2	T_3	T_4	$\Delta T_{1,2}$	$\Delta T_{3,4}$ TRVI	η_T
S 0301	WET	309	302	185	184	840	832	525	523	8	59	503
	P DRY	309	304	203	202	840	835	573	570	5	12	503
	DRY	309	315	215	214	840	836	588	595	4	+13	503
S 0202	WET	293	288	200	199	810	803	587	584	7	1	503
	P DRY	293	289	204	208	810	803	583	580		+15	498
M 165	P DRY	307	304	242	241	810	805	650	647	5	+7	38
	DRY	307	306	249	248	810	806	666	662	4	+22	38
M 167	WET	321	317	245	244	835	826	655	655	8	+10	354
	P DRY	321	318	257	256	835	828	682	679	7	+14	354
	DRY	321	319	264	263	835	830	691	686	5	+21	354

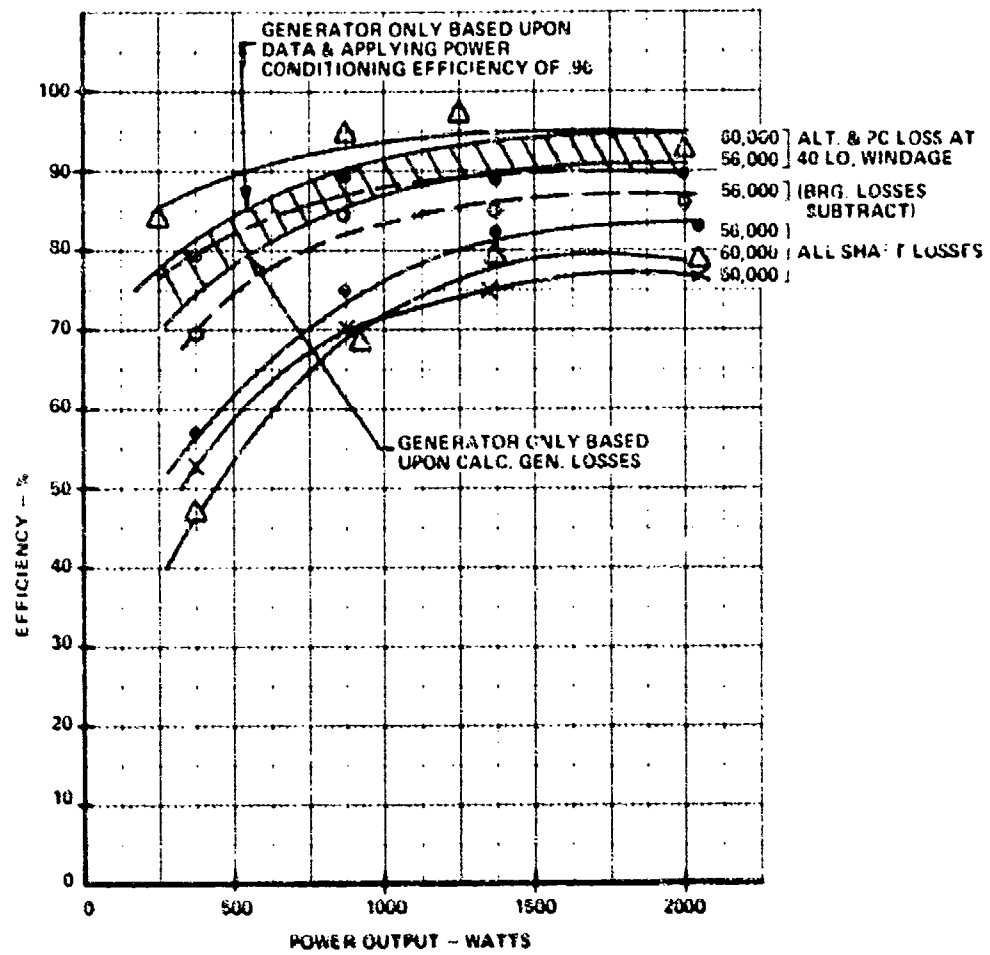


Figure VII-12 Alternator and Power Conditioning System Efficiency

Table VII-G Predicted Performance

Run 030-1 Partial Adm. losses & partial fire rate 120 lb/hr & $\eta_t = .58$		<u>120 lb/hr</u>	<u>$E_R = .85$</u>	<u>$\eta_{pp} = .35$</u>	<u>$\eta_H = .88$</u>
Shaft Power, w	2470	3017		3179	
Pump	<u>.900</u>	<u>496</u>		<u>496</u>	
	<u>1570</u>	<u>2521</u>		<u>2683</u>	
(B+W)	<u>.65</u>	<u>.65</u>		<u>.65</u>	
	<u>1505</u>	<u>2453</u>		<u>2618</u>	
G & R	<u>286 (.81)</u>	<u>422 (.83)</u>		<u>450 (.83)</u>	
	<u>1219</u>	<u>2034</u>		<u>2168</u>	
Parasitics	<u>600</u>	<u>600</u>		<u>600</u>	
	<u>619 w</u>	<u>1434 w</u>		<u>1568 w</u>	
<u>SUMMARY</u>		<u>Kilowatts output</u>			
Run	Comments	$\eta_t = .58$	Ht. Loss	Ht. Loss $\cdot E_R$	Ht. Loss $\cdot E_R \cdot \eta_{pp}$
030-1	Partial Adm & fire rate 120 lb/hr & $\eta_t = .58$.62		.43	.57
028-2	Partial Adm. Low η_{pp}	.58	.61	.58	.32
16-5	High back press	.65		.36	.47
16-7	High back press	.35	.38	.60	.12

Reducing the heat loss and increasing the performance of the regenerator, pitot pump and heater will bring output power to 1.2 – 1.6 KW at a 10.4 – 13.9% thermal efficiency.

Higher output power may be obtained by more fuel through-put.

SECTION VIII
IMPROVEMENTS

VIII. IMPROVEMENTS

STARTUP

Automatic startup was not achieved on Set 2. This was due to two factors:

- 1) Too high a degree of flow from the start pump which precluded enough temperature rise in the fluid prior to pitot pump takeover.
- 2) Possible takeover by the pitot pump at too low a turbine speed and/or at too low a working fluid temperature.

These conditions caused the system to reach a bootstrap equilibrium point at a temperature below the critical point, at a flow above the design point and at a speed below rated.

The start pump is oversized and needs to have its output reduced to effect a bootstrap start that is compatible with the fluid heat input and turbine/pitot pump dynamics.

OUTPUT POWER AND EFFICIENCY

As the discussion in Section VII indicates, these factors relate to several components.

TURBINE: The turbine appears to be operating close to design though low by several points. Increasing the lap ratio would allow more optimum entry of the gases into the blade passage. Design point efficiency of this same turbine with a higher lap ratio has been achieved on the Remcom program.

REGENERATOR: On Set 1 the regenerator showed better performance than on Set 2. The construction is that of a core slipped into a housing. The implication is that there may be a significant amount of side leakage around the core on the Set 2 regenerator that did not exist on Set 1. Tighter dimensional control, investigation of thermal fatigue/expansion characteristics and improved design quality should increase the effectiveness to the design value.

HEATER: The heater efficiency is also lower than that of Set 1 and a few percentage points lower than design. Fundamentally, a fin tube heater would be more reproducible than the present B-B design. The design point efficiency in a fin-tube design is achievable in the same volume and at reduced weight in the B-B type.

PARASITICS: The efficiency of the constant frequency motor reduced parasitics by a net of 50 watts factoring in the increased power of the quieter constant frequency gearbox. Further reduction can be achieved particularly if a single variable speed motor is used to support all parasitics rather than the present variable and constant speed motors each driving selected parasitic devices.

EFFICIENCY: In summarizing the efficiency that can be expected with another generation of hardware, from Section VII it is seen that improvements in heat loss control, pitot pump efficiency, regenerator effectiveness and heater efficiency will yield 1.2 - 1.4 KW at 10.4 - 13.9% thermal efficiency. Further improvement may also be made by increasing turbine lap ratio and reducing parasitic losses.

PITOT PUMP: The original prediction of pitot pump performance was 35%, that obtained on Set

1 was 28% and for Set 2 was about 15–16%. Figure VIII 1 illustrates the differences between the Set 1 and Set 2 probes. The probe for Set 2 was constructed in such a way as to be less expensive to fabricate. In so doing, several characteristics, such as the leading edge, X sectional symmetry, and inlet geometry of the nose changed. The housing cavity is also different. It is hypothesized that probe drag, recirculation and/or sidewall effects of the housing are inducing excessive losses.

An investigation was made to determine if the theoretical probe drag losses are consistent with achieving the original efficiency predictions which were obtained using scaling criteria. Table VIII A is a summary of measured power, predicted power and drag losses as a function of drag coefficient. Literature for streamline struts and foils indicate a $C_D = .009$ is common which results in a power loss of 63 w. Adding extra drag for the nose ($C_D = .1$ considering as a scoop) increases the power loss to 188 w including the centrifugal seal loss. This does not include recirculation, sidewall effects and internal inlet drag and is less than a 35% pump would permit (a total power of 215 w). However, the proximity of sidewalls can push C_D to .1 and in this case drag = 680 w which is comparable to that measured on Set 2.

This discussion indicates that there are geometric explanations for the higher Set 2 pitot pump power loss. To reduce the losses to that originally predicted is realistic but will require experimentation with the variables to arrive at the desired pump efficiency.

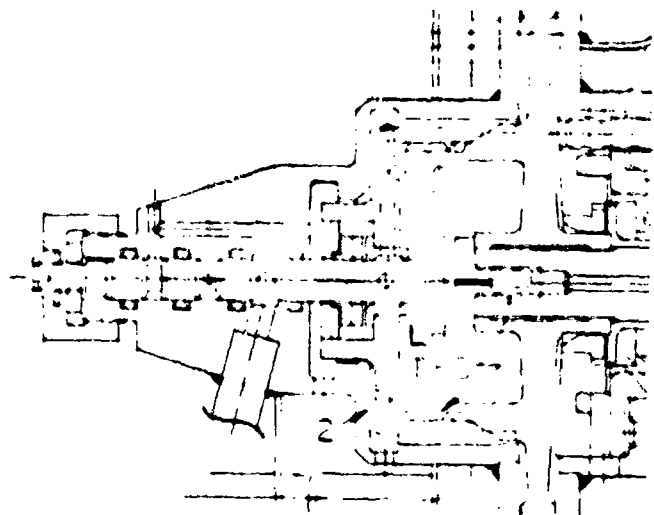
NOISE While significant improvement was made in gearbox emitted noise, the CRU is still the major noise producer. Although between Set 1 and Set 2 the noise level was reduced (stiffening the hotwell), it is not sufficiently low to meet the noiseless 100 meter requirement. The reason is largely due to all the resonances of the hotwell not being eliminated. Thus, the hotwell responds to the rotational disturbance of the turbine assembly. Further improvement could be made by reducing the input disturbance. This would require improving the balance of the rotating assembly by balancing in the operating speed region. Sundstrand's Remecon power plant is an example of a very quiet machine. It is heavy but nonetheless attests to the solution approach of stiffening the hotwell as the method to preclude responding to the one-per rev of the turbine rotating assembly. Minimal weight increase would be incurred by using ribs, better mount arrangement, elimination of flats on the hotwell which easily deflect, and a non cantilevered mounted turbine rotating assembly to eliminate its own self-induced vibration.

BOOST PUMP Between Set 1 and Set 2 an improved boost pump was developed; however, there are circumstances where boiling occurs as the condenser overcools the condensate during transient periods. Even the Set 2 boost pump will cavitate in these circumstances. Sundstrand has developed for Remecon a boost pump capable of handling boiling CP 25. This is a nominal 10,000 rpm centrifugal pump which has to date exceeded 8000 hours of operation and demonstrated its integrity. This pump is ideally suited to the MERDC 1.5 KW unit since it is designed for comparable flows and pressures.

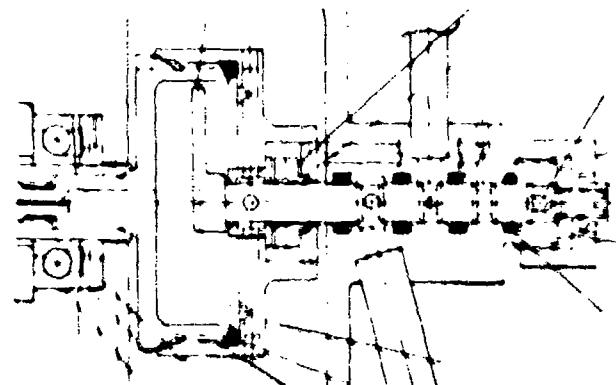
OTHER Other areas of improvement were presented in the Set 1 Final Report, ATR 1182, dated 6-24-74. Many of these were not incorporated into Set 2 and remain valid.

CONTROLS: The controllers used for Units 1 and 2 were designed to meet the requirements of the specification including use of preferred parts. To meet the circuit requirements over the specified temperature range and environmental conditions, it is not necessary to use the preferred parts of the specification.

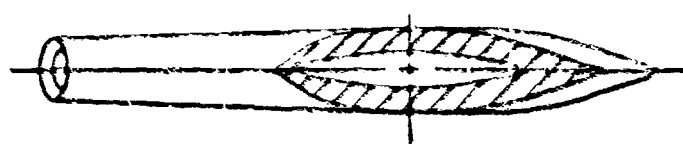
The following discussion of a simplified controller centers on circuits that were chosen to reduce



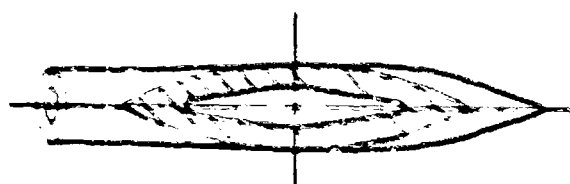
MERDC UNIT 1
EP 2559 1001



MERDC UNIT 2
EP 2559 5909



MERDC
EP 2559 1148
HAND FINISHED &
POLISHED WITH ROUND
LEADING EDGE
 $t = .070 \pm .001$
 $e = .285 \pm .006$



MERDC
EP 2579 5969
 $t = .070 \pm .001$
 $e = .306 \pm .006$

Figure VIII-1 Bar 1 and Bar 2 Probes

Table VIII-A Pitot Pump Characteristics

	MERDC EP2559	
	1148 <u>(UNIT 1)</u>	5969 <u>(UNIT 2)</u>
MEASURED EFFICIENCY (%)	28	15.6
Power (w)	470	840
Hyd. work (w)	130	130
P Hyd. wk (w)	340	710
Cent. Seal Est. (w)	32	32
Drag + Recirc. Losses (w)	308	678
PREDICTED EFFICIENCY (%)	35	
Power (w)	377*	@ $\eta_{SYS} - 10\%$
Hyd. work (w)	130	
P Hyd. wk (w)	247	
Cent. Seal Est. (w)	32	
Drag + Recirc. Losses (w)	215	
PROBE PREDICTIONS		
Vel Range (ft/sec)	60-300	
N_R Range	2.6×10^5 - 9.2×10^6	
Cent. Seal Loss (w)	32	32
Drag @ $C_D = .009$ (w)	63	
@ $C_D = .000$ (w)	410	
@ $C_D = .100$ (w)	680	
@ $C_D = .009 + .03$ Nose (w)	100	
@ $C_D = .009 + 1$ Nose (w)	188	

*Proposal Prediction = 330w

the overall parts count and meet the operational requirements. They are suggested circuits and have not been built and tested. In addition, they do not always use the military preferred parts list since this list lags the state of the art and, therefore, its use may induce less than ideal design.

The controller block diagram is shown in Figure VIII 2.

The auxiliary regulator can use a precision I.C. regulator instead of zener diode and op amps. The output stage can remain the same. The triangle generator output could be shared by both the auxiliary and main regulators.

The main alternator regulator uses an I.C. regulator for error amplification and reference voltage source. A comparator sums the output of the regulator and a ramp generator to produce a PWM signal to drive the field. The field driver circuit can remain the same.

The current limit circuit uses an F.E.T. as a variable resistance to lower the reference voltage coming from the voltage adjust pot. The current limit approximates a constant power slope.

The new regulator circuit as shown in Figures VIII 3 and VIII-4 has 35 parts compared to the previous design of 68 parts.

The proposed temperature regulator circuit uses the same block diagram approach to the control loop as the existing circuit. If deviation from the preferred parts list is allowed, CMOS and optical isolators can be used, simplifying the VCO and one shot circuitry (Figure VIII 5). The input amplifier will remain the same, an I.C. instrument amplifier. The transistor output stage can be simplified if Darlington transistors are used.

Three approaches to the control loop can be taken. A bang-bang loop would be the fastest and simplest circuit. Response to temperature changes would be immediate and high accuracy can be achieved. A bang-bang loop may cause thermal stressing of the fluid.

A second method which does not cause thermal stressing is a linear proportional loop. In order to make this loop stable, long time constants would be required which would also make it a slow loop. During load application, temperature undershoot would occur and during load removal, overshoot would occur.

A third method would use a linear proportional loop with load compensation. Alternator load would be sensed, and load change would be inserted into the heater loop to speed up the response.

Of the above methods, the first one would save the most parts and the third one the least. The first method would save 30 parts, the second approximately 20 parts and the third approximately 15 parts. Analysis and experimentation would be necessary to identify the optimum trade off.

With CMOS circuitry used extensively in this design, the +5 volt power supply will not be needed. The +15 and -15 v could be provided by pre packaged power supplies. The present design uses 42 parts for the three power supplies. This would be replaced by two power supply modules.

The battery charger will remain the same. The way it is attached to the battery is shown in Figure VIII 6.

Due to the present method of starting the turbine, the controller does not need any sequencing or

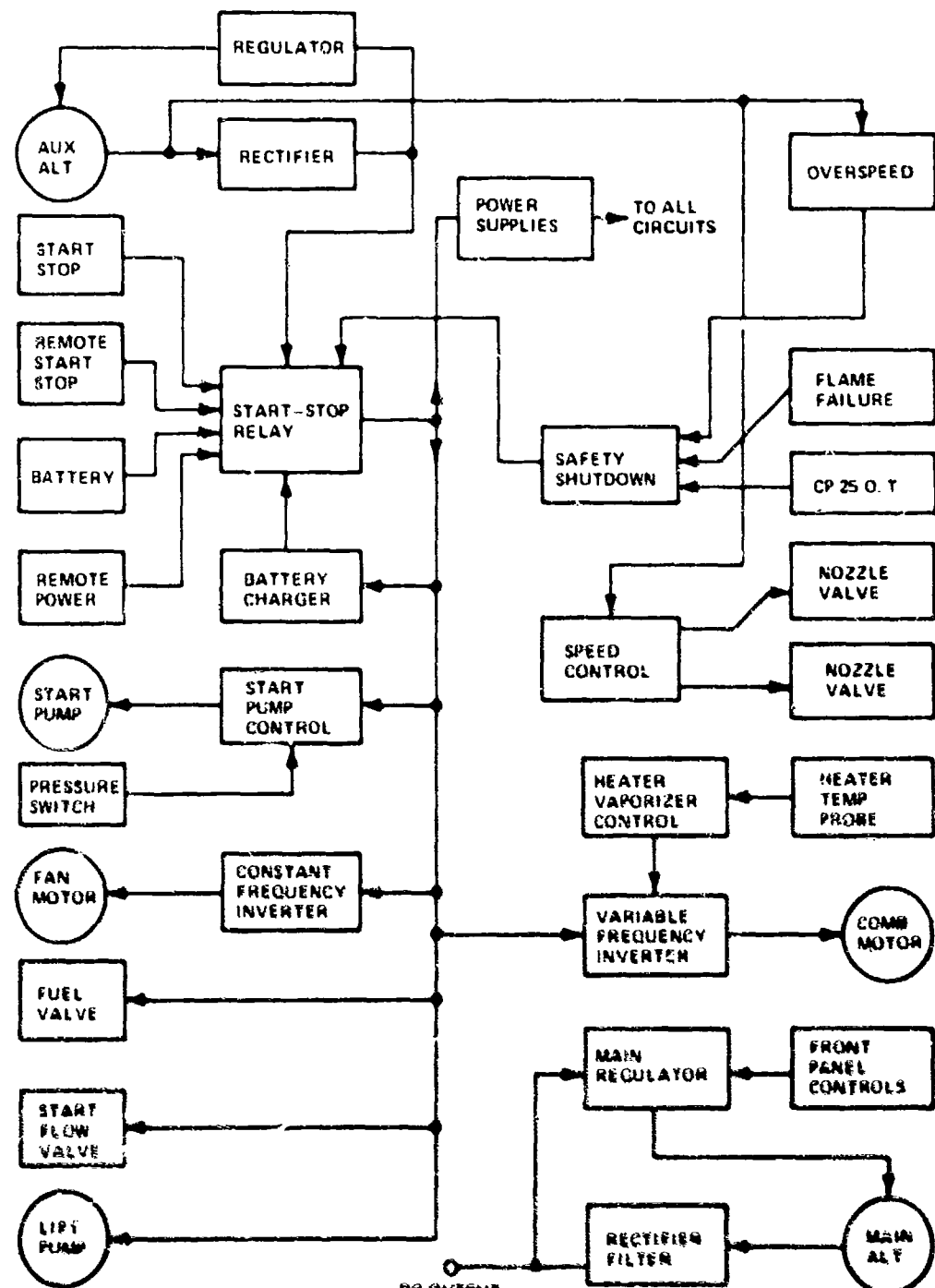


Figure VIII-2 MRDC Controller Block Diagram

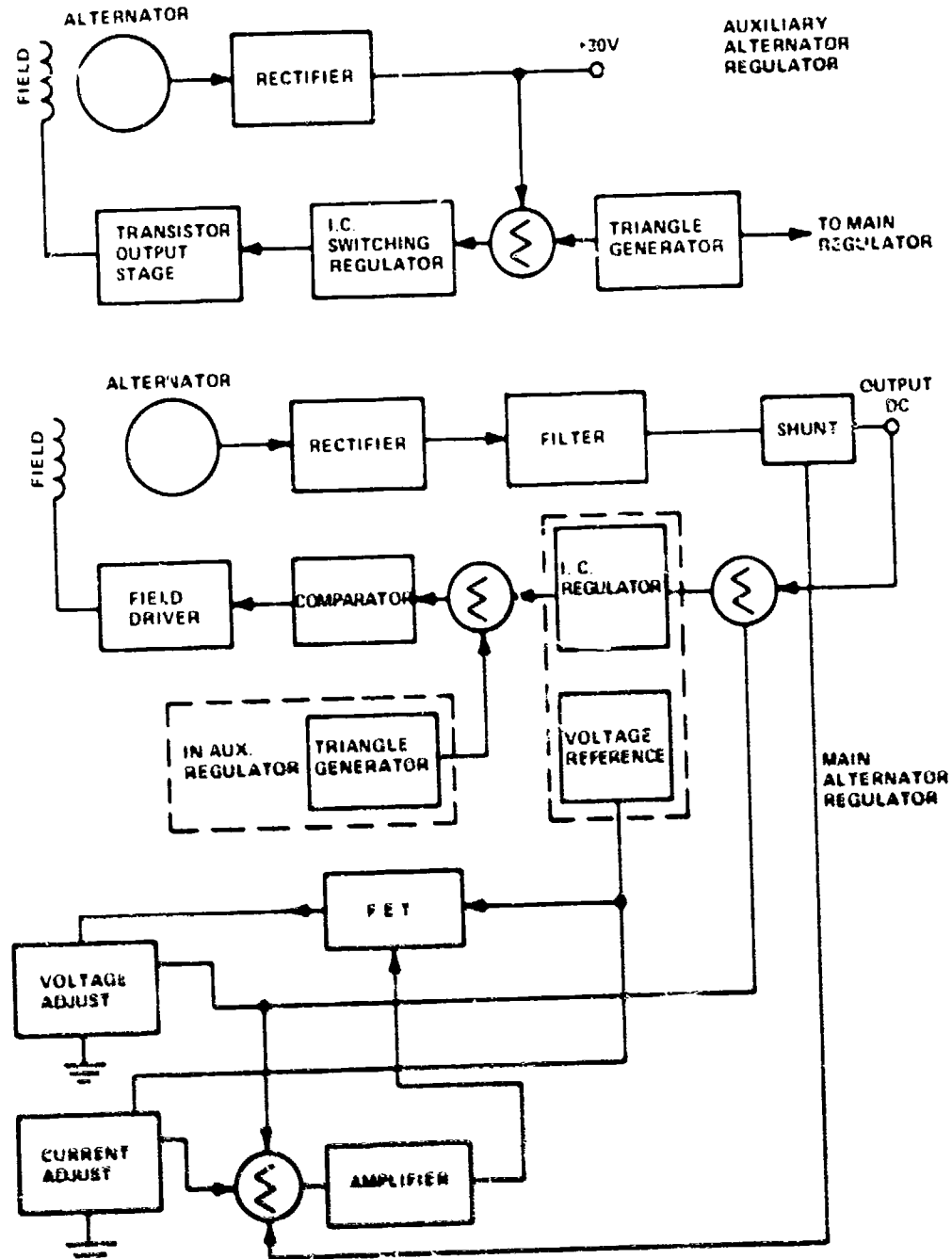


Figure V10-3 Main & Aux Alternator Regulator Block Diagram

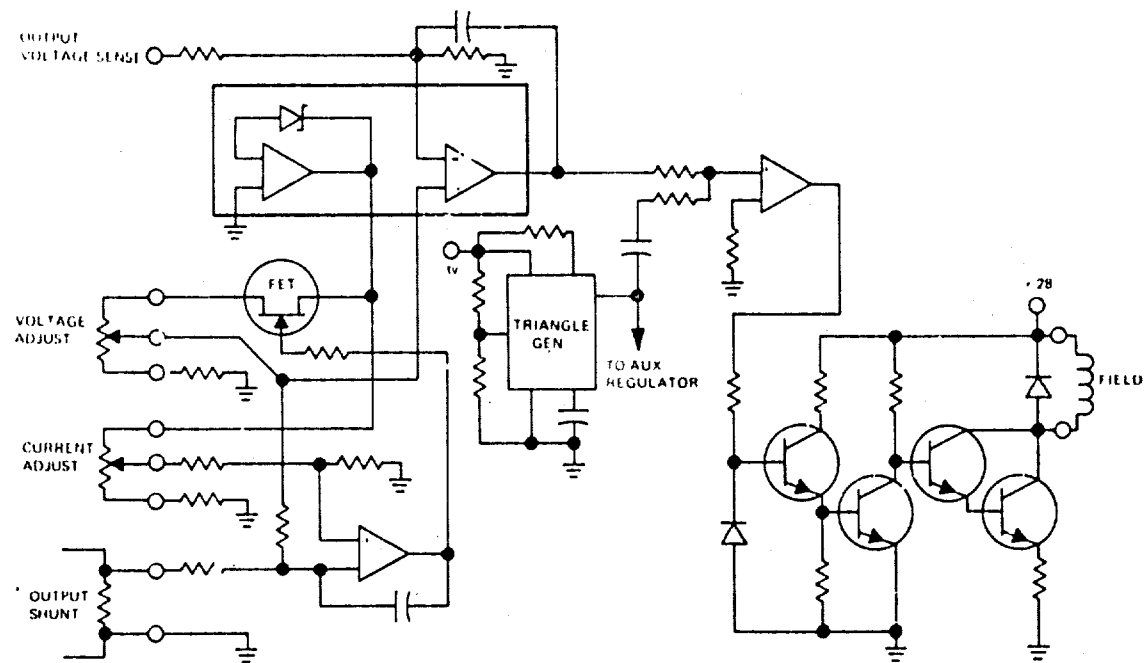


Figure VIII-4 Preliminary Schematic Main Alternator Regulator

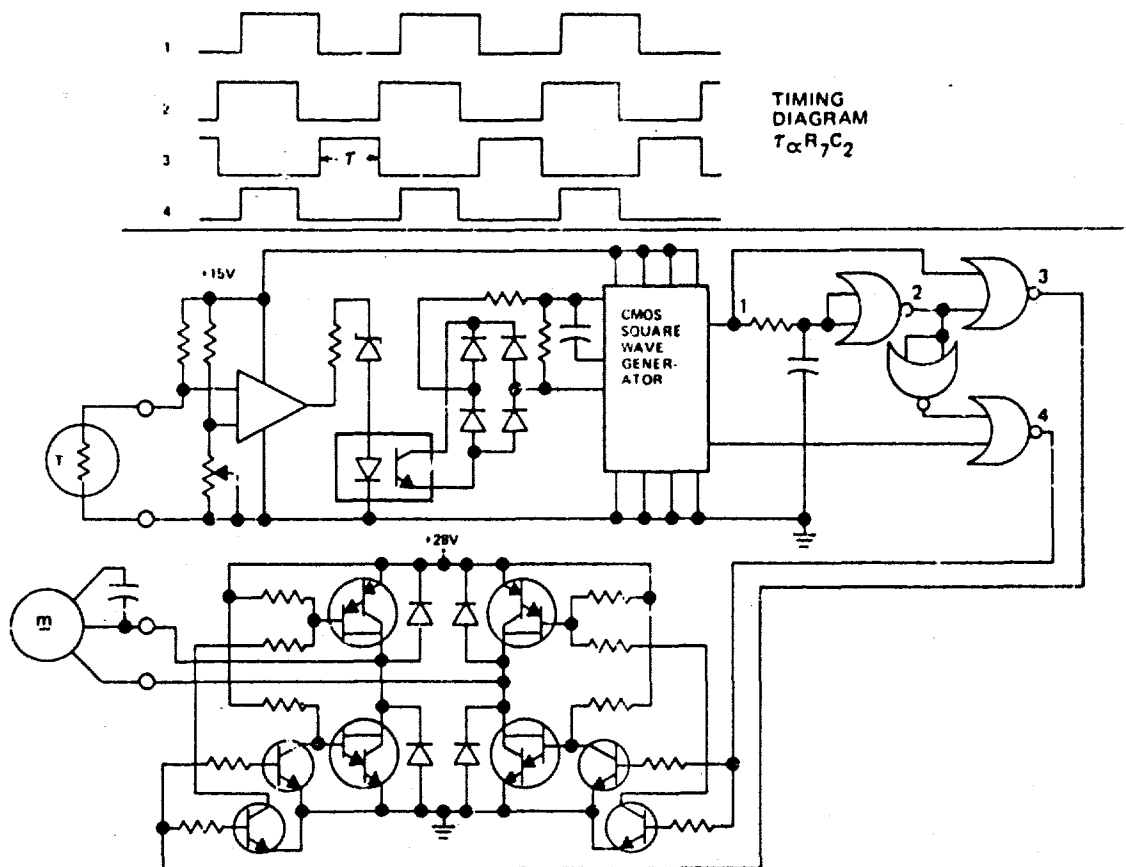


Figure VIII-5 Prelim. Schematic Temp. Reg. Circuit

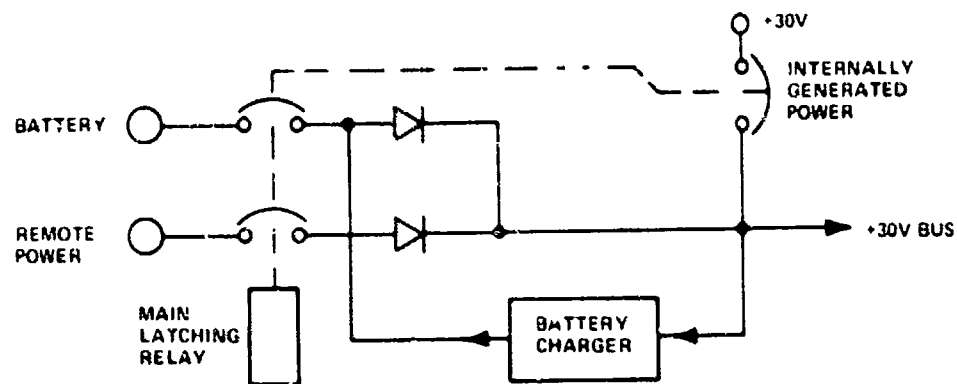


Figure VIII-6 Battery Charge Block Diagram

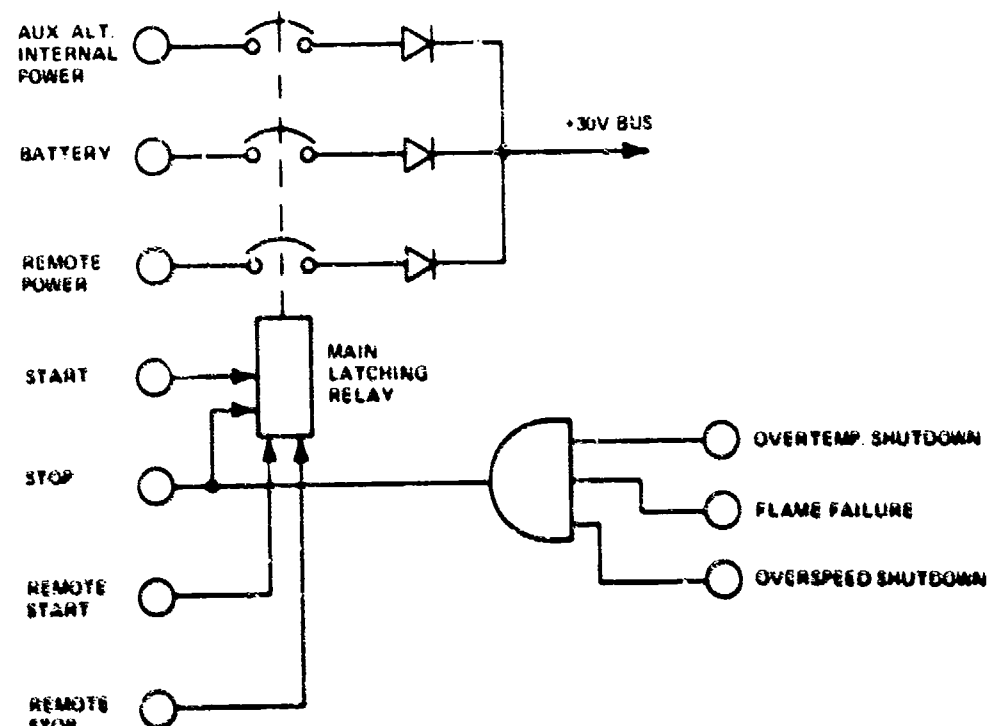


Figure VIII-7 Start-Stop Logic Diagram

time delays. One main latching circuit can control all power coming into the controller. This would consist of two power relays that have contact ratings compatible with the start pump and fan motor current requirements. The logic diagram is shown in Figure VIII 7.

The speed control and overspeed safety circuit will remain the same except that CMOS will replace the TTL logic.

The constant frequency inverter can remain a packaged purchased inverter or incorporated into the controls depending upon the cost trade-off.

The start pump control circuit which allows for starting the pump/motor will remain the same.

The main alternator rectifier filter circuit will also remain the same as the current Unit 2 controller.

REPACKAGING CONCEPT

The existing 2' x 2' x 2' package can be developed into a viable highly efficient power supply, however it is not the optimum package. Evidence from development data to date includes:

Noise emitted by condenser fan.

May not need both constant and variable frequency mechanical circuits. In fact, it is desirable to have condenser coolant fan speed follow working fluid flow rather than run at constant speed.

For increased operating margin, the boost pump should have more liquid head.

The burner operates better extended away from the heater rather than buried.

A repackaged unit would be 3.5' x 1.5' x 1.5' and is shown conceptually in Figure VIII 8. There is no volume or weight increase (currently 8 ft³ and 210 pounds). Further development of a bootstrap start, simplified controls and simplified accessory drive should reduce the parts count, weight, and cost. The repackaging effort will reduce noise and improve mechanical operation.

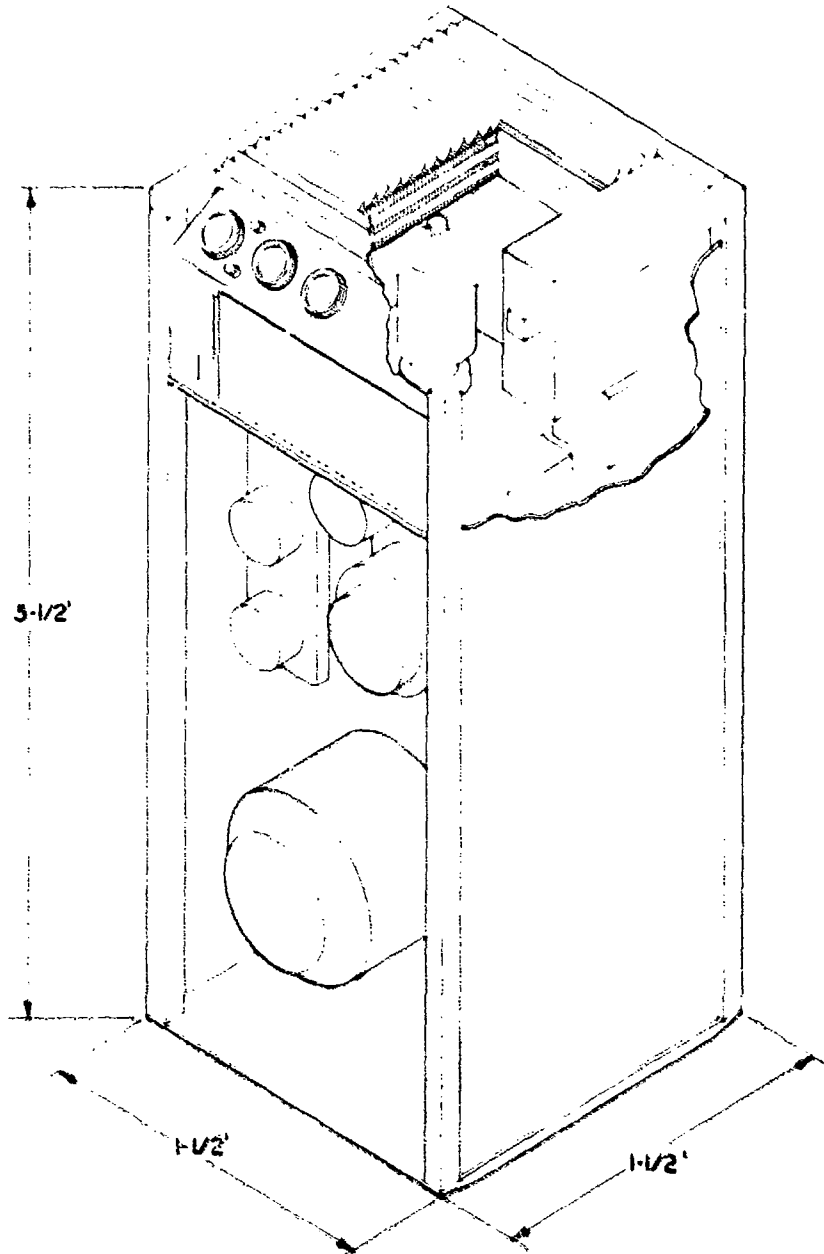


Figure VIII-8 1.5kW EBC Repackaged Canister

SECTION IX

CALIBRATION REQUIREMENTS SUMMARY

IX. CALIBRATION REQUIREMENTS SUMMARY

The calibration requirements summary establishes for the measured parameters the traceability of measurement from the operational equipment to the standards of the National Bureau of Standards.

Table IX A lists the parameters measured for which traceability is provided with the following records. Table IX B delineates thermocouple calibration.

Table IX-A Traceability and Record Identification

Parameter	Description	ID Number
TNI	Temperature nozzle inlet	0775100K
TRO	Temperature regenerator liquid out	0775074K
TRVI	Temperature regenerator vapor inlet	0775062K
THWL	Temperature hotwell liquid	0775099K
TVO	Temperature vaporizer out	0775103K
THE	Temperature heater exhaust	0775078K
TRVO	Temperature regenerator vapor out	0775087K
TRI	Temperature regenerator liquid inlet	0775085K
QE	Flow economizer	FL 205
QR	Flow regenerator	FL 308
QBP	Flow boost pump	FL 277
PNI	Pressure nozzle inlet	PT 204 & PT 160*
PC	Pressure condenser	PT 744 & PT 423
PBO	Pressure boost pump out	PT 232 & PT 760
PBI	Pressure bearing inlet	PT 186

* Used only during N₂ spin checks (PVO)

NOTE. The standard quality control period between calibrations is:

26 weeks for pressure transducers from the time of initial use after calibration

26 weeks for flowmeters from the time of initial use after calibration

52 weeks for thermocouples from the time of initial use after calibration

The test (use) period was from 1-21-76 through 4-18-76.

Table IX-B Thermocouple Calibration

Range: 0°F to 2400°F

Calibration date: Month 7, Year 1974

Usable period after calibration: 1 year

Instrument calibration: Model 1 8 x 12 K

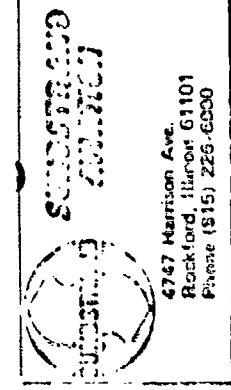
Calibration points: 32.0 + 5.0°F

/86.4 + 5.9°F

1761.4 + 13.2°F

Type - K

Type thermocouple: Chromel - Alumel



SEARCHED S/N: 1202

INDEXED S/N: 6-154

SERIALIZED S/N: ACK

FILED S/N: 6-153

SEARCHED S/N: 6-155

4747 Harrison Ave.
Rockford, Illinois 61101
Phone (315) 226-6500

N.	NAME	ADDRESS	PHONE	TYPE	TOTAL CYCLES	CPS	TRUENESS	GRAD M	GRAD S	GRAD M	GRAD S
1	800.8	80 . 765 . 0311	55367 10832	/98	0340						
2	800.3	8070 52392 12430	804	/0491							
3	500.4	5082 47244 47155	501	/0761							
4	700.6	.0941 54535 38265	702	/0353							
5	900.7	.1098 50358 45485	903	/308							
6	1200.9	.1411 49533 59443	1200	/709							
7	1500.11	.1235 49464 79409	1500	/292							
8	1800.13	.2038 49088 88318	1799	/3491							

SEARCHED S/N: 1202 S/N: 6-154

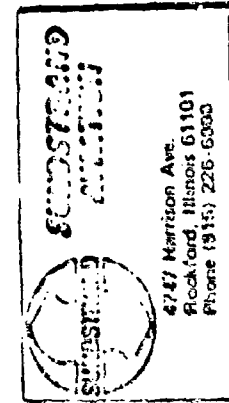
INDEXED S/N: 6-154 SERIALIZED S/N: ACK FILED S/N: 6-155

%

%

%

%



FLUTTER S/N: 14609
C.F. 6-1
J.C.
P.M.: 100%
FLUTTER S/N: 14609
C.F. 6-1
J.C.

RE	REVERSE	STUDIO VOL	STUDIO GAIN	REC	TRUE FREQ	FREQ/LBS/HR	GRAV. LBS/HR	VOL	GPM	CYCLES	GAL.	EPS
100.6	80.745	100%	10.34	5085	120	.1168						
100.7	80.811	100%	8.00			.1873						
100.7.5	83.52	51.09	15.382	307		.2761						
100.8	81.36	51.809	10.249	400		.3631						
100.9	84.04	51.204	31.392	601		.5902						
100.10	86.22	51.491	419.20	800		.7176						
100.11	88.40	51.511	51.602	1002		.9958						
100.12	90.07	51.002	63.376	1200		1.0690						

ENTRANCE STAND: CO. 100-1 3951, 2/1 6531

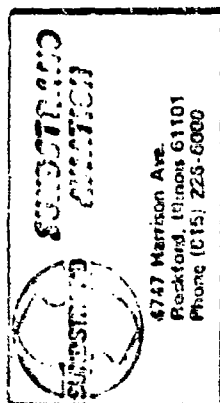
DATE OF LAST CHECK: 100% 100% 100% 100% 100% 100% 100% 100% 100% 100% 100% 100% 100%

% 100% 100% 100% 100% 100% 100% 100% 100% 100% 100% 100% 100% 100%

GRANTOR'S ST. N.D.: CGN 57221 335T, S/N 6537.

卷之三

CIVIL



PT-204 PRESSURE	02K 0 TO 1000	779	02.1 NI MEROC
10 NUMBER	TEST DATE	TEST	TEST
0000000000000000	1972	1972	1972
CAL POINT	STANDARD 14 R2		
0 - 10	AS LEFT		
	INPUT	ANALOG VOLTAGE	P.T.L. 0.204
LOW	0	0.000	2134
	20	1.000	X X
MED	40	1.925	X X
	60	3.000	X X
HIGH	80	3.992	X X
	100	5.000	2134
TECH	P2P		
CALIBRATION FIGURE	n 3 - 2.568 VDC		
CODE CH. NUMBER	DATE	DESCRIPTION	TEST
CODE TEST DATE	TEST	TEST	TEST
TEST NUMBER	TEST	TEST	TEST
TEST DATE	TEST	TEST	TEST
PT-236 PRESSURE	02K 0 TO 304	779	02. PPO (P00)
10 NUMBER	TEST DATE	TEST	TEST
0000000000000000	1972	1972	1972
CAL POINT	STANDARD 14 R2		
0 - 10	AS LEFT		
	INPUT	ANALOG VOLTAGE	P.T. 0232019
LOW	0	0.000	01205
	20	1.000	X X
MED	40	2.000	X X
	60	3.000	X X
HIGH	80	3.992	X X
	100	5.000	2134
See	Tidy Clean TECH 14 K		
CALIBRATION FIGURE	n 4 - 3.998 VDC		
CODE CH. NUMBER	DATE	DESCRIPTION	TEST
CODE TEST DATE	TEST	TEST	TEST
TEST NUMBER	TEST	TEST	TEST
TEST DATE	TEST	TEST	TEST
PT-744 PRESSURE	02K 0 TO 50 A	779	02. PC MEROC
10 NUMBER	TEST DATE	TEST	TEST
0000000000000000	1972	1972	1972
CAL POINT	STANDARD 14 R2		
0 - 10	AS LEFT		
	INPUT	ANALOG VOLTAGE	P.T. 0744
LOW	0	0.000	2134
	6	0.720	X X
MED	12	1.440	X X
	18	2.160	X X
HIGH	24	3.000	X X
	30	3.992	X X
	36	5.000	2134
TECH	P2P		
CALIBRATION FIGURE	n 3 - 3.507 VDC		
CODE CH. NUMBER	DATE	DESCRIPTION	TEST
CODE TEST DATE	TEST	TEST	TEST
TEST NUMBER	TEST	TEST	TEST
TEST DATE	TEST	TEST	TEST

PT 760 PRESSURE DOME Y		P.D. 0 TO 50 A		770 B. CELL 02 P	
12 NUMBER		TOTAL 5000		TEST	
CAL POINT		STANDARD 50-82		TEST	
0-		AS LEFT		TEST	
LOW		INPUT		TEST	
MED		0 0		0.000	
HIGH		20 6		0.95	
0.363		40 12		1.918	
		60 18		2.994	
		80 24		3.975	
		100 30		5.000	
TECH P.P.R.					
CALIBRATION FIGURE		3.3 664		VDC	
CALIBRATION FIGURE		3.4 3.674		VDC	
CALIBRATION FIGURE		3.4 3.767		VDC	
PT 160 PRESSURE DOME Y		P.D. 0 TO 1000		770 B. CELL 02 PVO	
12 NUMBER		TOTAL 5000		TEST	
CAL POINT		STANDARD 50-82		TEST	
0-		AS LEFT		TEST	
LOW		INPUT		TEST	
MED		0 0		0.00	
HIGH		20 200		1.001	
		40 400		2.002	
		60 600		3.003	
		80 800		4.004	
		100 1000		5.000	
TECH P.D.B.					
CALIBRATION FIGURE		4.3 674		VDC	
CALIBRATION FIGURE		4.4 3.767		VDC	
CALIBRATION FIGURE		4.4 3.767		VDC	
PT 176 PRESSURE DOME Y		P.D. 0 TO 50 P.S.I.		770 B. CELL 02 PBO	
12 NUMBER		TOTAL 5000		TEST	
CAL POINT		STANDARD 50-82		TEST	
0-		AS LEFT		TEST	
LOW		INPUT		TEST	
MED		0 0		0.000	
HIGH		20 10		0.995	
		40 10		2.000	
		60 10		2.001	
		80 10		2.002	
		100 10		2.003	
TECH S.G.					
CALIBRATION FIGURE		4.4 3.767		VDC	

BUNDESTRANZ AVIATION QUALITY CONTROL & RELIABILITY DEPARTMENT

六四：勿跛勿跛，勿

INSTRUMENT CERTIFICATION RECORD

ITEM CALIBRATED DIGITAL MULTIMETER CALIBRATION INTERVAL 30 YEARS

SECTION A

1 TYPE DC, INTL RMS, CHARGE TO-104: NO MFG NUMBER

2 MANUFACTURER FAULKE MODEL NO. 8375A

3 ACCURACY SEE BELOW RANGE 10, 100, 1000 CM. 0 - 104 CM. 3

4 IDENT NO. VE-150

5 SERIAL NO. 75405

CONTINUE ON SECTION 8

CALIBRATION DATA
John Fluke Digital Multimeter Model 8375A

Identification VE-150

Date Calibrated 01-15-75 By 611

Calibration Not Valid After 2-15-75

Standards Used X-44 X-51 X-31,32 33 34 35,41

Maintenance And Repairs Performed 72-2-C

PROCEDURE

No Adj.
Adjust _____
Read _____

1. DC Range Current (T.I. is Test Instrument)

Range	Standard	T.I. As Found	T.I. As Left	Error	Tolerance
0.1 VDC	+ .01000	<u>0.009997</u>		.000003	.000008
	- .01000	<u>2.00999</u>		.00002	.00003
	+ .10000	<u>0.00008</u>		.00002	.00003
	- .10000	<u>0.00004</u>		.00001	.00002
	+ .10.000	<u>0.00000</u>		.00001	.00001
	- .10.000	<u>0.00000</u>		.00001	.00001
	+ .1.0000	<u>0.00000</u>		.00001	.00005
	- .1.0000	<u>0.00000</u>		.00001	.00023
	+ .100.000	<u>0.00000</u>		.00002	.0021
	- .100.000	<u>0.00000</u>		.0001	.011
1.0 VDC	+ .10.000	<u>0.9999</u>		.00001	.00001
	- .10.000	<u>0.9999</u>		.00001	.00001
	+ .100.000	<u>0.9999</u>		.00001	.00001
	- .100.000	<u>0.9999</u>		.00001	.00001
	+ .1.0000	<u>0.9999</u>		.00001	.00001
	- .1.0000	<u>0.9999</u>		.00001	.00001
	+ .10.000	<u>0.9999</u>		.00001	.00001
	- .10.000	<u>0.9999</u>		.00001	.00001
	+ .100.000	<u>0.9999</u>		.00001	.00001
	- .100.000	<u>0.9999</u>		.00001	.00001
10.0 VDC	+ .100.000	<u>9.999</u>		.00002	.00012
	- .100.000	<u>9.999</u>		.00002	.00012
	+ .1.0000	<u>9.999</u>		.00002	.00012
	- .1.0000	<u>9.999</u>		.00002	.00012
	+ .10.000	<u>9.999</u>		.00002	.00012
	- .10.000	<u>9.999</u>		.00002	.00012
	+ .100.000	<u>9.999</u>		.00002	.00012
	- .100.000	<u>9.999</u>		.00002	.00012
	+ .1.0000	<u>9.999</u>		.00002	.00012
	- .1.0000	<u>9.999</u>		.00002	.00012
100.0 VDC	+ .100.000	<u>99.993</u>		.007	.012
	- .100.000	<u>99.993</u>		.007	.012
	+ .1.0000	<u>99.993</u>		.007	.012
	- .1.0000	<u>99.993</u>		.007	.012
	+ .10.000	<u>99.993</u>		.007	.012
	- .10.000	<u>99.993</u>		.007	.012
	+ .100.000	<u>99.993</u>		.007	.012
	- .100.000	<u>99.993</u>		.007	.012
	+ .1.0000	<u>99.993</u>		.007	.012
	- .1.0000	<u>99.993</u>		.007	.012
1000	+ .1000.000	<u>999.99</u>		.01	.02
	- .1000.000	<u>999.99</u>		.01	.02
	+ .100.000	<u>999.99</u>		.01	.02
	- .100.000	<u>999.99</u>		.01	.02
	+ .1.0000	<u>999.99</u>		.01	.02
	- .1.0000	<u>999.99</u>		.01	.02
	+ .10.000	<u>999.99</u>		.01	.02
	- .10.000	<u>999.99</u>		.01	.02
	+ .100.000	<u>999.99</u>		.01	.02
	- .100.000	<u>999.99</u>		.01	.02

NOTE: The following calibration steps are to be performed only if the above checks were found out of Specs.

5. Buffer Aero Adjustment.
6. Bias Current Adjustment.
7. Reference Voltage Adjustment.
8. A-D Zero Adjustment.
9. + Cal. Adjustment.
10. Ladder Cal.
11. Negative Cal. Adjustment.
12. Remainder Adjustment.
13. Comparator Level Adjustment.
14. RMS Range Amplifier Zero.
15. Balance Amplifier Zero.
16. Balance Gain.
17. AC Zero.
18. Calibration Adjustment/Check.
19. Coarse Calibration.
20. Buffer DC Calibration.
21. Active Filter.
22. Kilohms Calibration.
23. Ohms Calibration.

UNCLASSIFIED

Security Classification

DOCUMENT CONTROL DATA - R & D

(Security classification of title, body of abstract and indexing information must be entered when the overall report is classified)

1. ORIGINATING ACTIVITY (Corporate author) SUNDSTRAND AVIATION 4747 HARRISON AVE. ROCKFORD, ILLINOIS 61108		2a. REPORT SECURITY CLASSIFICATION UNCLASSIFIED
2. REPORT TITLE ORGANIC RANKINE CYCLE SILENT POWER PLANT 1.5 KW, 28 VOLTS D.C.		
3. DESCRIPTIVE NOTES (Type of report and inclusive dates) PROGRAM REPORT		
4. AUTHORITY (Title name, grade or rank, last name) RONALD F. McKENNA		
5. REPORT DATE AUG. 1975	6a. TOTAL NO. OF PAGES 0	6b. NO. OF APPENDIXES 0
7a. CONTRACT OR GRANT NO. DAAK02-72-C-0472	7b. ORIGINATING ACTIVITY REPORT NUMBER AND DATE	
8. PROJECT NO.		
9.	10. OTHER REPORT NUMBER (And other numbers that may be assigned this report) REF. FINAL REPORT ATR 1182, 24 JUNE 1974	
11. DISTRIBUTION STATEMENT [REDACTED]	DISTRIBUTION STATEMENT A	
	Approved for public release Distribution Unlimited	
12. SUBJECT TERMS (Key words)	13. SPONSORING ACTIVITY STATEMENT ELECTROTECHNOLOGY DEPARTMENT ELECTROMECHANICAL DIVISION U.S.ARMY MOBILITY R & D CENTER	
14. CATEGORIES		

- This report describes the design, fabrication and test of components subsystems and organic Rankine Cycle Power Plant. Design point net output power is 1.5 KW at 28 V.D.C. Power is produced by combustion of an air/fuel mixture and transferring the thermal energy to CP-25, the working fluid, which is expanded through a turbine. The turbine is part of a turbo-alternator which also powers internal accessory components. Specific design criteria involves precise quality of power, weight, volume, efficiency, life and noise limitations, severe environment and shock, and multi-fuel operating requirements. The set is portable, self-contained except for fuel supply and is intended to operate as a silent power plant.

DD FORM 1473

UNCLASSIFIED

Security Classification

14 KEY WORDS	LINE A		LINE B		LINE C	
	ROLE	WT	ROLE	WT	ROLE	WT
RANKINE CYCLE WORKING FLUID GENERATOR ALTERNATOR TURBINE BEARINGS PITOT PUMP GEARBOX HEATER VAPORIZER ECONOMIZER REGENERATOR CONDENSER BOOST PUMP HAND PUMP DIGITAL CONTROL VALVES VAPOR SHUTOFF VALVE CONTROL SYSTEM COMBUSTOR AIR/FUEL SYSTEM FUEL METERING PUMP ATOMIZING AIR COMPRESSOR MAGNETO CONDENSER FAN AIR BLOWER ACCUMULATOR ALTITUDE COMPENSATING VALVE START PUMP						

UNCLASSIFIED

Security Classification